UNIVERSITÀ
DEGLI STUDI
DI PADOVA

UNIVERSITÀ DEGLI STUDI DI PADOVA

Dipartimento di Ingegneria Industriale - DII

CURRICULUM: CHEMICAL AND ENVIRONMENTAL ENGINEERING

SERIES XXXV

EXPLORE CELLULAR REPROGRAMMING PROCESS AND MICROFLUIDICS-BASED NASCENT IPSCS FOR INVESTIGATING HUMAN DEVELOPMENT IN VITRO

Thesis written with the financial contribution of Chinese Scholarship Council

Coordinator: Prof. Andrea Claudio Santomaso

Supervisor: Prof. Nicola Elvassore

Ph.D. student: Wei Qin

Summary

The discovery of induced pluripotent stem cells (iPSCs) circumvents the ethical concerns of human embryonic stem cells, which fasten the stem cell research. After that, various types of transfection methods have emerged to induce cellular reprogrammig, in order to generate iPSCs in an effective and safe manner. Out of all the integrating and non-integrating ways, message RNA (mRNA) reprogramming is found to be one of the most efficient and safe methods, which lays also the basis of my project. Combining with the expertise of microfabrication, we tested the mRNA reprogramming in a microfluidic chip system and found out that the cellular reprogramming was improved greatly (~50folds) comparing to the standard cell culture conditions, like the multi-well plate of petri dishes. Thus, by making the fully use of microfluidics-based mRNA reprogramming, we explored the reprogramming process itself and later the applications of iPSCs.

The first chapter contains brief but fundamental background information for this work. It tells us how the iPSCs have been discovered and the advantages of non-integrating method, mainly on the mRNA transfection ways. Also, we introduce illustrate how the human embryo development *in vivo* and the demanding *in vitro* 3D organoids models to study embryogenesis. Basic principle of microfabrication is also introduced.

The second chapter talks about the main aim of my whole project.

The thrid chapter gives detalied information to all the experiment materials and protocols that I have been used in this project.

The fourth result chapter is the core chapter. Here I listed the results obtained until now. In the this charpter, to anwser the first question of exploring the reprogramming process and identify the intermediate stages, cell populations, gene trajactory and possible signaling pathway, we make use of highy efficient reprogramming in microfluidics by mRNA transfection and temporal multi-omics.

We combined secretome analysis with single-cell transcriptomics to reveal the functional extrinsic protein communication channels between reprogramming sub-populations and the reshaping of a favorable extracellular environment. We moved forward with the help of the microfluidic culture setup by objectively identifying the reprogramming subpopulation trajectories and relationships based on an integrative secreted proteome and scRNA-seq study. The former found several secreted cytokines, growth factors, and extracellular matrix(ECM)-related proteins that were truly present in the extracellular space during reprogramming and helped to construct an environmental signaling system that resembled the early embryonic basal lamina. Two primary pathways during reprogramming were found by scRNA-seq. One of them was entirely committed to secretory activity and the other one was committed to cellular reprogram.

Previous investigations may have overlooked the importance of the extracellular environment by failing to recognize immature hiPSCs as a secretome target due to their low abundance or limited secretory activity. On the basis that cellular reprogramming is a transcriptional factores driven processm our findings combine also the idea that human cellular reprogramming is dependent on extracellular context and cell populations, in this work, we followed an unbiased approach that supported the idea that the route to pluripotency can be broadened by cell-non-autonomous mechanisms. Paracrine signalling is established by highly regulated dynamics with multi-factorial contribution.

We identified the HGF/MET/STAT3 axis as a significant facilitator of reprogramming that functions through HGF accumulation in the constrained environment of microfluidics but requires exogenous supply in standard dishes to increase efficiency. We showed the use of HGF for gain of function during reprogramming in a conventional culture system, but this efficiency was amenable to further enhancement when multifactorial contributions were used. In particular, we used IL6 and soluble IL6R for a more effective downstream activation of STAT3. Moreover, we found that NRG1 contribute to enhance efficiency of hiPSC formation

consistently with previous works, which upon binding ERBB2/ERBB3 receptors activates MAPK/ERK pathway and showed improved mainte nance and passage of hiPSCs.

For the second aim of my project, we tested the overall ability of nascent iPSCs, which were newly generated right after the 14day of mRNA reprogramming, were able to form 3D epiblast cyst then later the organoids from three germ layer of the human embryo. We found that nascent iPSCs were less methylated compared to the high passage of iPSCs line, which is part of epigenetics that hampering gene expressions. Also, nascent iPSCs required less cells (as low as 5000cells per one 24well) for generating a 3D epiblast cyst on a matrigel bed. 5000n ascent iPSCs were able to produce around 1200 3D epiblast cysts while high passage iPSCs lines only produced 800 of that. Also, in terms of the quality, nascent iPSCs derived epiblasts cysts were homogeneous and at high proliferate rate, while the high passage counterparts were only half of their size(diameter). Germ layer differentiation experiments showed that these nascent iPSCs epiblast cysts were able to produce cells, primitive tissue from endoderm, mesoderm and neuroectoderm, which was an ideal model for investigate the human embryogenesis *in vitro*. The long-term maturation organoids, like the liver organoids, the cardiac organoids and forebrain organoids were still maintained in culture. Characterization experiments were ongoing.

The microfluidic reprogramming fibroblasts to organoids happened in a continuum, which could be established within three weeks, while the established iPSCs lines usually take two to three months. It is low cost as well as timesaving, which could be promoted to studying large cohort of patients. Apart from investigating the human embryogenesis, nascent iPSCs derived organoids could also be utilized in the field of studying liver, intestine, lung, kidney and brain, which facilitates the detailed research of disease mechanism or tissue regeneration *in vitro*.

In order to solve the third problem, we moved to peripheral blood as the blood cell supply for sources of reprogramming since they were easier accessible by venipuncture. We were kindly donated 40ml of peripheral blood from the Padova

hospital to start the first trial from blood to iPSCs. Whole blood was processed firstly by gradient centrifugation to remove most of the plasma and erythrocytes. The mononuclear cell layer was our target cells. They were plated on a type I collagen-coated flask to ensure the attachment. During the endothelial progenitor cells (EPCs) generation process, medium change was strictly kept three times per week guaranteeing the growth factors supplement, which was a crucial point from my experience in generating EPCs after one week. After 28days, we saw the cobblestone morphology like adherent cells appear, forming a cluster. They were the blood outgrowth endothelial cells (BOECs). The reprogramming procedure of BOECs shared the same protocol with skin fibroblasts, but there was a gradual medium adaptation to balance the BOECs survival and transition since they were more delicate to the microenvironment inside the microchannels. Only 12days of transfection, iPSCs were clearly appeared and they were kept another 5days in IPS-Brew medium for stabilization before the extraction from the chips. BOEC-iPSCs were able to differentiate into three germ layer cells with distinguished marker expression. 3D organoids characterization of development potential was ongoing.

This work is a compresive and systematic exploration as well as utilization of highly efficient cellular reprogramming in microfluidics. We have established the standard mRNA reprogramming in microfluidic chips to produce high-quality iPSCs in a fast and cost-saving manner. Then we developed the fibroblasts to organoids process, since the newly generated nascent do not ask for any extra expansion, leading to a direct generation protocol of epiblast cysts and later on various types of organoids. What is more, our organoids models only require as few as 5000 cells per organoid to start the differentiation process, which is also of great benefits to large-scale studies, like the toxicity testing, drug screening and and antibodies selection. We have successfully reprogrammed fibroblasts from Alzheimer patients(~70 years old) and Duchenne muscular dystrophy patients into iPSCs within 20days, which were considered as a challenge to achieve in other reprogramming systems. These patient-specific iPSCs and later patient-specific organoids are accessible to disease modeling.

Bear the inconvenience of skin fibroblasts obtain in mind, we expolored alternative cell sources for broader application of iPSCs. We demonstrated that the isolation of blood outgrowth endothelial cells from the peripheral blood was an feasible way for generating patient-specific organoids, which is beneficial personalized medicine.

In the fifth chapter, there is the brief conclusion to all the experiment results and discussion of the potential optimization and future plans.

RIASSUNTO

La scoperta delle cellule staminali pluripotenti indotte (iPSC) supera le controversie etiche dell'uso delle cellule staminali embrionali umane, accelerando la ricerca sull'embriogenesi. In seguito, sono emersi vari tipi di metodi di trasfezione per indurre la riprogrammazione cellulare, al fine di generare iPSC in modo efficace e sicuro. Tra tutti i metodi integranti e non, la riprogrammazione con RNA messaggero (mRNA) è risultata essere uno dei metodi più efficienti e sicuri.

Questa strategia costituisce anche la base del mio progetto. Combinandola con la tecnologia di microfabbricazione, abbiamo testato la riprogrammazione dell'mRNA in un sistema di piattaforma microfluidico e abbiamo scoperto che la riprogrammazione cellulare è stata notevolmente migliorata (~50 volte) rispetto alle condizioni di coltura cellulare standard, come la piastra Petri. Utilizzando pienamente la riprogrammazione dell'mRNA basata sulla microfluidica, abbiamo quindi esplorato il processo di riprogrammazione stesso e successivamente le applicazioni delle iPSC.

Il primo capitolo contiene brevi ma fondamentali informazioni di base per questo lavoro. Ci spiega come sono state scoperte le iPSC e i vantaggi di metodi non-integranti, soprattutto per quanto riguarda le modalità di trasfezione dell' mRNA. Inoltre, viene illustrato lo sviluppo dell'embrione umano in vivo e gli impegnativi modelli di organoidi 3D in vitro per lo studio dell'embriogenesi. Vengono anche introdotti i principi di base della microfabbricazione.

Il secondo capitolo parla dell'obiettivo principale di tutto il mio progetto.

Il terzo capitolo fornisce informazioni dettagliate su tutti i materiali e i protocolli utilizzati in questo progetto.

Il quarto capitolo, sui risultati, è il capitolo centrale. Qui ho elencato i risultati ottenuti finora. Per rispondere alla prima domanda di esplorare il processo di riprogrammazione e identificare le fasi intermedie, le popolazioni cellulari, la traiettoria dei geni e le possibili vie di segnalazione, ci avvaliamo della riprogrammazione ad alta efficienza in microfluidica mediante trasfezione di mRNA e della multi-omica temporale.

Abbiamo combinato l'analisi del secretoma con la trascrittomica di una singola cellula per rivelare i canali di comunicazione funzionali delle proteine estrinseche tra le sottopopolazioni di riprogrammazione e il rimodellamento di un ambiente extracellulare favorevole. Abbiamo identificato le traiettorie e le relazioni tra le sottopopolazioni di riprogrammazione sulla base di uno studio integrativo del proteoma secreto e dell' scRNA-seq. Lo studio del secretoma ha individuato diverse citochine secrete, fattori di crescita e proteine correlate alla matrice extracellulare (ECM) realmente presenti nello spazio extracellulare durante la riprogrammazione e ha contribuito a costruire un sistema di segnalazione ambientale che assomiglia alla lamina basale embrionale iniziale. Due percorsi primari durante la riprogrammazione sono stati individuati mediante scRNA-seq. Uno di essi era interamente impegnato nell'attività secretoria e l'altro era impegnato nella riprogrammazione cellulare.

Le indagini precedenti potrebbero aver trascurato l'importanza dell'ambiente extracellulare, non riconoscendo le hiPSC immature come target del secretoma a causa della loro bassa abbondanza o della limitata attività secretoria. Sulla base del fatto che la riprogrammazione cellulare è un processo guidato da fattori trascrizionali, i nostri risultati combinano anche l'idea che la riprogrammazione cellulare umana dipenda dal contesto extracellulare e dalle popolazioni cellulari; in questo lavoro, abbiamo seguito un approccio imparziale che ha supportato l'idea che il percorso verso la pluripotenza possa essere ampliato da meccanismi cellulari non autonomi. La segnalazione paracrina è stabilita da dinamiche altamente regolate con un contributo multifattoriale.

Abbiamo identificato l'asse HGF/MET/STAT3 come un importante facilitatore della riprogrammazione che funziona attraverso l'accumulo di HGF nell'ambiente confinato della microfluidica, ma che richiede un apporto esogeno nelle piastre standard per aumentare l'efficienza. Abbiamo dimostrato l'uso di HGF per l'aumento della funzione durante la riprogrammazione in un sistema di coltura convenzionale, ma questa efficienza poteva essere ulteriormente migliorata quando venivano utilizzati contributi multifattoriali. In particolare, abbiamo utilizzato IL6 e IL6R solubile per una più efficace attivazione a valle di STAT3. Inoltre, abbiamo riscontrato che NRG1

contribuisce a migliorare l'efficienza della formazione di hiPSC, coerentemente con i lavori precedenti, che al legame con i recettori ERBB2/ERBB3 attiva la via MAPK/ERK e ha mostrato un migliore mantenimento e passaggio delle hiPSC.

Per il secondo obiettivo del mio progetto, abbiamo testato la capacità complessiva delle iPSC nascenti, che sono state generate subito dopo i 14 giorni di riprogrammazione dell'mRNA, sono state in grado di formare cisti dell'epiblasto 3D e successivamente gli organoidi dai tre strati germinali dell'embrione umano. Abbiamo riscontrato che le iPSC nascenti erano meno metilate rispetto alle linee iPSC ad alto passaggio, il che ha ostacolato l'espressione genica. Inoltre, le iPSC nascenti richiedevano meno cellule (fino a 5000 cellule per letto) per generare una cisti epiblastica 3D su un letto di matrigel. 5000 iPSC nascenti sono state in grado di produrre 1200 cisti di epiblasto 3D, mentre le linee di iPSC ad alto passaggio ne hanno prodotte solo 800. Inoltre, in termini di qualità, le cisti di epiblasti derivate da iPSC nascenti erano omogenee e ad alto tasso di proliferazione, mentre le controparti ad alto passaggio avevano solo la metà delle loro dimensioni (diametro). Gli esperimenti di differenziazione dello strato germinale hanno dimostrato che queste cisti di epiblasti iPSCs nascenti erano in grado di produrre cellule, tessuti primitivi da endoderma, mesoderma e neuroectoderma, un modello ideale per studiare l'embriogenesi umana in vitro. Gli organoidi a maturazione a lungo termine, come gli organoidi del fegato, gli organoidi cardiaci e gli organoidi del prosencefalo, sono stati mantenuti in coltura. Gli esperimenti di caratterizzazione sono in corso.

La riprogrammazione microfluidica dei fibroblasti in organoidi avviene in modo continuo e può essere realizzata entro tre settimane, mentre le linee di iPSCs realizzate richiedono solitamente due o tre mesi. Si tratta di un metodo a basso costo e a risparmio di tempo, che potrebbe essere promosso per lo studio di ampie coorti di pazienti. Oltre a studiare l'embriogenesi umana, gli organoidi nascenti derivati da iPSCs potrebbero essere utilizzati anche nel campo dello studio del fegato, dell'intestino, del polmone, del rene e del cervello, facilitando così la ricerca dettagliata del meccanismo della malattia o della rigenerazione dei tessuti *in vitro*.

Per risolvere il terzo problema, ci siamo orientati verso il sangue periferico come fonte di cellule ematiche per la riprogrammazione, in quanto più facilmente accessibile tramite prelievo venoso. Ci sono stati gentilmente donati dall'ospedale di Padova 40 ml di sangue periferico per iniziare la prima sperimentazione dal sangue alle iPSC. Il sangue intero è stato trattato in primo luogo mediante centrifugazione a gradiente per rimuovere la maggior parte del plasma e degli eritrociti. Lo strato di cellule mononucleate era il nostro target. Sono state piastrate su una fiasca rivestita di collagene di tipo I per garantire l'attaccamento. Durante il processo di generazione delle cellule progenitrici endoteliali (EPC), il cambio del terreno di coltura è stato effettuato rigorosamente tre volte alla settimana, garantendo l'integrazione dei fattori di crescita, un punto cruciale per la mia esperienza nella generazione delle EPC dopo una settimana. Dopo 28 giorni, abbiamo visto apparire la morfologia a ciottoli delle cellule aderenti, che formavano un ammasso. Si trattava di cellule endoteliali ematiche (BOEC). La procedura di riprogrammazione delle BOEC condivideva lo stesso protocollo dei fibroblasti cutanei, ma c'è stato un adattamento graduale del terreno di coltura per bilanciare la sopravvivenza e la transizione delle BOEC, poiché erano più delicate al microambiente all'interno dei microcanali. Dopo soli 12 giorni dalla trasfezione, le iPSC sono emerse chiaramente e sono state mantenute per altri 5 giorni nel terreno IPS-Brew per la stabilizzazione prima dell'estrazione dai chip. Le BOEC-iPSC sono state in grado di differenziarsi in tre cellule dello strato germinale con espressione di marcatori distinti. La caratterizzazione del potenziale di sviluppo degli organoidi 3D è in corso.

In conclusione, il presente lavoro rappresenta un'esplorazione completa e sistematica e l'utilizzo di una riprogrammazione cellulare altamente efficiente in microfluidica. Abbiamo stabilito la riprogrammazione standard dell'mRNA in chip microfluidici per produrre iPSC di alta qualità in modo rapido e a basso costo. Abbiamo poi sviluppato il processo di trasformazione dei fibroblasti in organoidi, poiché i nascenti appena generati non richiedono alcuna espansione supplementare, portando a un protocollo di generazione diretta di cisti dell'epiblasto e successivamente di vari tipi

di organoidi. Inoltre, i nostri modelli di organoidi richiedono solo 5000 cellule per organoide per avviare il processo di differenziazione, il che è di grande utilità per gli studi su larga scala, come i test di tossicità, lo screening di farmaci e la selezione di anticorpi. Abbiamo riprogrammato con successo fibroblasti di pazienti affetti da Alzheimer (~70 anni) e da pazienti affetti da distrofia muscolare di Duchenne in iPSC entro 20 giorni, un risultato considerato difficile da raggiungere con altri sistemi di riprogrammazione. Queste iPSC paziente-specifiche e i successivi organoidi paziente-specifici sono accessibili alla modellazione delle malattie. Tenendo presente l'inconveniente di ottenere fibroblasti cutanei, abbiamo esplorato fonti cellulari alternative per un'applicazione più ampia delle iPSC. Abbiamo dimostrato che l'isolamento delle cellule endoteliali della crescita ematica dal sangue periferico è un modo fattibile per generare organoidi specifici per il paziente, a vantaggio della medicina personalizzata.

Nel quinto capitolo, si riportano le conclusioni e si discutono le potenziali ottimizzazioni e i piani futuri.

Content

Chapter 1 Introduction

1.1 Cell pluripotency

1.1.1 Pluripotent state maintenance

The property of pluripotency was first exposed by Driesch in 1892, when he separated the two cells of an early sea urchin blastocyst and observed the development of two complete sea urchin[1]. The term cell pluripotency has been stressed to a variety of cell types with a wide range of functional capacities. In a broader range of definition, pluripotency means a cell that could generate all cell types from each of the three embryonic germ layers: the endoderm, mesoderm and ectoderm. From a strict point of view, however, pluripotency describes a cell that can give rise to an entire organism, generating every cell type within the organism[2].

Cell potency could be divided into three more specific categories, totipotency, pluripotency and then multipotency. There also exist oligopotency and unipotency, which are not frequently discussed, thus they are excluded in this chapter. Totipotency is the greatest, totipotent cells could form all the cell type in the body, plus the extraembryonic or placental cells. Embryonic cells from the first rounds of cell division after fertilization are totipotent. Pluripotent cells are more familiar to people and are most frequently studies by people. Pluripotent cells could generate all cell types in the body like we mentioned above, embryonic stem cells are considered as pluripotent, which were first isolated by Thomson and his colleagues in 1998. They were isolated from the inner cell mass when the human embryo was at the blastocyst stage[3]. Multipotent refers to a more limited cell potency state, which generate only specific cell types within circulatory system, immune system or other systems of the body.

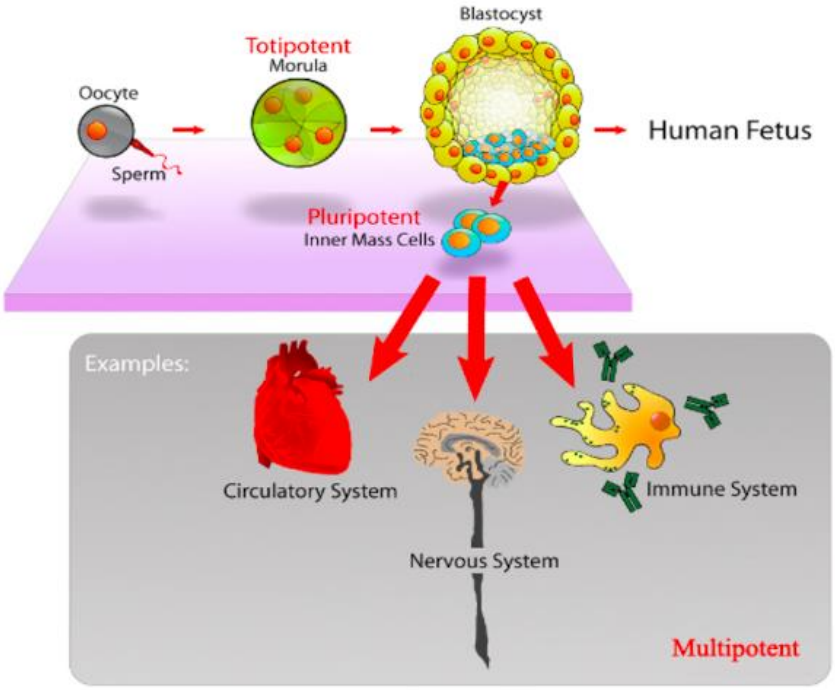

Figure 1.1 The brief classification and relation of cell potency

The cell potency from totipotency to multipotency is descending, which means the cell stemness decreases while the differentiation ability increases, generating only specific cell types in human organism. Even though the ability of pluripotent cells differentiating into various cell types that matters, self-renewal ability is also considered as much as an important and unique aspects of pluripotent cells. However, pluripotency is a transient state *in vivo*. Pluripotent cells, derived from different stages of early embryonic development, must be supplied with exogenous factors to maintain indefinitely passaging once they are cultured *in vitro*[4]. Therefore, it is important to understand that self-renewal is not a defined feature of pluripotency and is only a transient feature during early development[5].

Because of the limited and precious human embryos source for study human embryo development *in vivo*, thus *in vitro* pluripotent cell models are necessary. The first pluripotent cell line was derived in 1976 from a mouse germline tumor[6] , then the isolation of mouse embryonic stem cells (mESC) was achieved in 1981[7]. The first human embryonic stem cell line (hESC) was established in 1998 from the cells of the inner cell mass (ICMs) of a human blastocyst mentioned above.

Compared to the *in vivo* transient pluripotent cell states during development, the establish pluripotent stem cell lines is of great help in presenting different stages of the developing embryo, staying at a relative static state for studies. As the Figure 1.2 shows, mESCs are established from pre-implantation stage ICMs at (E3.5-E4), post-implantation epiblast stem cells (EpiSCs) are established from peri-gastrulating embryo (E4.5–E8.0). The called post-implantation epiblast stem cells (EpiSCs) are meant to distinguish from mESCs that are established from pre-implantation-stage epiblast[8]. For ethical consideration, there is no counterpart of EpiSCs isolated from human embryos. EpiSC lines share some similarities to human ES cells that are established from human blastocysts[3]. For example, growth factor requirements for these cells are basic fibroblast growth factor (bFGF) and activin instead of leukemia inhibitory factor (LIF). The morphology is a flat, two-dimensional colony, with a high ratio between nucleus and cytoplasm, whereas mESCs are dome-shaped, three-dimensionally organized, and the single cells cannot be distinguished from the cell mass. Both human ESC and mouse EpiSCs are delicate when dissociated at the single cell level; they activate the pathway to apoptotic cell death, therefore, Rho-associated kinase (ROCK) inhibitor (ROCKi) is needed to block this pathway, increasing the cell survival rate[9].

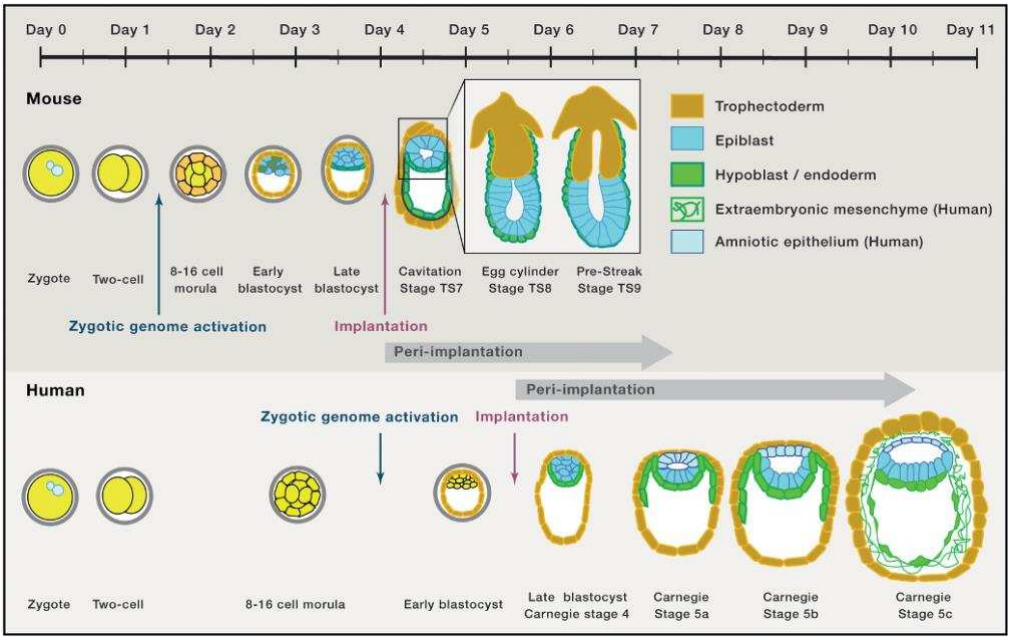

Figure 1.2 Species-specific schedule of developmental events and differences during embryogenesis from pre-implantation to peri-implantation of mouse embryo and human embryo. (Adapted from Janet Rossan, 2016).

In mice, another type of pluripotency-related cell observed in the developing embryo is the germ cell. Germ cells are unipotent cells that normally give rise to sperm or egg. Primordial germ cells (PGCs) in mice first show up as a tiny number of alkaline phosphatase (AP)-positive cells in the posterior proximal epiblasts during the pre-gastrulation stage[10]. Then PGCs migrate until around E12.5 to become mature germ cells. Though PGC itself *in vivo* is not pluripotent but unipotent, these PGCs are found to be the origin of embryonal carcinoma[11].

mESCs forms the dome-like morphology while mouse EpiSCs and hESCs are still in a flat colony shape, which has been given two terms, naïve and primed for these two pluripotent stages. mESCs are in a naïve pluripotent state while the latter two EpiSCs and hESCs are called primed stem cells. At first, primed hESCs need to be cultured on a layer of mitotically inactivated (by mitomycin or γ-irradiation treatment) mouse embryonic fibroblast (MEF) as surrounding feeder layer, but recently many substitution have been developed to replace the MEF layer[12]. Since they are two states of pluripotency, they share some similarities but also there are many differences between naïve and primed pluripotent states, they are summarized in Figure1.3.

	ES/EG cells	EpiSCs
Embryonic stage of origin	E3.5–E4.5(ES)/E8.5–E12.5 (EG)	E5.5–E8.0
Culture condition	2i/2iL	Activin, FGF
Morphology	Dome shape, psuedo-epithelial (no polarity)	Flattened, epithelial
X state in female cells	XaXa	XaXi
Global DNA methylation	Hypo in 2i LIF culture	Hyper
Histon marks	Low to modelate global H3K27me3 marks. Some bivalent (both H3K4 and H3K27 at the same loci)	Moderate to high global H3K27me3 marks. Some bivalent (both H3K4 and H3K27 at the same loci)
Germ line competency	Yes	Not clear
FGF signal	Differentiation	Self renew
LIF signal	Enhance self-renewal	No effect, enhance reprogramming back to naïve cell
Extraembryonic linage potential	Trophectoderm, primitive endoderm (by artificial gene overexpression)	None

Figure1.3 Features of naïve and primed ESCs. (Adapted from Masaki Kinoshita,2015)

1.1.2 Human embryonic stem cells lines

In the year of 1998, James Thomson and colleagues reported the first isolation of human embryonic stem cells from the human blastocyst, and this cell line had kept the pluripotent state in culture more than 4-5 month[3]. The functional definition of embryonic stem cells includes four criteria: 1) origin from a pluripotent cell population;

2) capability of self-renewal indefinitely in the undifferentiated state; 3) capability of maintaining normal karyotype during growth and clonally derived cells capable of differentiation into all three embryonic germ layers *in vitro* or into teratomas *in vivo*[14].

In culture, hESCs appear as tightly packed colonies with distinct borders. Within the colonies, individual cells have a high ratio between nucleus and the cytoplasm. Human stem cell identification and characterization *in vitro* also includes demonstration of a high level of alkaline phosphatase activity and expression of specific embryonic stem cell markers. Transcriptional factors, such as Oct4[15], Nanog[16] and Sox2[17] also the tumor rejection antigens Tra-1-60[18] and Tra-1-81[18] are expressed by pluripotent hESCs. In addition, hESCs are tested negative for stage-specific embryonic antigens SSEA1[19], while tested positive for SSEA3 and SSEA4[20]. Any newly derived hESC lines must pass multiple testing to prove that they are pluripotent. This should also show the ability to differentiate and the positive identification of all three germ layers in teratomas or embryoid bodies (EB) generated *in vitro* or *in vivo*. Also, karyotypic stability during *in vitro* culture is also mandatory.

Usually, the inner cell mass (ICM) of embryos at the blastocyst stage is where human embryonic stem cells formed. These distinct cells have the capacity to constantly divide and can differentiate into each of the three embryonic germ layers. Over a thousand different hESCs lines have been derived worldwide as a result of the development of the original hESC lines. Mechanical dissection[21], micro-surgery[22] and laser dissection[23] have been used to isolate the pluripotent ICM. After the dissection, the pluripotent stem cells are plated and grown to produce the ESC line. Even though the pluripotency of the cells from ICM is transient, but they still have the potentiality to be maintained *in vitro* and stay undifferentiated.

Huge effort from researchers has been carried out and focused on the pluripotent property of these cells to differentiate into the three germ layers and later nearly all the somatic cells. The differentiation ability, which ensures that stem cells have a wide range of potential applications in therapeutic and clinical settings, is the primary research issue in the study of stem cell biology. Human embryonic stem cells can, as

we already know, develop into almost every type of human cell. Apart from the common cell linages differentiation usage of hESCs, there are many established trials of the utilization of them, for example, the earliest embryoid bodies, which expresses markers associated with the development of three germ layers, is an experimental model that researchers are able to produce *in vitro* from hESCs. Despite the biggest obstacle that the isolation and utilization of hESCs face ethical concerns, they are still the foundation of stem cell research and greatly promote the emergency of embryonic stem cell replacement for the potential application of human development modelling and cell therapies.

1.1.3 The discovery of human induced stem cells (hiPSCs)

In 2006, the groundbreaking discovery was made with the report that cells with similarity to mouse embryonic stem cells can be generated from mouse somatic fibroblasts by four factors cocktail. These cells were named induced pluripotent stem cells(iPSCs), and the factors-OCT4, KLF4, SOX2 and C-MYC (OKSM) were called Yamanaka factors[24]. The same result achieved one year later in human fibroblasts[25]. Meanwhile, Yu's group also independently identified four factors-OCT4, SOX2, NANOG, and LIN28 that were able to produce iPSCs from human fibroblast in 2007[26].

These hiPSCs have normal karyotypes, express telomerase activity, express cell surface markers and genes that characterize human ES cells and maintain the developmental potential to differentiate into advanced derivatives of all three primary germ layers. Human iPSC technology, which has evolved rapidly since 2007, has ushered in an exciting new era for the fields of stem cell biology and regenerative medicine, should also be useful in the production of new disease models and in drug development, as well as for applications in transplantation medicine, which have brought great value to biology field and caught the attention of researchers. Since the initial derivation of iPSCs line in 2006, tremendous headway has been made in better understanding stem cell biology the culture requirements for maintenance of pluripotency. The Figure 1.4 briefly summarized the main research on reprogramming

and induced pluripotency. Human iPSCs technology holds great promise for stem cell-based therapy, human disease modelling and drug discovery.

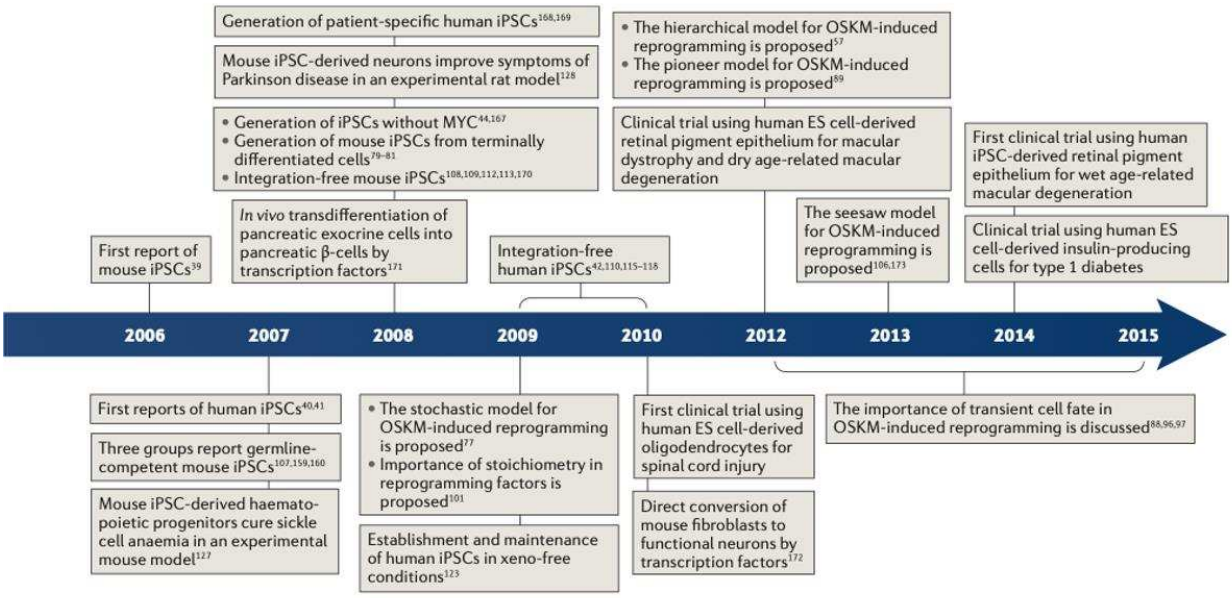

Figure 1.4 The timeline of hiPSCs research from 2006 to 2015(Adapted from Takahashi and Yamanaka 2016).

There are various ways for change cell fate, from somatic cell nuclear transfer (SCNT)[27], cell fusion[28], transduction of OSKM transcription factors to transfections with small molecules. Out of the OKSM factor reprogramming, iPSCs were generated via integrating viral vectors at the beginning, such as retroviral or lentiviral vectors, there was always a concern about the clinical application of these iPSCs owing to the potential for insertional mutagenesis caused by the integration of transgenes into the genome of host cells[29].

In order to make hiPSCs more clinically applicable, various non-integrating methods have been developed to minimize the risk of insertional mutagenesis and genetic alterations associated with retroviral and lentiviral transduction-mediated introduction of reprogramming factors[30]. These non-integrating methods include reprogramming using episomal DNAs[31], adenovirus[32,33], Sendai virus[34], PiggyBac transposons[35], recombinant proteins[36], synthetically modified mRNAs[37], non-modified RNAs[38], microRNAs[39], small molecules[40,41,42]. Table 1.1 has briefly summarized the efficiency comparison between various reprogramming methods.

Table 1.1 Different reprogramming efficiency by different factor delivery method to human fibroblasts

		Reprogramming factors	Cell sources	Reprogramming efficiency (Approximate)	Advantages
	Retroviral transduction	OKSM	Mouse Fibroblasts	0.01%-1%	efficiency reproducible;
	Lentiviral Transduction	OKSM	Human fibroblasts	0.1%-1%	Reasonable efficient;
	Inducible lentiviral	OKSM	Human fibroblasts	0.1%-2%	Appropriate efficient; controlled factors expression
	Adenoviral transduction	OKSM	Mouse Fibroblasts	0.001%	Low frequency of gene integration
	Sendai virus	OKSM	Human fibroblasts	0.1%	No gene integration
	Plasmid DNA transfer	OKS	Fibroblasts	0.001%	No insertion on the genome
	PiggyBac	OKSM	Fibroblasts	0.01%	Accurate gene deletion
	Protein mediated	OKSM	Neonatal fibroblasts	0.001%	No risk of gene modification
	Modified synthetic RNA	OKSM	Human fibroblasts	4.4%	High efficiency;

(Data from Vimal K.S,et al 2015)

According to the Table 1.1, the OKSM factors reprogramming methods could be divided into mainly two approaches: integrating and non-integration. Integrating methods includes the retroviral and lentiviral transfections, which have relative higher efficiency, but also bring genome modifications. Non-integrating methods contain plasmids, proteins, RNAs and small chemical molecules. They are safer in not bring gene mutation, but they need to be optimized to increase the efficiency.

1.1.4 mRNA-based cellular reprogramming

Despite such progress, considerable limitations accompany the non-integrative iPSC generation strategies urge people to move further. For example, In protein-based strategies, the recombinant proteins used are suspected to generate and purify in the quantities required[43]. The DNA-transfection-based methodologies are kind of safe, they also bring some risk of genomic recombination or insertional mutagenesis. Use of Sendai virus requires strict steps to purge reprogrammed cells of replicating virus, and the sensitivity of the viral RNA replicase to transgene sequence content may limit the generality of this reprogramming vehicle[44]. Daley'group has compared some of the non-integrative methods, the Sendai virus (SeV)[34], the episomal (Epi)[45] and the mRNA transfection approaches[46,47]. They compared the success rate of generating iPSCs, defined as the percentage of samples for which at least three hiPSC colonies emerged. the efficiency of iPSCs produce from the same number of fibroblasts plated initially and the workload of generating iPSCs with these three methods, including reagent, media and feeder cell preparations, from initial seeding of the target somatic cells to the picking of iPSC colonies. The results are summarized in Figure1.5.

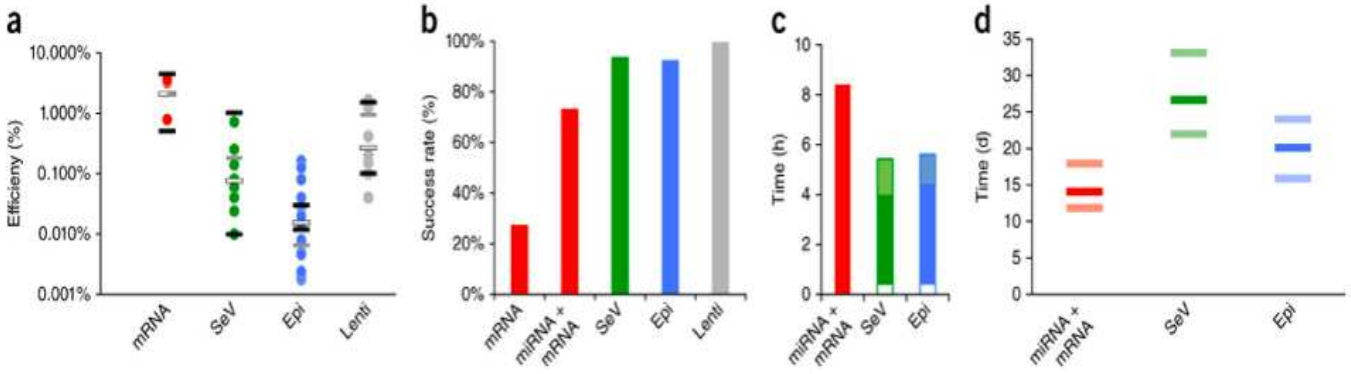

Figure 1.5 Performance comparison of mRNA, SeV and Epi reprogramming methods. (Adapted from Thorsten.M.S, et al, 2014)

Epi (93%) and SeV (94%) methods very reliably generated multiple iPSC colonies. In contrast, with the mRNA method, the success rate was significantly lower (27%). When they used a modified protocol that employed transfection of microRNAs (miRNAs) and mRNAs, the success rate improved significantly to 73% (Figure 1.5b); mRNA-based reprogramming was found to be the most efficient (Fig. 1.5a). The mean

efficiency of successful reprogramming experiments was 2.1% for the mRNA transfection, followed by SeV (0.077%) and Epi (0.013%) reprogramming; Epi reprogramming consumed about 4h, with colonies appearing around day 20. The SeV way demanded the least amount of work, requiring around 3.5h while iPSCs colonies were ready to be picked at day 26, and the miRNA + mRNA method required about 8h, but colonies appeared the earliest at day 14; SeV and Epi reprogramming required pre-test for the loss of reprograming agents and more passages of colonies, which added to the workload[47].

Out of all the OKSM factors reprogramming methods mentioned above, one of the most promising approaches is the use of mRNA, including a synthetic modified mRNA for reprogramming[46,48] by Warren's and Plew's group respectively and the non-modified mRNA by Poleganov's group in 2015[38]. In the first mentioned mRNA way, after the delivery of synthetic mRNA into the cytosol, ribosomes rapidly convert mRNA into proteins, entrance into the nucleus is not necessary. After mRNA is degraded, the production of reprogramming factors stops, and no traces are left behind. Additionally, to enhance the stability and translation of proteins, the synthetic mRNA can be changed during in vitro transcription with a cap structure, poly(A) tail, and modified nucleosides[49]. One of the issues is that prior research has demonstrated the ability to integrate modified nucleosides, such as pseudouridine (Pseudo-UTP) and 5-methylcytidine (5mCTP), into synthetic mRNA to replace cytidine and uridine and so suppress the innate immune response[49]. The activation of an innate immune response after many daily mRNA transfections, which causes increasing cellular stress and severe cytotoxicity, is still one of the major challenges. Therefore, the interferon inhibitor B18R produced from vaccinia virus must be present in the reprogramming medium to avoid interferon-response driven cell death, which is the one of the main improvements that done by Poleganov's group. They coupled immune evasion mRNAs (E3, K3, and B18R [EKB]) from the vaccinia virus with non-modified reprogramming mRNAs (OKSM, NANOG, and LIN28 [OSKMNL]) and the incorporated mature,

double-stranded microRNAs (miRNAs) from the 302/367 cluster, which are known to improve the reprogramming procedure.

In conclusion, the inconvenience and limited resource of hESCs have encouraged the rapid development on hiPSCs. For more than 15 years, various of reprogramming methods have been fully explored, to reach the overall goal that iPSCs could be clinical applied and patients-friendly, with the hope that hiPSCs could be used for disease modeling, cell therapy, drug screening and personalized medicine.

1.2 Microfabrication in biology

1.2.1 Microtechnology and microfabrication

In every area of research, the introduction of new tools increases feasibility. Biology research is starting to be affected by micro-technology, which is the manufacturing and utilization of materials, structures, and systems with features at the micron or even submicron scale. The design and handling size of micro-technology is well matching to physical dimensions of most microorganisms, and micron-scale tools make it possible to manipulate among individual cells, their immediate extracellular environments, which usually referred to as the microenvironment, and also their shape and more deep, the interaction and communication between cells[50]. The microenvironment refers to the region that could be sensed and monitored by a cell via molecular contact, mass transport and diffusion, and the dimensions could range from a few nanometers to perhaps a millimeter. Microfabrication builds up the bridge between the micro-scale precisely handling and microorganisms research like we mentioned at the beginning. The intersection of microfabrication and biology, with a focus on soft lithography, is particularly well suited for generating microscale or nanoscale structures in soft materials[51].

Soft lithography uses a polymeric substrate and/or an elastomeric stamp or mold with a pattern to print, mold, and emboss microstructures[51], which was created as an alternative to photolithography and electron-beam lithography. It has been employed

more frequently in cell biology due to their ease of use, low cost, and compatibility with cells. In particular, soft lithography offers the capacity to regulate the molecular structure of surfaces and pattern the complex molecules crucial to biology, to construct channels structures that are appropriate for microfluidics, and to pattern and manipulate cells[52].

There are various types of elastic polymers that have been tested in soft lithography, Polydimethylsiloxane (PDMS) and other siloxane-based polymers are widely used[52]. PDMS is non-toxic and commercially available. The main features of PDMS are they are optical transparent and moderately stiff elastomer, although it is quite hydrophobic, but a quick plasma treatment could make it hydrophilic[53]. The lateral dimensions of PDMS ranges between 1–1000μm and vertical dimensions between 100nm and hundreds of microns. Detailed steps of fabricating the PDMS are summarized in Figure 1.6.

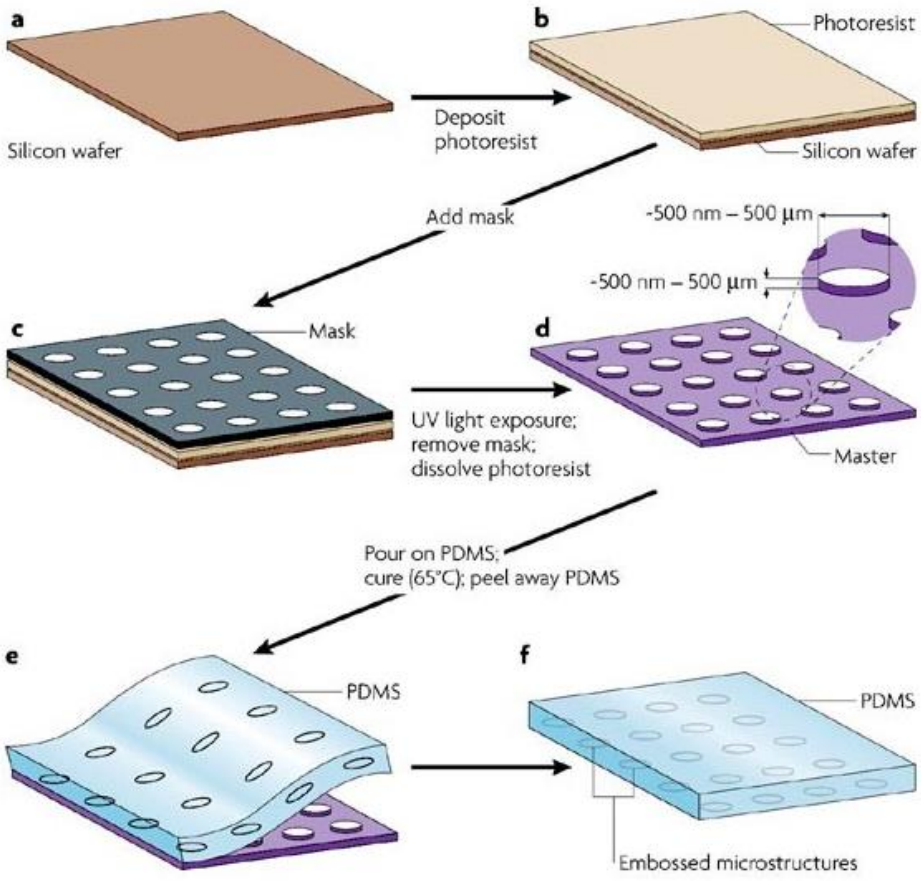

Figure 1.6 The key production of PDMS in microfabrication. (Adapted from Douglas W.B, et al, 2016)

The silicon master is produced using photolithography[54]. A layer of photoresist material is spinning-coated evenly over the silicon water, then your targeted pattern mask, designed by using a CAD (computer-aided design) tool, touches the photoresist layer. Pattern mask is printed on a high-resolution photoplotter with transparency (a sheet of transparent polymer). Through the mask, ultraviolet (UV) light illuminates the photoresist, transferring your pattern from the mask to the photoresist material. The photoresist solution was crosslinked by the UV light and became rigid. The residual non-crosslinked photoresist can be removed and dissolved later using an organic solvent, leaving behind the bas-relief structure in the polymer layer. The master copy, or simply the master, is a silicon wafer having polymeric photoresist structures etched on its surface by pouring the PDMS solution over it. Through heating at 65-100 ℃ for more than 30 minutes, then the pre-ready PDMS layer could be peeled away from the photoresist mask. The thickness of the photoresist layer initially applied to the silicon wafer's surface determines the polymer structure's height, it can be calculated from the spinning-coating machine, which affected by the acceleration speed and the time, while the mask determines its shape and lateral dimensions. Later silicon and photoresist masks can be recycled and reused many times.

PDMS replica molds are transparent to ultraviolet and visible light, flexible, biocompatible, insulating, soft, and unreactive, so they have been widely utilized for soft lithography applications in biology in general.

In many situations, the entire procedure takes less than twelve hours, from a CAD design to a finished microfabricated structure in PDMS, as we could see that thermally heating of PDMS solution fastens the cooking process. The resulting patterned layers of PDMS can be utilized as masters to replicate the structure in another material. There are many biological applications of utilizing PDMS, the microfluidics[55], the micromolding in capillary[56], the microcontact printing[57], microtransfer molding[58], and so on, they are shown in the following Figure1.7. Using a patterned PDMS stamp, designs are transferred to the surface of a substrate by microcontact printing as

Figure1.7(b) shows. “Micromolding in capillaries” creates a network of microchannels, which involves placing a layer of PDMS that has been printed in contact with a surface. When the PDMS layer is in conformal contact with a solid substrate, like a glass slide, liquid prepolymer is added to the PDMS layer's edge, capillary action draws the prepolymer into the channels, where it is then cured to form solid structures. On the substrate surface, a pattern of micropatterned material is left after carefully peeling the stamp away. Fabricating microfluidics is one of the most frequent usage of PDMS. A glass surface that serves as the floor of the channel and a layer of PDMS with channels etched on it are brought into contact to create microfluidic channels, as the Figure 1.7(e) describes.

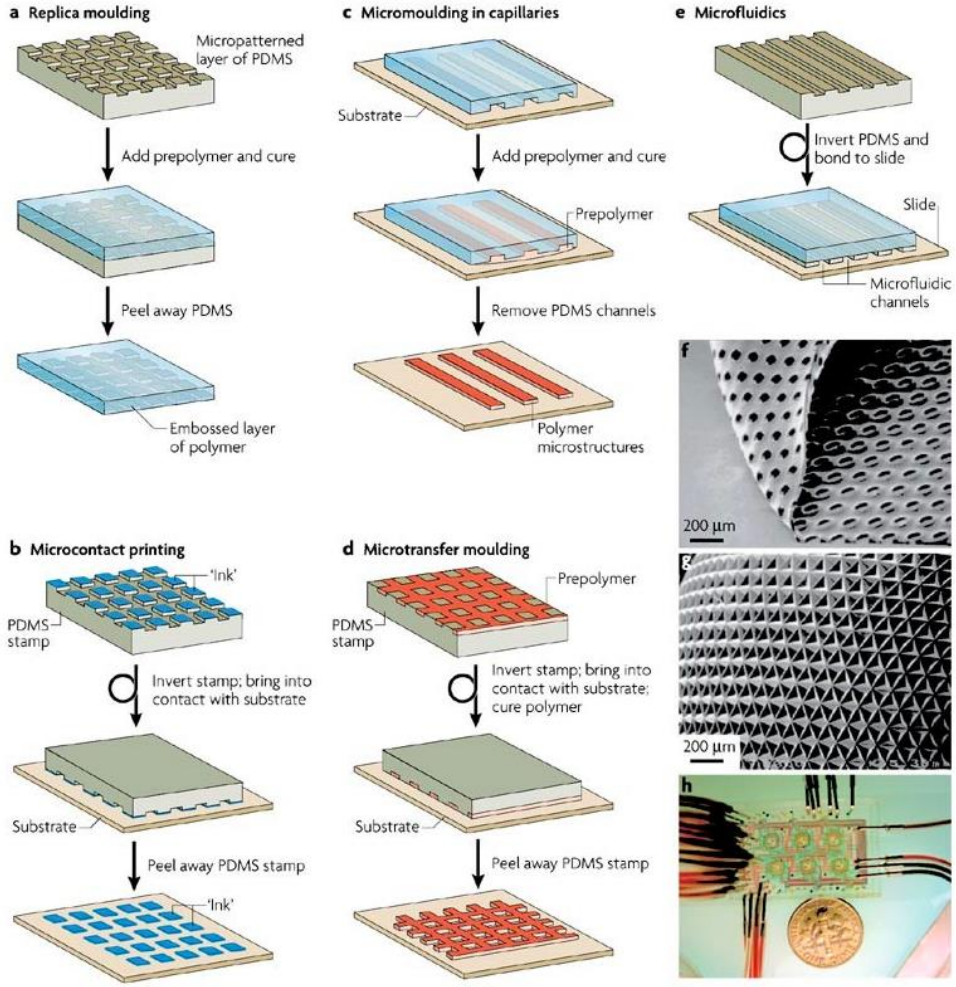

Figure 1.7 The main techniques for soft lithography. (Adapted from Douglas W.B, et al, 2016)

There are many devices made from microfabrication available and is of great importance in biology research field. Microfabrication under the help of soft

lithography has offered new possibility and feasibility in precisely manipulating and observing cell behaviors under micron or submicron scale, which helps people understand better how cells behave in physiological environments *in vivo*. They also allow us to design and modulate the microenvironment to investigate how cells and the surrounding environment affect each other.

1.2.2 How microfluidics utilized in biology

We move the focus of microfabrication to microfluidics. Microfluidic devices refer to the channels with sizes ranging from tens to hundreds of micrometers to process or manipulate small (10^{-6} to 10^{-12} liter) volumes of fluid. As devices get smaller, their surface-to-volume ratios rise, and their surface qualities play a bigger role in determining how well they work. Initially, microfluidics has an impact on fields including microelectronics, integrated circuit industry, information technology, optical synthesis (Figure 1.8). The development of the transistor marked the beginning of microfluidics and the growth of 3D printed devices. Cell biology is an area of research into which microfluidic systems bring a new capability as mentioned before[59].

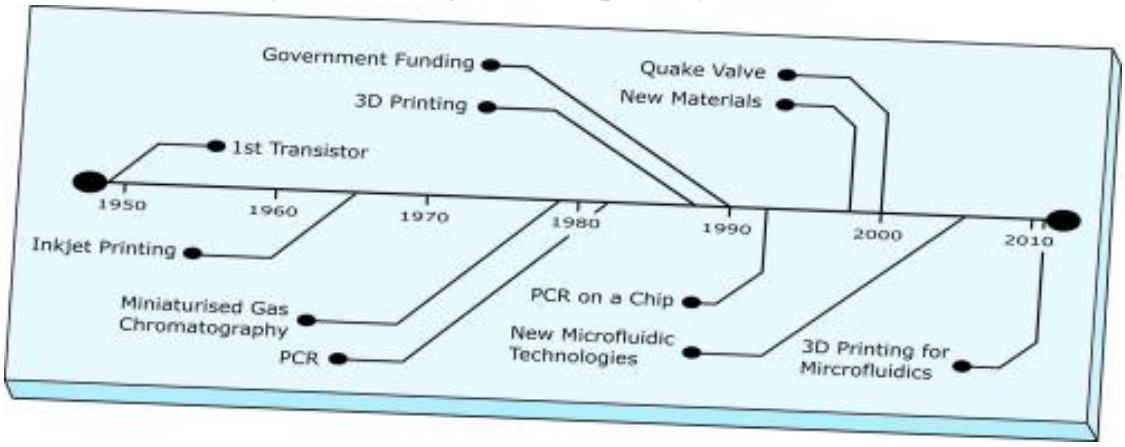

Figure 1.8 Timeline highlighting the main advances in the field of microfluidics(Adapted from Neil C,et al, 2019)

"Organ-on-chip" is a system that is combined with the biology and microtechnology, which is filling up with cells, or either natural or engineered small tissues that are grown inside microfluidic chips. The chips are made to regulate cell microenvironments and keep up tissue-specific functions in order to more closely

replicate human physiology[60]. An organ-on-chip device (Figure 1.9) basically has to contain the following criteria: 1) the flow and exchange of fluid, which means the fluid inlet, outlet and the flowing channels, and the reasonable ratio between the surface and the volume; 2) Geometrical confinement and patterning, which means cells could be co-cultured spatially and morphology and phenotypes will change correspondingly due to the confined environment;3) External control, this means oxygen, carbon dioxide, pH, nutrition, and growth factors could be add or remove manually, as well as the presence endogenous toxins. mechanical stimulation or electrical stimulation could be applied according to the experiments aim[61].

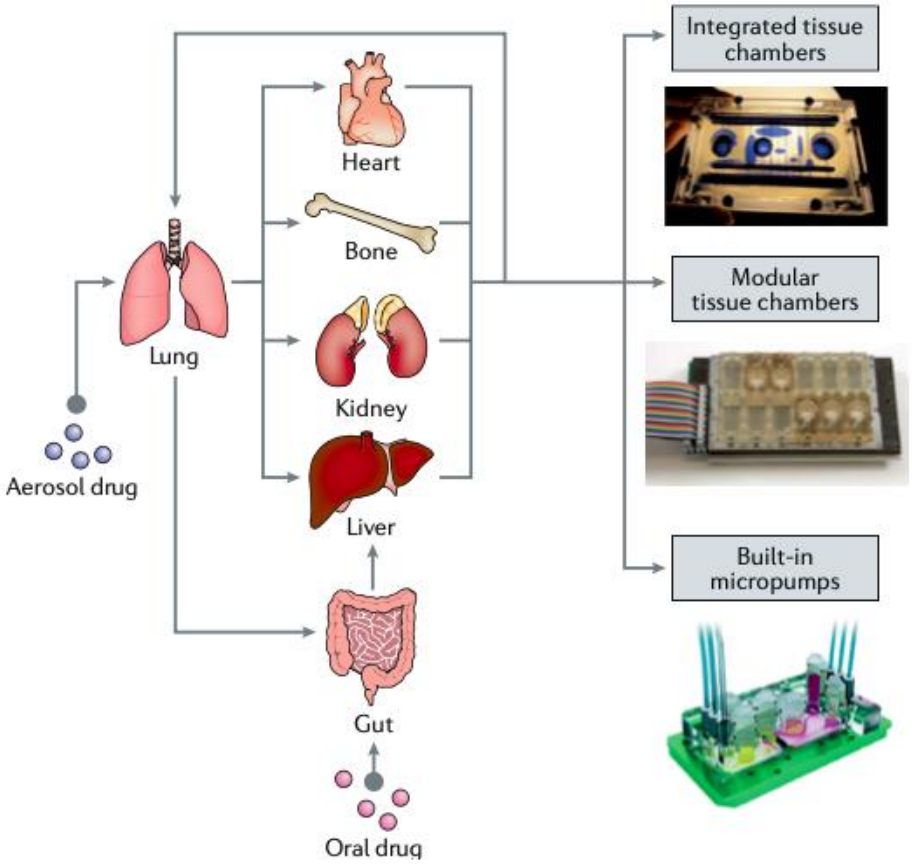

Figure 1.9 Organ-on-chip device. (Adapted from Boyang Z, et, al 2018)

Organ-on-a-chip technologies simulate the fundamental operation of an organ's tissue. Single organ-on-a-chip allows to investigate the basic principle and cellular mechanism inside one specific organs, for example, like observing how the lung change the air with the external environment and how the liver biodegrades the alcohol once people drink wine. Moreover, the multi organ-on-chip, with more complex units inserted and modulated inside a single chip, more complicated actions between organs

could be investigated, mimicking the real situation in human bodies. Also, organ-on-chip can be used the test the potency of some drugs, which is another important application.

Our lab, since 2015, has been working on integrating microfluidics into the cellular reprogramming process, to be more specific, to understand how the confined microfluidic environment could affect the reprogramming efficiency, the pluripotency induction, the genome trajectory, the cell populations, the iPSCs differentiation ability and other aspects. We designed an microfluidic platform with the channel height only has 200μm, ensuring the accumulation of endogenous factors[62]. We demonstrated that downscaling mRNA reprogramming to microliter quantities produces an environment that is conducive to the development of pluripotency. We discovered that a confined cell microenvironment significantly affects self-regulated autocrine and paracrine signaling[63]. Over 120 hiPSC colonies were produced on average from 100 seeded cells from our microfluidic chips, with only 14 days of daily mRNA transfections. Also there hiPSCs have been successfully differentiated into cells from three germ layers[64]. In 2019, we have optimized the whole microfluidics-based reprogramming system[65].

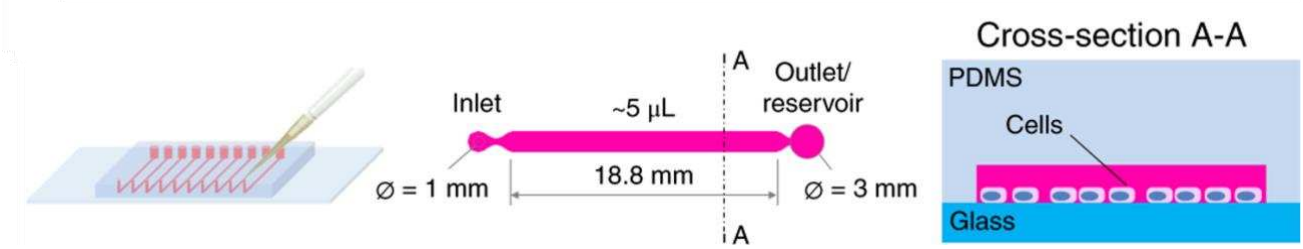

Figure 1.10 Schematic representation 10-channel microfluidic chips developed in the lab.

The inlet is 1mm in diameter meant for the medium injection and the reservoir is 3mm in diameter to store the consumed medium and secretion factors produced by the cells, also the big volume of medium could efficiently prevent the evaporation inside the channel. The bottom layer of a chips is made by glass that has been coated before with extracellular components, like vitronectin, fibronectin or other collagens. Cells (usually skin fibroblasts) are seeded via cell suspension injection, and later cells would attach to the bottom glass because of the coating. The quality of coating highly influences the percentage of cell attachment, which is a key factor whether the reprogramming would succeed or not. Then the daily mRNA transfection is conducted

by the same way. A cautions visual check of the cell status is recommended because then the dose of RNA could be adjust according to the how cells react the toxic transfection. mRNA reagent is mixed with the base medium and injected from the inlet, then the next morning, by medium changing, they are all removed from the outlet, this is how our homemade microfluidic reprogramming system work.

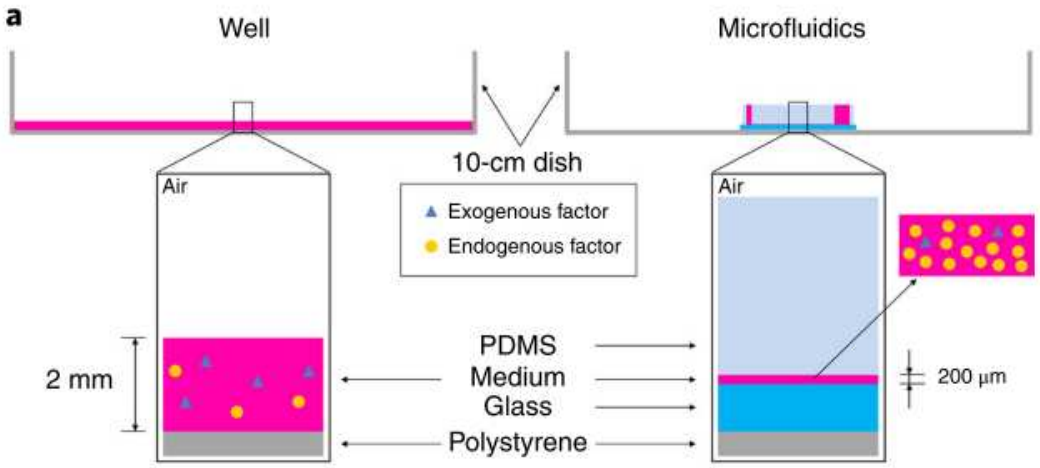

Figure 1.11 Comparison between conventional multi-well plate and downscaled micro-channel.

From the Figure1.11 showed, we could see clearly that the endogenous factors have been highly accumulated inside the micro-channel, which corresponded with our previous work that we found limited cell microenvironment has a significant impact on self-regulated autocrine and paracrine signaling when mRNA reprogramming is scaled down[63].

This protocol makes use of the benefits of mRNA, which can be cleaned quickly due to the 24-hour lifespan in conventional systems. In microfluidic chips, a large number of hiPSC colonies are produced per culture chamber after only 15 days of reprogramming (up to 160±20 mean ±s.d. (n = 48)). Once removed from the setup, these colonies can be utilized in other ways. Besides, comparing the protocol we apply here to that in our initial publication[64], it has been improved. B18R protein was combined added in the transfection to reduce the interferon response.

In conclusion, there are numerous applications for microfluidic reprogramming. After adjusting the parameters to perfection, there are not any significant restrictions on downscaling other reprogramming techniques to the microfluidic system. Moreover,

considering that the viability of producing customized mRNAs in standard biological laboratories, the combination of microfluidic and mRNA technologies also offers tremendous flexibility for additional applications.

1.3 Human embryonic development

1.3.1 Human embryonic development

Embryo is an early stage of animals. Human embryonic development or human embryogenesis, starting from the totipotent zygote, proceeds to develop four days later a continuous manner. It starts out as cell mass and gradually develops into the fetus, an obvious human shape. Human embryogenesis defined as a series of early developmental processes that involve the embryonic cell division and cellular differentiation[66]. They are summarized in Figure 1.12.

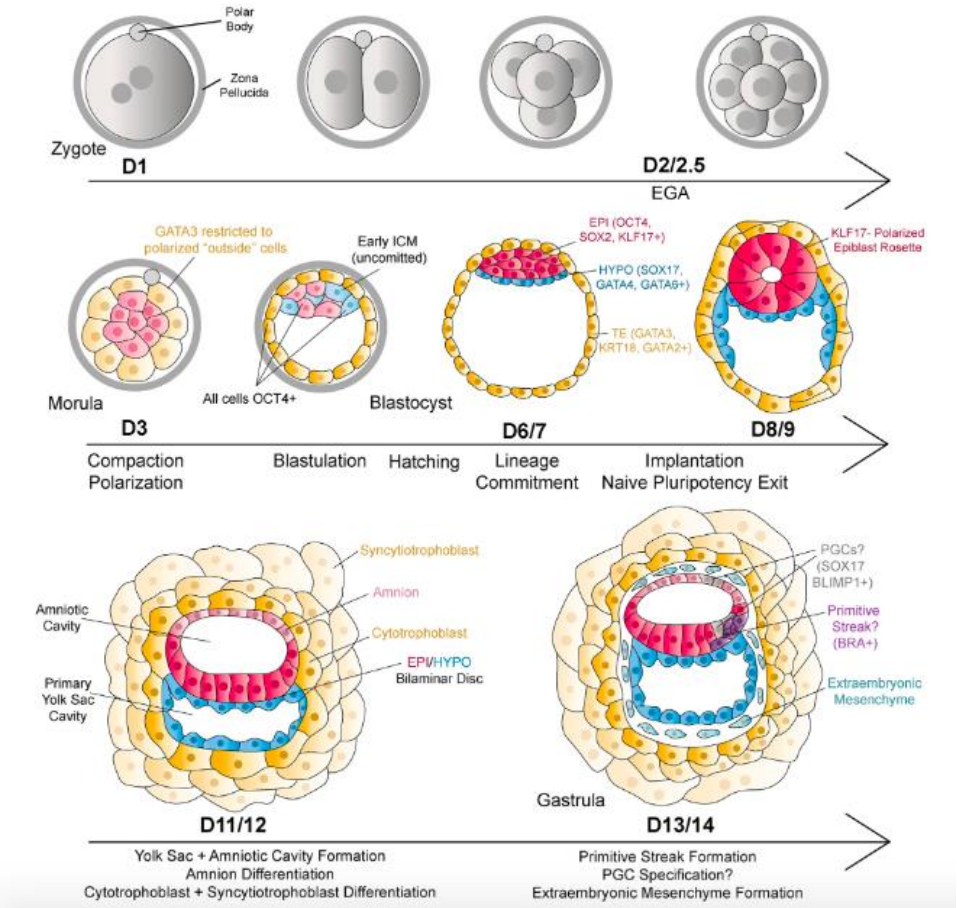

Figure 1.12 The initial two weeks after fertilization in human embryogenesis (Adapted from Bailey A.T, et al, 2021)

The zygote starts off as a single cell in the oviduct and develops into a compact cell mass called a morula, which is made up of 16cells, after undergoing a series of mitotic divisions during the first three days of pregnancy. The embryo has entered the uterus by the morula stage. The 32-cell morula cell mass develops into a blastocyst, which is structured as a hollow sphere made up of an exterior layer called the trophoblast and an inner group of cells termed the inner cell mass. This morula stage is characterized by the onset of fluid production and cell self-organization, and it is feasible to see a difference in gene expression between the cells in the inner cell mass and the cells on its surface, for example, inner cell mass is all Oct4 positive, while the surface cells are Gata3 expressed. The cell division from 16-32 cells morula to blastocyst represents the end of embryo totipotency, which means that the cells of the trophoblast will become the fetal portion of the placenta, while the cells residing in the inner cell mass will give rise to all body tissues and therefore, they are regarded as pluripotent.

By the first week of gestation, the embryo implants in the uterine wall following the blastocyst formation. It is a remarkable stage because pre-implantation and post-implantation embryogenesis are separated here by the embryo implantation.

After the implantation, the inner cell mass differentiates into the epiblast and hypoblast, two layers that form the bilaminar disc, which separates the blastocyst into two cavities. The extraembryonic yolk sac will develop from the cavity on the hypoblast side, while the amniotic cavity will develop from the cavity on the epiblast side, to enclose the developing fetus[67].

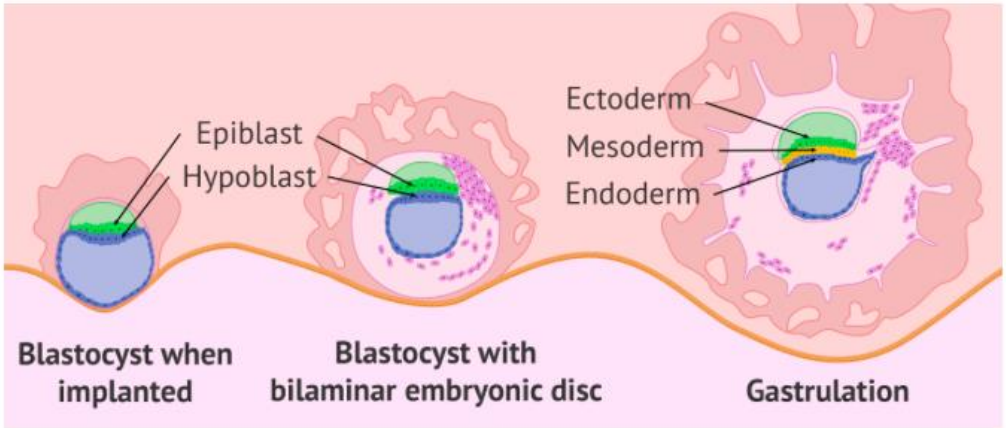

Figure 1.13 Implantation and gastrulation stage of embryogenesis (Miguel Barea, et al, 2019)

The epiblast exits its pluripotency condition and migrate to a primitive streak during the third week of gestation, developing into three germ layers, the ectoderm, the mesoderm, the endoderm and the ectoderm, which is also known as the gastrulation. Three germ layers are all regarded as multipotent due to the fact they can differentiate into a variety of tissues.

The primitive streak is a transient structure, which marks the beginning of gastrulation at day 14 of human development[68], when epiclastic cells divide and proliferate rapidly, so they need to migrate to new locations and take up more space in the embryo. Cells from the epiblast migrate into the interior of the embryo via the primitive streak, in a process termed ingression, which involves a cellular epithelial-to-mesenchymal transition (EMT). The initial wave of migrating cells streams through the primitive streak, replacing the hypoblast cells to become definitive endoderm, which ultimately produces the future gut derivatives. Then the mesoderm layer is created when the migrating cells fill up the space between the epiblast and the definitive endoderm. The intraembryonic mesoderm cells eventually give rise to five cell subpopulations, the paraxial mesoderm, the intermediate mesoderm, the lateral plate mesoderm, the cardiogenic mesoderm and a population known as the notochordal process, which forms a midline tube[68]. The notochordal process develops from the primitive node and is the progenitor of the flattened notochordal plate, which, after separating from the endoderm, merges the free edges together to create a rod known as the notochord[69]. The upper side of epiblast cells stop migrating and start to form the ectoderm. The surface ectoderm and the neural ectoderm are two different lineages that develop from the ectoderm[70].

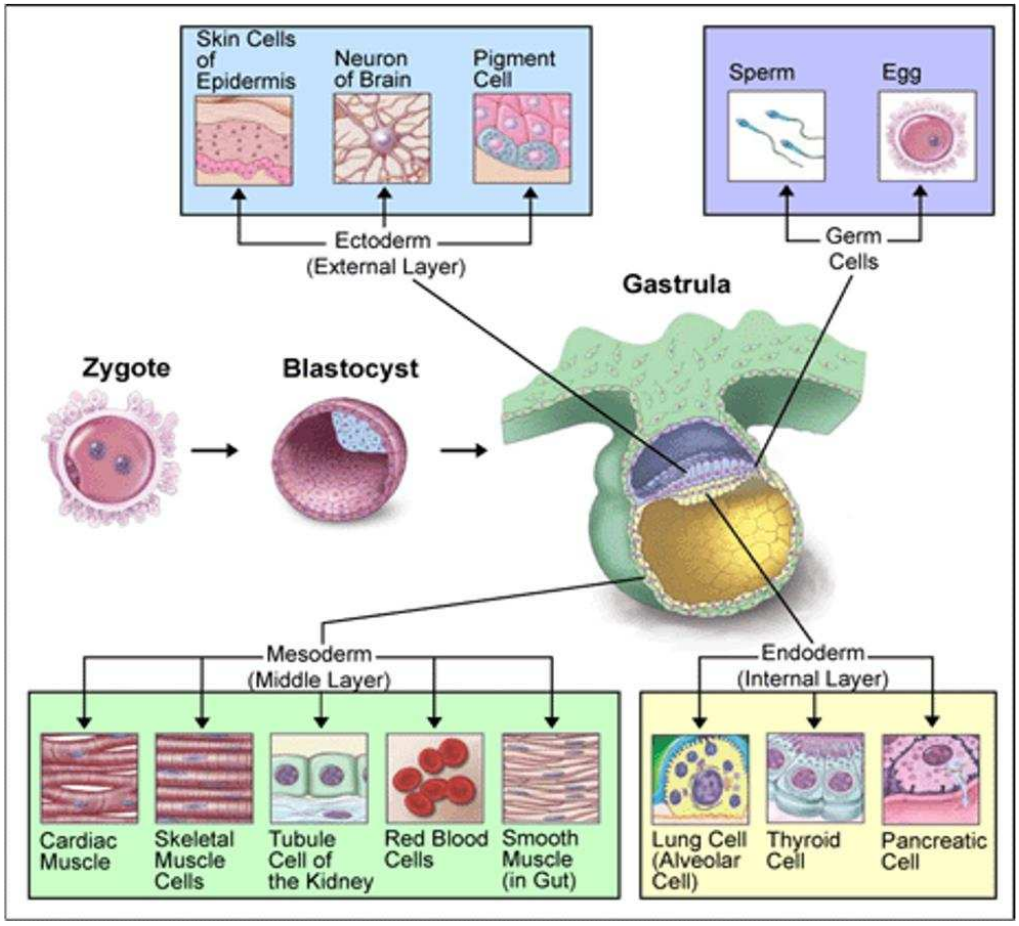

Figure1.14 The germ layer derivative cells, tissues and organs. (Adapted from Wikipedia)

Each germ layer derives various types of cells, tissues and organs. For example, ectoderm includes brain, skin, cord and peripheral nervous system. Muscle, bone and circulatory system, connective tissue belong to mesoderm, while endoderm give rise to bladder, pancreas lung, stomach and liver. They are summarized in Figure 1.14. Organogenesis starts after the gastrulation, which organs from different germ layer before to form[71].

There are debates on when an embryo could be considered as a real human, thus, to prohibit the human embryo research *in vivo*. Some opinions insist that the emergence primitive streak is the crucial moment, which marks the beginning of the individual development of the embryo[72], especially the neurological development, so the research must be prohibited before this time, in order to guarantee that there is no embryo suffering[73]. Thus we have the "14-days" rule for human embryo research. However, the scientific developments in embryo culture suggest that sustaining human embryos

*in vitro fo*r as long as 14 days may be theoretically possible[74], which move forward the human embryonic development research *in vitro* despite all the difficulties.

1.3.2 Organoid in a dish

One of the greatest advantages of human pluripotent stem cells(hPSCs), including the embryonic stem cell (ESCs) and later the discovery of induced pluripotent stem cells (iPSCs), is that they harbor the potential to differentiate into hundreds of cell type, while it is also a challenge to exclusively differentiate hPSCs into a single desired cell type. Many differentiation protocols *in vitro* are focus on microenvironment simulation; however, it is still unclear how many and what kinds of intermediate steps a pluripotent cell goes through in order to differentiate into a particular cell type *in vivo*. As a result, throughout the past few decades, the study of stem cell differentiation has made inconsistent progress. The intended lineage frequently makes up a portion of the entire population, and the majority of differentiation techniques provide a variety of lineage results[75]. The differentiation efficiency between individual hPSCs lines have been found to varied significantly with suboptimal differentiation methods[76]. On the contrary, instead of avoiding generating heterogenous cell population, the new discovery of organoid utilizes this disadvantage to investigate cell behavior and communication in the process of cell linage in a real cellular microenvironment, which assists in solving some biological problems, like the cell-cell interaction, cell-environment communication, dynamic development and so on.

Organoids, which are often known as "mini-organs," are cell clusters that self-organize and differentiate into functional cell types *in vitro* to mimic the shape and function of an organ *in vivo*[77]. They grow in a pre-determined three-dimensional (3D) environment. Organoids can be produced from embryonic stem cells, induced pluripotent stem cells, neonatal or adult stem cells[70] (Figure 1.15). Through spatially constrained lineage commitment and cell sorting, which are mediated by intrinsic

cellular components or extrinsic environments like the extracellular matrix (ECM) and media, self-organization takes place within the organoid[78].

Organoids produced using this method frequently recapitulate organogenesis, developing from immature tissues into organotypic cultures that resemble their fetal counterparts (Figure 1.15). Organoid cultures can be produced from adult tissue using either purified single cells, such as Lgr5+ stem cells[79], or minced tissue fragments, for example, the intestinal crypts. In the presence of niche factors, single cells are, instead, directly embedded into matrigel to produce epithelial organoid cultures, they are without a cellular niche. Before generating epithelial and mesenchymal organoid cultures using matrigel, minced tissue fragments are typically transferred to create spheroid cultures similar to those described above. By using this method, organoids with completely differentiated cell types are produced, which is most closely resemble the adult original organs[80]. 3D cell system in suspension culture avoids the direct physical contact to a plastic dish. Scaffolding or approaches without scaffolding can be used to accomplish this. Scaffolds are hydrogels that are either biological or synthetic and resemble the extracellular matrix (ECM) in nature. Matrigel, a heterogeneous and gelatinous protein mixture released by Engelbreth-Holm-Swarm (EHS) mouse sarcoma cells, is the one that is most frequently utilized nowadays[81].

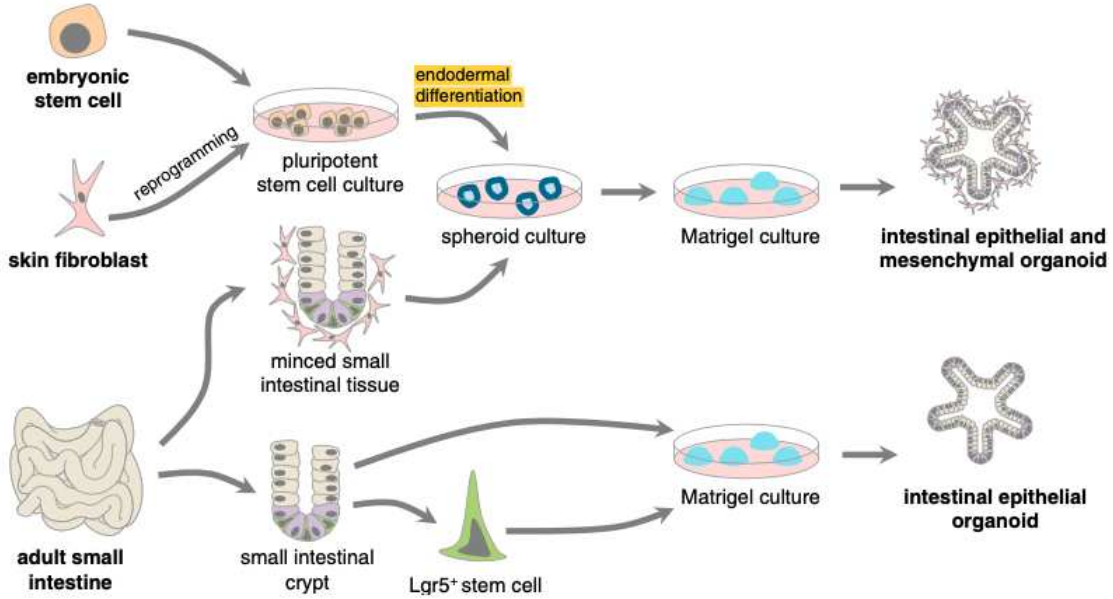

Figure1.15 Organoid cultures are generated from embryonic pluripotent stem cells, induced pluripotent stem cells, adult stem cells or tissue pieces. (Adapted from Kai K, et al, 2016)

Matrigel is mainly composed of adhesive proteins, like collagen, entactin, laminin and heparin sulfate proteoglycans that resemble the extracellular environment, that can give support and signals to the cells. Along with the timeline of organoids development, in 1907, Wilson HV's group initially attempted to regenerate an organism in a dish, demonstrating that separated sponge cells can self-organize to create a new creature. Then later Paul Weiss conducted dissociation-reaggregation procedures[82] to create various organ types from dissociated chick embryos. The isolation of human embryonic stem cells in 1998 and later the breakthrough discovery of human induced pluripotent stem cells thrives the organoids research. In 2008, when Eiraku M and her colleagues used the 3D aggregation culture technique to produce cerebral cortex tissue from human embryonic stem cells[83], the field of organoid research started to transition from 2D to 3D. The first report on creating a 3D organoid culture from a single adult stem cells was conducted in 2009 by Clever Hans group in Netherlands[79]. This landmark work demonstrated that in the absence of a mesenchymal niche, adult intestinal stem cells expressing the single leucine-rich repeat-containing G protein-coupled receptor 5(Lgr5) may create 3D intestinal organoids in matrigel that develop into crypt-villus[79], which provided the foundation for numerous subsequent organoid works in other systems, like the mesoderm (i.e. liver, lung and kidney) and neuroectoderm(i.e. retina and brain) using adult stem cells or iPSCs.

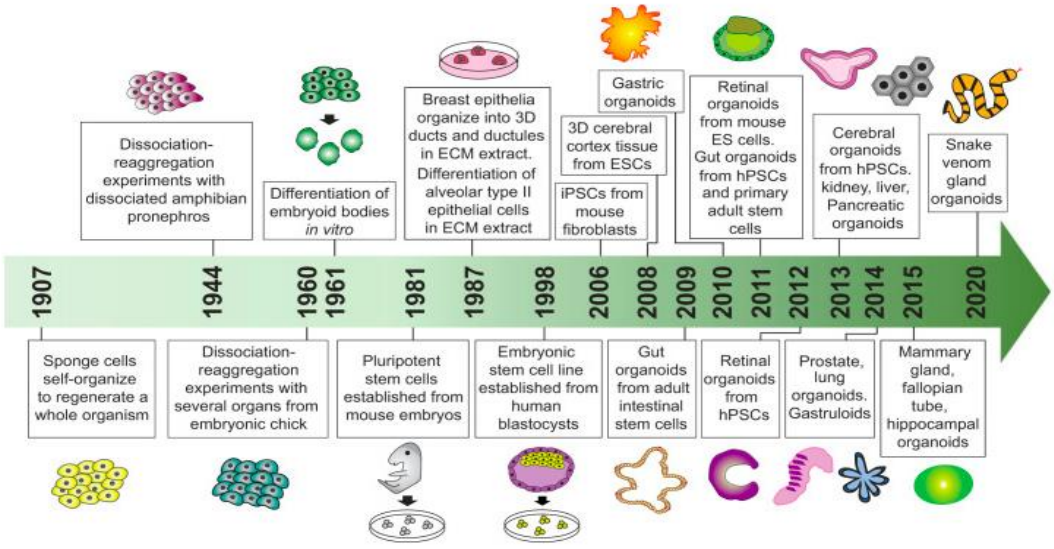

Figure1.16. Timeline for the development of organoid cultures. A summary of key landmark studies and breakthroughs leading to the establishment of various organoid technologies. (Adapted from Claudia C, et al, 2020)

As Table 1.2 shows, the 2D monolayer cell culture and animal models have many disadvantages. 2D cell system could not mimic the dynamic cell microenvironment in *vivo*, lack of cell-cell communication and cell-matrix interaction, while the extracellular matrix plays a very important role not only in mechanical support, but also cell signals transduction.

Table 1.2 Disadvantages of 2D cell culture and animal model systems.

Systems	Disadvantages
2D cell monolayer	Cells lose their phenotype; Lack cell communication and cell-matrix interaction; it could not mimic cellular functions and signaling pathways as in vivo conditions.
Animal model	High cot; difference between animals and human; Limited feasibility in imaging and high-throughput studies.

On the other hand, animal models are at high cost. They are not able to receive timely feedback because of the long time period. What is more important is that there exist species difference between rodent animals and human, even between other primates and human. Any mechanism could not be 100 percent promoted from animal models to human. The limited availability of animal models at the same time is as well as obstacle for high-throughput utilization, like drug screening or antibodies screening. 3D organoids address the limitations of existing model systems by providing self-organize into organotypic structures compare to the 2D cell culture system. They are capable of self-renewal, self-organization and exhibit organ functionality. Organoids can differentiate into cells of all major cell lineages, with similar frequency as in physiological condition. Besides, organoids are more biologically relevant to any animal model system and are amenable to manipulate niche components and gene sequence. Last but not least, organoids can be cryopreserved as biobanks and expanded indefinitely by leveraging self-renewal, differentiation capability of stem cell and intrinsic ability to self-organize.

In all scenarios, self-organization and differentiation ability are the two main aspects of organoids formation, also, they are the results of the instructive signaling cues that given by the base medium, the extracellular matrix, the 3D structure itself once the organoids formed[84].

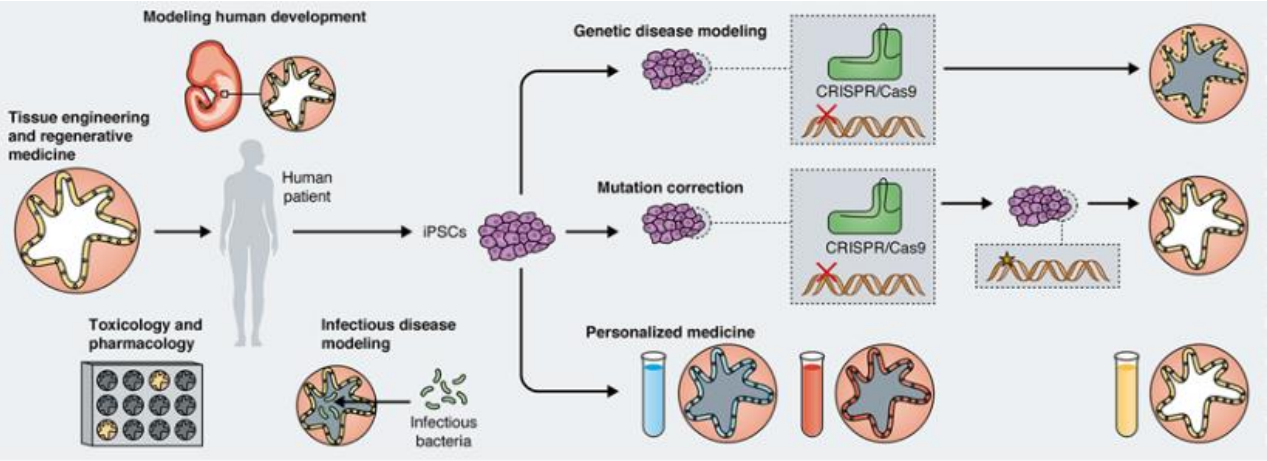

Figure 1.17 Various biomedical applications of organoids. (Adapted from Heather A, et al, 2017)

There are enormous opportunity arising from the organoids field. For example, the diseases modeling. As we know, it is quite challenging to simulate some human diseases in animals, such as those that influence human brain development. Transcriptome analysis of organoids made from the iPSCs of autistic patients revealed that these individuals have excessive GABAergic inhibitory neuron production[85]. The group of Paula C. has used the 3D organoids as a model to study idiopathic form of Parkinson's disease[86]. Also, in 2015, Lancaster's research on neural organoids from people who had loss-of-function mutations in the CDK5RAP2 gene that caused microcephaly demonstrated that inactive CDK5RAP2 caused early neural differentiation, which in turn caused brain hypoplasia[87]. Another important application of organoids is that they are widely used in investigating human development models. For example, studying on human organoids has found that inhibiting bone morphogenetic protein (BMP) signaling is an vital step in specifying human posterior foregut endoderm and for stomach formation[88]. As the Figure 1.17 shows, apart from diseasing modeling and human development investigation, there are bunches of applications of organoids in biomedical field. Organoids allow for a high throughput

drug discovery and screening[89], CRISPR gene editing in kidney organoids to mimic kidney disease[90] and regenerative medicine research[91].

1.4 Alternative cell source for cellular reprograming

1.4.1 Peripheral blood plays an important role in human health

Peripheral blood is the flowing, circulating blood of the body. It is composed of leukocytes, erythrocytes and thrombocytes. These blood cells are suspended in blood plasma, which allows the blood cells to travel throughout the body. But the blood that circulates inside organs including the liver, spleen, bone marrow, and the lymphatic system differs from peripheral blood. These regions have their own distinct blood cell types.

All body organs and systems receive nutrition from peripheral blood circulation. Because peripheral blood transports cellular waste from cells to the excretory system, it also contributes significantly to excretion. Peripheral blood also plays a crucial role in the body's general immune system since it can eliminate or stop infections from settling in various parts of the body. Peripheral blood also improves immunity because of the defense mechanisms it transports to sickness or infection sites. After consumption, peripheral blood can carry more water and oxygen, which contributes to the body's continued disease-purification.

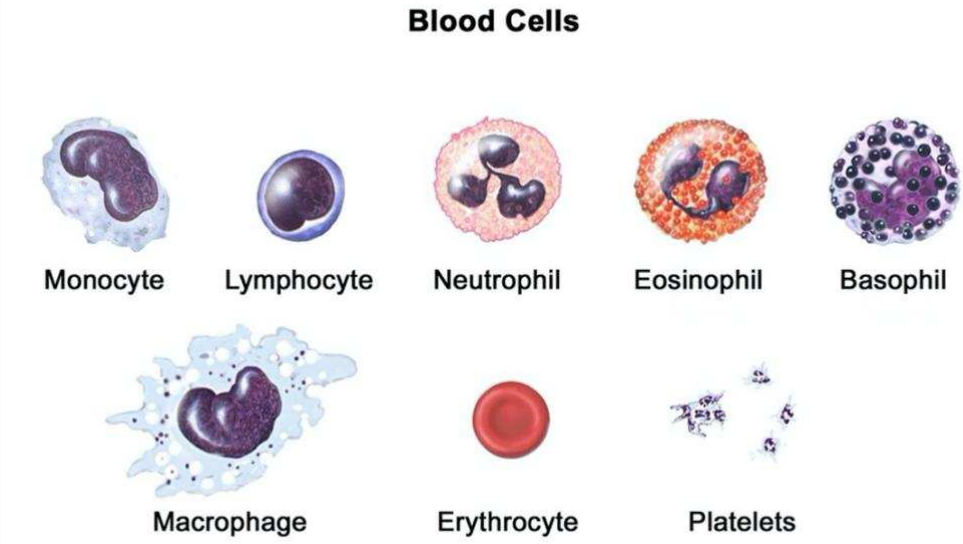

Figure 1.18 Blood cell type in human bodies.

Erythrocytes are the red cells present in the peripheral blood[92]. Leukocytes, known as white blood cells, are found in the lymphatic system and peripheral circulation. Granulocytes and agranulocytes are the two types of lymphocytes. Eosinophils, basophils, and neutrophils make up granulocytes[93]. The macrophages, lymphocytes, and monocytes are agranulocytes. The concentration of platelets is determined by thrombocytes. Plasma in the blood serves as a vector for the flow of constituent parts throughout the body. Blood plasma is composed of around 90% water, glucose, dissolved proteins like fibrinogen, mineral ions, clotting agents, carbon dioxide, and other hormones. Peripheral blood oversees refueling every system, including the immune system and the ability to absorb nutrients. Personal live quality is dependent on the healthy peripheral blood affects.

1.4.2 Blood cell reprogramming

Beyond the original fibroblast skin cells, the category of reprogrammable cell types has advanced to more readily available cell sources, including hair[94], urine[95,96], dental pulp[97], and human blood[98,99]. In contrast to these shortcomings of fibroblasts, peripheral blood is already widely used in medical diagnostics and is obviously the most accessible resource for cellular reprogramming. In the blood reprogramming, firstly, people are focus on the hematopoietic $CD34^+$stem cells by using retrovirus transduction, but this method involved a difficult, time-consuming isolation process of $CD34^+$ cells from peripheral blood using granulocyte colony-stimulating factor[98]. In 2016, Youngkyun Kim's group worked on cord blood mononuclear cells (CBMCs) reprogramming by Sendai virus, which is the most common transfection method used in blood reprogramming[100,101]. There are various of cell types, like T cell[102,103], mononuclear cells[104,105] from the peripheral blood that have been reprogrammed into iPSCs.

The differences between the most important cell types present in peripheral blood are shown in Figure 1.19.

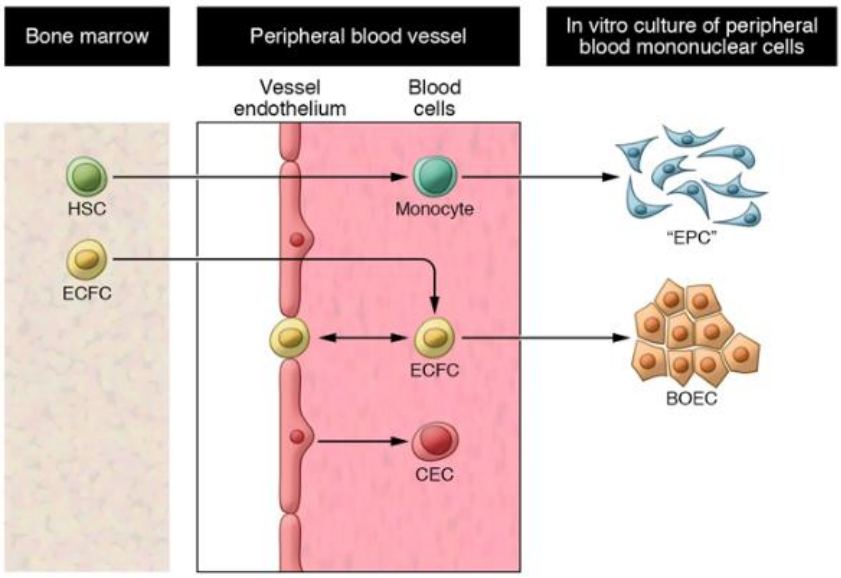

Figure1.19 Blood endothelial cell types, origins, and culture. HSC, hematopoietic stem cells; ECFC, endothelial colony–forming cells; CEC, circulating endothelial cells; EPC, endothelia progenitor cells. (Adapted from Robert P. Hebbel, 2017)

Endothelial progenitor cells (EPCs), referred to as blood outgrowth endothelial cells (BOECs) and endothelial colony forming cells (ECFCs), can be produced from cord and peripheral blood samples[106,107]. BOECs are characterized as mature endothelial cells, they are regarded as the progeny of ECFCs. Eventually, it is discovered that the cells formerly known as EPCs are hematopoietic in origin, have a restricted capacity for proliferation, Accessible from peripheral blood, while BOECs growth are robust, continuing to proliferate until around 60 passages, after which they stop growing but remain viable[108]. Also, BOECs have the ability to contribute to neovascularization and have been employed to model endothelial diseases[109]. In addition, they have been used therapeutically in cell transplantation and iPSC derivative translation[110].

In conclusion, the workflow from the patient blood to patient specific iPSCs later towards cell therapy is summarized in Figure 1.20.

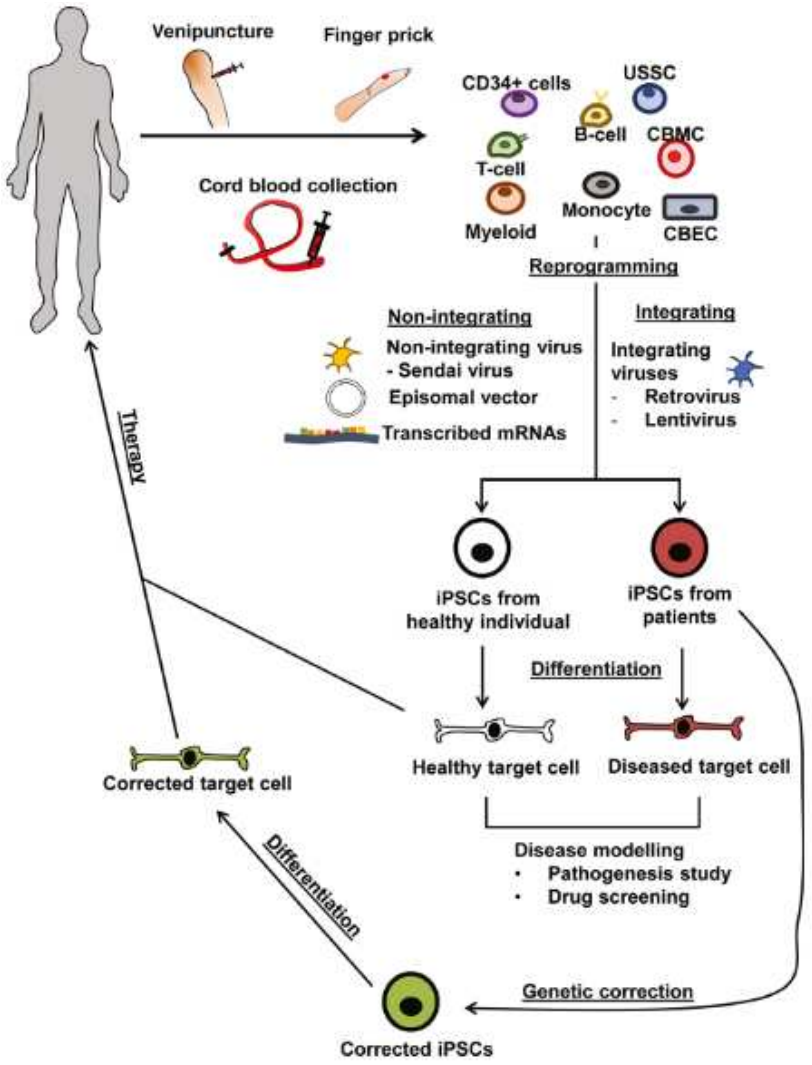

Figure1.20. Summary of blood cell reprogramming process (Adapted from Ying Chen, el al, 2019)

Cells from cord blood or peripheral blood have both been successfully reprogrammed into iPSCs, while peripheral blood is more favorable because they are easier accessible by venipuncture. Also, a smaller blood volume is likely to be clinically more favorable. The most frequently used blood cells in reprogramming are hematopoietic cells, mononuclear cells or T, B cells. Sendai virus is most widely used among the non-integrating methods. In the meantime, mRNA transfection has caught the attention of more groups. Integrating methods, like retrovirus face great challenge because they hinder the clinical application of blood derived iPSCs. Usually the appearance of blood-iPSCs colonies would take around one month of transfection, but

the efficiency is quite dependent on the cell sources and methods. The blood derived iPSCs, either from the healthy doner or patient doner, are of great help in disease modeling and clinical diagnosis. With the gene editing technique, patient specific blood-iPSCs benefit to personized medicine and cell therapies.

Chapter 2 The Project aim

Human embryonic stem cells could generate all cell types in the body, which gives possibility to study disease mechanism, intrinsic signaling pathways, human development process, autoimmune reaction, antibody targets and other biological questions. Due to the ethical and clinic concerns about using human embryos in research, people started to look for other possible alternative models to circumvent this obstacle. In 2006, the cellular reprogramming experiment was firstly carried out in mouse, and one year late followed by the success in human fibroblasts using the same factors and methods in human fibroblasts, which has done by Yamanaka's group, showing that terminal differentiated cells have the potential to be converted back into stem cell state. This process was called cellular reprogramming and also the obtained stem cells were named induced stem cells (iPSCs), and the core protein transcriptional factors Oct3/4, Klf4, Sox2 and c-Myc (OKSM) have been named Yamanaka factors. The discovery of iPSCs was of great help to avoid using the human embryos in research, thus has drawn great attention to the crowds. For more than a decade, people are working hard in understanding the detailed mechanism of this cellular reprogramming and also the downstream application of iPSCs

The first aim of my study is focus on the reprogramming process itself. Many groups have been working on various aspects of this reprogramming process. For example, search for other factors that could also trigger or even improve the efficiency of iPSCs generation (in general the efficiency is around 0.001%-0.1%), looking for some other methods, like plasmids electroporation, RNA infections, and proteins or small chemical molecule instead of using the retrovirus by Yamanaka group, which interferes the genotype and may induce teratocarcinoma later. Also, the retrovirus needs passages of splitting to remove the residual virus particles. On the other hand, people spend time in understanding the how does the reprogramming process could happen, which cells they are when are in the transition phase and how much similarity they share with the embryonic stem cells. Since our group has expertise in microscale

design and fabrication, we conduct cellular reprogramming process in homemade microfluidic chips, to mimic the three-dimension microenvironment *in vivo,* so we could test if the reprogramming efficiency could be improved in such confined micro-chips. We hypotheses that some subpopulations during human cellular reprogramming control fate decisions toward pluripotency through cell-extrinsic factors. We take advantage of microfluidics that has the confined environment, where secreted signals are accumulated, and distinctive intermediate subpopulations can be effectively captured and characterized.

The second aim is that we use newly generated iPSCs, which are called nascent iPSCs as an ideal model to study human development *in vitro*. There are *in vivo* zebrafish, mouse models that helps to understand the events that happen in human body, however, due to the great difference between mice and human, or even between the primate animals and human, we could not use the non-human species to fully mimic the biological way and metabolism in human. The emergence of organoid, which is a three-dimension cell aggregates of primary tissues or stem cells that are capable of self-renewal, self-organization and exhibit organ functionality. Organoids address the limitations of existing model systems by providing self-organize into organotypic structures. With the high efficiency of microfluidic reprogramming system in our lab, we study the three germ layers development *in vitro* and especially focus on brain organoids generation and maturation.

The third aim of my project that we carry out the reprogramming experiments in blood extraction cells. Up to date, most of the cellular reprogramming experiments are carried out in fibroblasts, but most of fibroblasts are taken from the skin biopsies (some are also isolated from the dental pulp or urine), which is an invasive process, especially to small kids. Thus, we were thinking about other cell source alternatives, where we are more interested in cells from the peripheral blood. Peripheral blood could be easily got from the venous blood collection. Also, they are less mutant because of the fewer exposure to the sunlight rays comparing to the skins. Many groups have successfully reprogrammed T cells, B cells and so on, into iPSCs. But in my project, we work on

the blood outgrowth endothelial cells (BOECs) as the cell source. They are adherent to the glass bottom of our microfluidic chips, and readily to receive the daily mRNA transfection. Besides, we want to test if we could get patient-specific iPSCs by only taking 5ml to 10ml peripheral blood from the patients, which could greatly facilitate the personal medicine research.

To summarize, the whole aim of my Ph.D. period is to explore better the cellular reprogramming process in microfluidics, then the application of iPSCs derived organoids to understand the human embryonic development *in vitro,* mainly focused on the brain organoids generation, maturation and optimization. Last but not least, in parallel to the downstream research of hiPSCs, we turn back to the start point to study broader cell sources scale for large and more feasible cellular reprogramming.

Chapter 3 Materials and methods

3.1 Experiment materials

3.1.1 Base cell culture medium and supplements

Human fibroblasts-BJ cells (ATCC, cat. no. CRL-2522)

Human fibroblasts-HFF-1 cells (ATCC, cat. no. SCRC-1041)

DMEM high glucose (Gibco/Thermo, cat.no. 41965-039)

DMEM KnockOut (Gibco/Thermo, cat.no.10829-018)

DMEM/F12 (-/-) (Gibco/Thermo, cat.no.21331-020)

Nutristem HPSC XF W/O TGF & FGF (Resnova, cat.no.06-5100-01-1A)

TeSR-E8 (Voden, cat.no.05990)

TeSR-E8 25X supplement (Voden, cat.no.05990)

StemMACS iPS-Brew XF, human (Miltenyi Biotech, cat.no.130-104-368)

RPMI 1640 (Gibco/Thermo, cat.no. 22400089)

EGM^{TM-2} Endothelial Cell Growth Medium-2 BulletKit (Euroclone, cat.no.CC-3162)

EGM^{TM-2} Endothelial SingleQuots^{TM} Kit (Euroclone, cat.no.CC-4176)

Neurobasal (Gibco/Thermo, cat.no.21103-049)

Advanced DMEM/F12 (Gibco/Thermo, cat.no.12634-010)

Fetal bovine serum (FBS) (Gibco/Thermo, cat.no.10270106)

Fetal bovine serum defined (Defined FBS) (Hyclone, cat.no.SH30070.03)

Horse serum (Gibco/Thermo, cat.no.16050-122)

Donkey serum (Merck, cat.no.S30-100ML)

KnockOut Serum Replacement (Gibco/Thermo, cat.no.10828028)

N2 (100X) (Gibco/Thermo, cat.no.17502048)

B27 complete (50X) (Gibco/Thermo, cat.no.17504044)

B27 without insulin (Gibco/Thermo, cat.no.A1895601)

B27 without vitaminA (Gibco/Thermo, cat.no.12587010)

3.1.2 Solutions and reagents

MEM NEAA (Gibco/Thermo, cat.no. 11140-50)

β-Mercaptoethanol (Gibco/Thermo, cat.no. 31350-010)

StemMACS mRNA transfection kit (Miltenyi, cat. no. 130-104-463)

StemRNA-NM reprogramming kit (Stemgent, cat. no. 00-0076)

Sodium pyruvate (Sigma, cat.no. 11360070)

TrypLE™ Select (Gibco/Thermo, cat.no.12563-011)

EZ-LiFT Stem Cell Passaging Reagent (Sigma-Aldrich, cat.no SCM139)

MACS Running Buffer (Miltenyi, cat.no.130-091-221)

Insulin-transferrin-selenium (Gibco/Thermo, cat.no. 41400-045)

Vitronectin (Gibco/Thermo, cat.no. A14700)

IRGACURE 2959 (Ciba, cat.no.0298913AB)

DPBS(10X) (Gibco/Thermo, cat.no.14200-067)

DPBS(1X) (Gibco/Thermo, cat.no 14190-144)

Ficoll-paque plus (Merck, cat.no.GE17-1440-02)

GlutaMax 100X (Gibco/Thermo, cat.no.35050-061)

Trypan Blue (Logos Biosystems, cat.no. L12002).

Collagen IV (R&D, cat.no. 3410-010-01)

Fibronectin (Corning, cat.no. 354008)

HEPES (1M) (Gibco/Thermo, cat.no.15630-080)

RNaseZap RNase decontamination solution (Invitrogen, cat. no. AM9780)

Trypsin 0.05% (Gibco/Thermo, cat.no.25300-054)

Trypsin 0.25% (Gibco/Thermo, cat.no.25200-056)

BSA (cell culture) (Sigma,cat.no.A7030-10g)

BSA (no cell culture) (Sigma, cat.no.A2153-50g)

EDTA (Gibco/Thermo, cat.no.15575020)

Penicillin–streptomycin(Gibco/Thermo, cat.no.15140-122)

Puromycin (Gibco/Thermo, cat.no.A11138-03)

MitomycinC (Sigma/Merck, cat.no.M0503-5X2MG)

Sucrose (Sigma, cat.no. 84097-250G)

PFA, Paraformaldehyde (Sigma, cat.no. P6148)

Triton-100 (Sigma, cat.no. 93426)

Sylgard 184 silicone elastomer base

Sylgard 184 elastomer curing agent

Ethanol 75%

Distilled water/ MilliQ water

3.1.3 Growth Factors and small molecules

Activin-A (Qkine, cat.no. QK001)

Fibroblast growth factor 2 (FGF2; Peprotech, cat.no.10018B)

Recombinant Human/Murine/Rat BDNF (Peprotech, cat.no.450-02,50ug)

Recombinant human HGF (Peprotech, cat.no.100-39)

Recominant human IL6 (Peprotech, cat.no.200-06)

Recominant human soluble IL6 receptor (sIL6r) (Peprotech, cat.no. 200-06R-20)

Recombinant Human NT-3 (Peprotech, cat.no. 450-03, 50 ug)

Recombinant Human FGF4 (aa 71-206) (R&D, cat.no. 7460 - F4)

Recombinant Human BMP-4 (Peprotech, cat.no. 120-05ET)

Recombinant Human BMP-4 (R&D, cat.no. 314-BP)

Recombinant Human FGF-10 (Peprotech, cat.no. 100-26 50ug)

Human FGF basic (154 aa) (Peprotech, cat.no. 100-18B-100 ug)

recombinant human NRG1 (R&D, cat.no. 396-HB)

Oncostatin (R&D, cat.no. 8475-OM)

LSD1 Inhibitor (Mllipore, cat.no. 489479-10MG)

LDN193189 (Sigma, cat.no. SML0559-5MG)

Chiron (ABCR, cat.no. AB 253776)

SB 431542 (Axon, cat.no. 1661,10mg)

DOXYCYCLIN (Sigma/Merck, cat.no. D9891)

Y27632 Rock inhibitor (Milteny, cat.no. 130-103-922)

3.1.4 Matrigel

Corning Matrigel Matrix - Growth Factor Reduced (MRF, Corning, cat.no. 354230)

M01(Corning, cat.no. 354234, Lot 0324001)

M02(Corning, cat.no. 354234, Lot 0232002)

M07(Corning, cat.no. 354234, Lot 0076007)

3.1.5 Antibodies

Primary antibodies

Anti-cMYC (Santa Cruz, cat.no. sc-764)

Anti-Col VI (Fitzgerald cat.no. 70R-CR009x)

Anti-GATA-4 (Santa Cruz, cat.no. sc-1237)

Anti-Ki-67 (Abcam, cat.no. ab16667)

Anti-KLF4 (Santa Cruz, cat.no. sc-20691)

Anti-MAP2 (Abcam, cat.no. Ab5392)

Anti-Nestin (Millipore, cat.no. MAB5326)

Anti-Oct4 (Santa Cruz, cat.no. sc-5279)

Anti-Pax6 (Santa Cruz, cat.no. sc-81649)

Anti-Pax6 (Biolegend, cat.no. 901301)

Anti-PECAM-1 (CD31) (Millipore, cat.no. 04-1074)

Anti-Sox2 (Millipore, cat.no. AB5603)

Anti-SOX2 (Y17) (Santa Cruz, cat.no. sc-17320)

Anti-SSEA-1 (Millipore, cat.no. MAB4301)

Anti-SSEA-4 (Santa Cruz, cat.no. sc-21704)

Anti-Tra-1-60 (Millipore, cat.no. MAB4360)

Anti-Tuj1 (Biolegend, cat.no. 801213)

Anti-Brachyury (R&D, cat.no. AF2085)

Anti-Brachyury (Abcam cat.no. ab20680)

Anti-E-Cadherin (Cell Signaling, cat.no. 3195S)

Anti-E-Cadherin (GeneTex, cat.no. GTX100443)

Anti-E-Cadherin (BD, cat.no. 610182)

Anti-FoxA2/HNF3b (Cell Signaling, cat.no. 8186S / D56D6)

Anti-Klf17 (Atlas, cat.no. HPA024629)

Anti-NANOG (Cell Signaling, cat.no. 4903S)

Anti-TUJ1 b-III-tubulin (Sigma, cat.no. T3952)

Anti-Zo-1 (GeneTex, cat.no. GTX108627

Anti-CDX2 (Abcam, cat.no. ab157524)

Anti-Ctip2 (Abcam, cat.no.18465)

Anti-FoxG1 (Abcam, cat.no. ab18259)

Anti-Map2 (Sigma, cat.no. M2320)

Anti-Map2 (Abcam, cat.no. AB5392)

Anti-NeuN (Abcam, cat.no. AB104225)

Anti-Otx2 (R&D, cat.no. AF1979)

Anti-SATB2 (Abcam, cat.no. ab51502)

Anti-Sox1 (R&D, cat.no. AF3369)

Anti-Sox17 (R&D, cat.no. AF1924)

Anti-TBX6 (Abcam, cat.no. AB38883)

Anti-Tbr1 (Abcam, cat.no. Ab31940)

Anti-Vimentin (Sigma, cat.no. SAB1305445-40TST)

Anti-E-Cadherin (Cell Signaling, cat.no. 24E10-3195)

Secondary antibodies

Alex 647 donkey anti rabbit (Life Tech, cat.no. A31573)

Alex 594 donkey anti rabbit (Life Tech, cat.no. A21207)

Alex 568 donkey anti rabbit (Life Tech, cat.no. A10042)

Alex 488 donkey anti rabbit (Life Tech, cat.no. A10043)

Alex 647 donkey anti mouse (Life Tech, cat.no. A31571)

Alex 594 donkey anti mouse (Life Tech, cat.no. A31573)

Alex 568 donkey anti mouse (Life Tech, cat.no. A10037)

Alex 488 donkey anti mouse (Life Tech, cat.no. A31573)

Alex 647 donkey anti goat (Life Tech, cat.no. A21447)

Alex 594 donkey anti goat (Life Tech, cat.no. A11058)

Alex 568 donkey anti goat (Life Tech, cat.no. A11057)

Alex 488 donkey anti goat (Life Tech, cat.no. A11055)

Alex 488 donkey anti rat (Life Tech, cat.no. A21208)

Alex 647 donkey anti rat (Life Tech, cat.no. A48265)

Nuclear staining

DAPI (LifeTech, cat.no. 62248)

Hoechst 33342 (LifeTech, cat.no. 62249)

3.2 Experiment equipments

Laminar flow hood;

CO_2 incubator;

Glass microscopy slides (Menzel, cat. no. 10756991);

Coverslips, 24 × 60 mm (Menzel, cat. no. 15747592);

Water bath;

Phase contrast and epifluorescence microscope;

Stereomicroscope;

Sterile tweezers;

Cell strainer (Biosigma, cat.no.010198Z)

Sterile scalpel;

Disposable glass pasteur pipettes;

DNase- and RNase-frees microcentrifuge tubes (0.2ml,1.5ml and 2ml);

RNase-free sterile 15-mL conical tubes(15ml and 50ml);

Serological tube(2ml,5ml,10ml,25ml and 50ml);

Sterile filter tips (10, 20, 200 and 1,000 µL);

Cryostat (Leica, cat.no.CM1860UV);

Confocal microscope (Zeiss,cat.no. LSM900);

3.3 Experiments protocols

3.3.1 Microfluidic chips fabrication

The microfluidic chip used in the whole experiments are all 5-channel chips, they are developed internally using soft-lithographic methods and was molded from polydimethylsiloxane (PDMS), as described before in chapter 1. It consists of 10 separate microfluidic channels, with a surface of 27 mm^2 (18mm long, 1.5mm wide) and with a height of 200 μm.

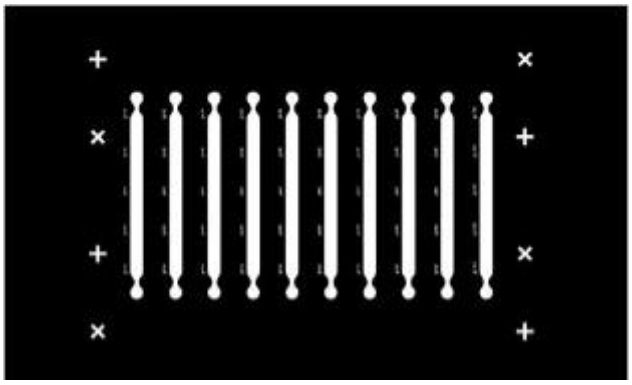

Figure 3.1 the design of the microfluidic chips

1. Two components of PDMS (Sylgard 184 base and curing agent) liquid is thoroughly mixed at the ration of 10:1 inside a plastic cup, room temperature;
2. Place the cup inside a desiccator and vacumm for 30 minutes to remove all the oxygen;
3. Pour the mixed liquid over the mask plate showed in Figure 3.1.
4. Put the whole mask back to a desiccator again and vacuum for another 30 minutes, room temperature;
5. Thermally heat the mask plate for 1hour at 75℃ on a hot plate. Cover the whole mask plate with a plastic lid or aluminum foil to prevent any dust comtamination;
6. After cooked and the PDMS cooling down, it become solid and can be peeled off easily from the mask;

7. The peeled off 10-channel PDMS stamp is shown as Figure 3.2. Use a 1mm biopsy punch to cut the inlet from one side and a 3mm biopsy biopsy punch to cut the outlet reservoir;

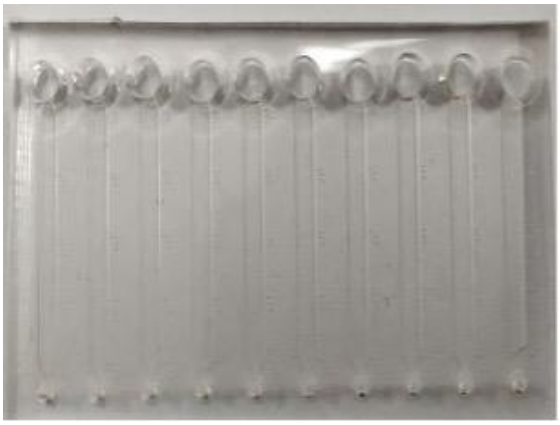

Figure 3.2 The punched PDMS stamp

The 10-channle PDMS stamps are cut into 2 piece of 5-channle stamp according to the experiment requirements.

8. The PDMS stamp was covalently attached a 75x25 mm microscope glass slide by plasma treatment;
9. Once the PDMS stamp attaches to the bottom glass (we call it a chip now), place the chip on the hot plate 100 ℃ for 15 minutes to validate the plasma attachment;
10. Wash the chip with isopropanol and dry it on the hot plate for 15 minutes;
11. Wash the chip with distilled water and dry it on the hot plate for 10 minutes;

Washes help to check if the fluid could go smoothly inside the channel and also to remove the non-reactive polymers.

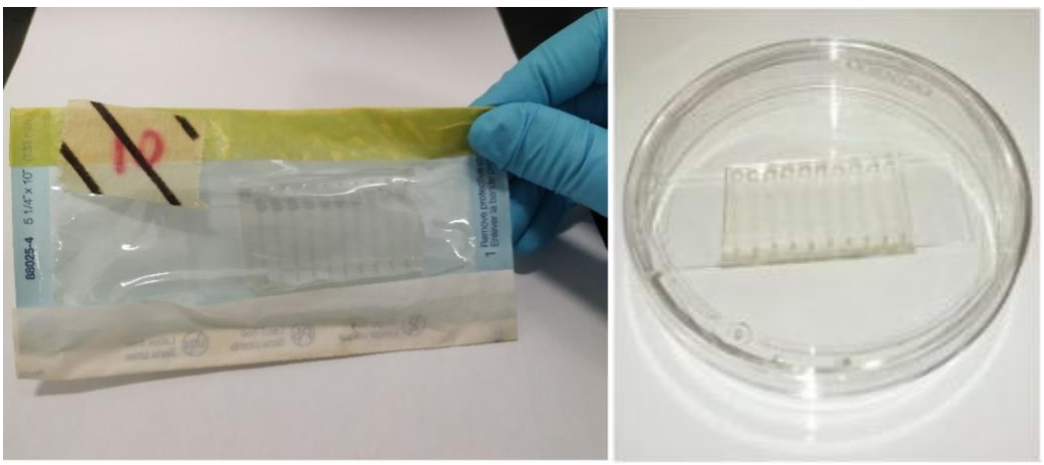

Figure 3.3 the autoclaved chip (in the autoclave bag and in a petri dish)

Put the chips inside a autoclave bag and sterilize at 121℃ for 20 minutes and dry in the oven overnight before they are ready to be used (Figure 3.3). Once chips are ready, open the chips under the biological safe hood and place them inside a petri dish. Fill with distilled water or PBS solution around the chamber to increase the humidity and prevent media evaporation.

3.3.2 Fibroblasts culture

The human fibroblasts lines -BJ cells (ATCC, cat. no. CRL-2522) and HFF-1 cells (ATCC, cat. no. SCRC-1041)are cryopreserved in -80℃ or in liquid nitrogen tank for long term store.

BJ cells thawing:

1. The media for culturing BJ fibroblasts are high glucose DMEM +10% FBS+ 1% Pen/Strep (antibiotics is not mandatory);
2. Set the water bash at 37℃, add 3ml of fibroblasts medium inside a 15ml falcon tube and warm it in the water bath;
3. Quickly move a BJ cryovials from liquid nitrogen and shake the vial inside the water bash gently, until there is only one small piece of ice left;
4. Spray ethanol over the BJ vial and the pre-warmed medium, do not let any water or ethanol leaking into the vial;
5. Open the vial under the hood and carefuly, move all BJ cell suspension from the vial and drop by drop adding to the 15ml falcon tube;
6. Mix the BJ cell suspension and medium for 2 or 3 times to let the DMSO solution quickly diluted by the DMEM medium;
7. Centrifugate the 15ml falcon tube at 300g for 5 minutes;
8. Remove the supernatant and resuspend the BJ cell pellet with 10ml fresh DMEM medium;
9. Replate all BJ cells suspension inside a 10cm petri dish and put the petri dish into a 37℃, 5%CO_2 incubator.

10. Medium needs to be changed every 2 or 3 days.

BJ fibroblasts should be split every 3 or 4 days when they reach 80% of confluency. Cells should not reach 100% confluency before spliting because they will become senescent and start to not proliferate. BJ fibroblasts are split with 0.25% EDTA-trypsin.

BJ cells passaging:

1. Remove the DMEM medium and wash the BJ cells with PBS, twice;
2. Remove the PBS solution and add 1.5ml 0.25% EDTA-trypsin over the 10mm petri dish evenly; the 0.25% EDTA-trypsin volume has to be adjusted according to the culture format you use;
3. Incubate back in the incubator for 3-5 minutes, check under the microscope to see if all cells are detached and start to float inside the dish;
4. Stop the trypsin reaction with DMEM medium(mainly because of the FBS), the ratio of stopping medium and trypsin is 3:1; collect all solution in a 15ml falcon tube;
5. Wash the left cells inside the dish with 3ml PBS and collect into the tube used in the previous step;
6. Centrifugate the 15ml falcon tube at 300g for 5 minutes;
7. Remove the supernatant and resuspend the BJ cell pellet with 1ml fresh DMEM medium;
8. Take out 100μl of BJ cell suspension and replate in a new 10cm petri dish, the spliting ration ranges from 10:1 to 8:1;
9. Add 10ml fresh DMEM medium in the new dish and put back into the incubator;

When we split the BJ cells, apart from keep a portion in culture, the rest of the cells could be also frozen for future usage.

BJ cells freezing:

1. Remove the DMEM medium and wash the BJ cells with PBS, twice;

2. Remove the PBS solution and add 1.5ml 0.25% EDTA-trypsin over the 10mm petri dish evenly; the 0.25% EDTA-trypsin volume has to be adjusted according to the culture format you use;
3. Incubate back in the incubator for 3-5 minutes, check under the microscope to see if all cells are detached and start to float inside the dish;
4. Stop the trypsin reaction with DMEM medium(mainly because of the FBS), the ratio of stopping medium and trypsin is 3:1; collect all solution in a 15ml falcon tube;
5. Wash the left cells inside the dish with 3ml PBS and collect into the tube used in the previous step;
6. Centrifugate the 15ml falcon tube at 300g for 5 minutes;
7. Remove the supernatant and resuspend the BJ cell pellet with 1ml fresh DMEM medium;
8. Prepare 2 cryovials, add 400µl of FBS and 100µl of DMSO, mix thoroughly and wait for vials to cool down (DMSO release heat);
9. Add 500µl of BJ cell suspension in each cryovial and mix 1 time; tightly close the lid and put in a cryobox;
10. The cryobox has filled up with isopropanol to slow down the freezing procedure; The cryobox firstly has to be put in -80℃ fridge for at least 24 hours, then the cells cryovials have to be moved into liquid nitrogen for long term and high-quality storage.

3.3.3 mRNA transfection preparation

The reagent kit used in our reprogramming method are the StemRNA-NM reprogramming kit (Stemgent, cat. no. 00-0076) and StemMACS mRNA transfection kit (Miltenyi, cat. no. 130-104-463).

In the StemMACS mRNA transfection kit, there are two components, 0.5 mL StemMACSTM Transfection Reagent and 25 mL StemMACS Transfection Buffer; all

components have to be stored at 2−8°C. This kit is a lipid-based transfection system for efficient mRNA delivery into various cell types.

In the StemRNA-NM reprogramming kit, there are three mRNA components, 1 vial of OKSMNL NM-RNA, 30 μg; 1 vial of EKB NM-RNA, 22 μg; 1 vial and 1 vial of NM-microRNAs,15μg; from the manufactor's instruction, the NM-RNA reprogramming cocktail is set to reprogram one well of a 6-well plate. The daily NM-RNA reprogramming cocktail is composed of 0.8 μg OSKMNL NM-RNA, 0.6 μg EKB NM-RNA (total mRNA= 1.4 μg), and 0.4 μg NM-microRNAs per transfection per well (6-well plate format). Thus the volume ratio between 3 components is around 51:39:10. Since the volume of each vial could be different from every batch to batch, every time when we get a new package of the StemRNA-NM reprogramming kit, we measure the precise volum of each vial and mix the correct NM-RNA components, pre-mixed NM-RNA cocktail is aliquoted 5μl per vial and stored at -80℃. There is no need to aliquot StemMACS mRNA transfection kit, they are stable at +4℃.

3.3.4 Daily mRNA transfection

According to our standard fibroblasts reprogramming processe in microfluidics, daily mRNA transfection lasts for 8days. Twice of medium change is required every time during the whole process until the iPSCs are extracted from the chamber. The transfection is always performed in the afternoon, around 6.pm.-7.pm, and the morning medium change is set between 9.a.m-10.a.m. During the transfection process, we also adjust the transfection dose according to the morphology change and the cell death ratio because of the toxicity and stress from the transfection. Basically, we set three dose of transfection, low dose, medium dose and high dose. The detalied information is listed in Table1.

Table 3.1 Composition of transfection solutions for a five-chamber microfluidic chip

Low dose		
Solution 1(μl)	Solution 2(μl)	Medium(μl)
RNA:0.468	TR:0.140	55.327
TB:1.869	TB:2.196	

Medium dose		
Solution 1(μl)	Solution 2(μl)	Medium(μl)
RNA:0.780	TR:0.234	52.189
TB:3.125	TB:3.672	
High dose		
Solution 1(μl)	Solution 2(μl)	Medium(μl)
RNA:1.247	TR:0.375	47.503
TB:5.000	TB:5.875	
TB:transfection buffer; TR:transfection reagent		

The detalied daily mRNA transfection steps are as follwing:

1. Prepare two sterile, RNase-free microcentrifuge tube, labelled as 1 and 2;
2. 60μl of total transfection and medium is calculated for 1 chip and the daily transfection started from low dose; According to how many chips you have and the dose you choose, add the required amount of TB (Transfection Buffer) in tube 1 and tube 2, separately;
3. Add the required amount of RNA cocktail and TR (Transfection Reagent) to tube 1 and tube 2, remember adding RNA cocktail as the last step; Mix tube 2 firstly and mix tube 1 for around 10 times, take everything from tube 1 and pour into tube 2, then mix two tubes for another 10 times, and incubate under the biological hood for 20 minutes at room temperature;
4. During the incubation, prepare another tube 3, add the required amount of reprogramming medium (usually the Nutristem+20ng/ml FGF2). After 20 minutes incubation, transfer the cocktail mix to tube 3 and mix gently no more than 5 times. Because at this moment, the RNA cocktail is tightly wrapped by the lipid reagent, violent mixture would break the lipid spheres;
5. Distribute equally 60μl of transfection mixture to 5 channels. Leave a drop on each inlet of the channel, check if the mixture go smoothly without producing any bubble inside the channel. Keep the reservoir full to prevent evaporation from the channel itself;

6. The next more, repeat the operation in step 5, change with 60µl of reprogramming medium, remove the extra waste from the reservoir but keep the reservoir full;
7. Check under the microscopy every day after medium change to track the morphology change and adjust the transfection dose;
8. The microfluidic chips are kept in 37 °C , 5% CO_2, 5% O_2 incubator, because low oxygen can help increase the reprogramming efficiency[111]. The whole process is performed under a hypoxia incubator;
9. Daily mRNA transfection lasts for 8days; From day9, the medium is switched to IPS-Brew, and no more transfection is needed.

3.3.5 Tra-1-60 live staining in microfluidics chips

1. Remove the medium from the reservoir and wash with PBS;
2. Dilute the Anti-Tra-1-60 488 antibody in the ratio of 1:100 in fresh iPS-BREW medium, calculate the diluted antibody volume for 15 µl/channel;
3. Replace the PBS with the Tra-1-60 antibody solution.
4. Incubate for 30 minutes at 37 °C, 5% CO_2, 5% O_2 incubator;
5. Aspirate antibody solution (from the reservoirs) and gently wash the channel with PBS twice, the last wash is with IPS-brew medium;
6. Check the staining using a fluorescence microscope.
7. The microfluidic chips can be put back into the incubator for culturing.

3.3.6 Microfluidic chips immunofluorescence

1. Two washes of the micro-channels with PBS, 200 µl/chip, empty reservoir;
2. Add 200µl of 4%PFA to one chip, keep the reservoir full,10 minutes;
3. Empty reservoir, two washes with PBS, 200 µl/chip, 1 min interval;
4. Add 200 µl/chip 0.1%PBST, keep at room temperature for 10 minutes, empty the reservoir;

5. Wash with 200 µl/chip of 5% (or 10%) horse serum in 0.1%PBST, empty the reservoir;
6. Add 200 µl/chip 5% (or 10%) horse serum in 0.1% PBST, keep at room temperature for 45 minutes;
7. Two washes with 200 µl/chip of 0.1%PBST, empty the reservoir;
8. The primary antibody is diluted in 5% (or 10%) horse serum in 0.1%PBST solution, 12 µl/channel;
9. Store the microfluidic chip inside a petri dish with parafilm and PBS around, leave the dish at +4°C overnight;
10. The next day, wash the primary antibody with 200 µl/chip of 0.1% PBST, three times, 5 min interval;
11. Dilute the secondary antibody with 5% (or 10%) horse serum in 0.1% PBST solution, 12 µl/channel, keep at room temperature, protect from the light for at least1 hour;
12. Three washes 200 µl/chip of 0.1%PBST, 5 min interval;
13. Replace the PBST solution with PBS+1%Pen/Strep; check the signal under a reverted microscope due to the PDMS layer is at the top.

3.3.7 iPSCs extraction from the microfluidic channels

After 8 days of daily transfection and 5 days of maintenance, iPSCs are extracted from the microchamber at day14.

1. Prepare a multi-well coating with 1% MRF, wait for 30 minutes at 37°C in the incubator.
2. Wash 2 times the chips with PBS. Add 60µl of EZ-LiFT solution for 1 chip, leave it for 3 minutes in the incubator. Add IPS-Brew medium to block the reaction. Pipette up and down for several times and collect all the volume from the channels in a new 1.5 ml Eppendorf tube. Check under the microscope if all the iPSCs colonies are detached;

3. Centrifuge the 1.5 ml Eppendorf tube at 500*g* for 5 minutes, remove all the supernatant and resuspend again in 1ml of fresh IPS-Brew medium, at 1:1000 ROCK inhibitor in the cell suspension;
4. Replate all cells back to the multi-well coated at the beginning, put the plate back into the incubator and keep it in culture.

3.3.8 iPSCs establishment in multiwell

After extracted from the microfluidics, iPSCs colonies are cultured in multi-well plate. Commercially available stem cell medium-E8 and iPS-Brew XF medium are most frequently used iPSCs medium used by us. Medium needs to be changed every other day (E8 medium should be changed every day). iPSCs should be split every 3 days, when colonies start to merge together, the over confluent would induce the differentiation, lower the iPSCs puritity and quality.

iPSCs passaging:

1. Coat a new well with 0.5% MRF, put back in incubator for 30 minutes;
2. Remove the medium from the iPSCs and wash with PBS twice;
3. Single cell dissociation: add TrypLE solution to cover the all iPSCs colonies and put back the incubator for 3-4 minutes, check under the microscopy to see if the incubation time is enough to detach all the iPSCs colonies;
4. Add IPS-Brew (or E8 medium) to stop the reaction of TrypLE, pipette up and down to dissociate all colonies into single cells, collect everything from the well and put in a falcon tube;
5. Centrifuge at 300g for 5 minutes, remove the supernanant, resuspend the cell pellet in 1ml IPS-Brew medium (or E8 medium), add 2μM of ROCK inhibitor to keep cell attachment and viability after spliting. Usuall the passage ratio between 1:8 to 1:10;
6. Remove the ROCK inhibitor after 24 hours by medium changing. If the cell viability is too low, keep ROCK inhibitor for another day to ensure the cell survival.

7. Non-single cell dissociation: add 0.5mM EDTA solution to cover the all iPSCs colonies and put back the incubator for 3-4 minutes, check under the microscopy to see if the colony start to become bright from the edge to the center;
8. Remove EDTA gently, do not aspire any iPSCs colony piece, take 1ml of IPS-Brew medium (or E8 medium) and push strongly on the iPSCs surface, pipette up and down no more than 4 times;
9. Check under the microscopy to see if the iPSCs colonies are dissociated into small pieces of colonies, instead of single cells;
10. Take the suspension volume at 100µl-125µl and compensate with fresh IPS-Brew medium (or E8 medium) to reach the medium volume required by the cell plate format you use; There is no need to add ROCK inhibitor in this spliting method, but if you see the colony pieces are too small, it is strongly recommended to add also ROCK inhibitor like we do in the TryPLE dissociation method to increase the cell survival rate.

iPSC thawing:

1. Coat a new well with 0.5% MRF, put back in incubator for 30 minutes;
2. Set the water bash at 37℃, add 3ml of DMEMF12+20% KSR medium inside a 15ml falcon tube and warm it in the water bath;
3. Quickly move a iPSCs cryovials from liquid nitrogen and shake the vial inside the water bash gently, until there is only one small piece of ice left;
4. Spray ethanol over the iPSCs vial and the pre-warmed medium, do not let any water or ethanol leaking into the vial;
5. Open the vial under the hood and carefuly, move all iPSCs cell suspension from the vial and drop by drop adding to the 15ml falcon tube;
6. Mix the iPSCs cell suspension and DMEMF12+20% KSR medium for 2 or 3 times to let the DMSO solution quickly diluted by the DMEMF12+20% KSR medium;
7. Centrifugate the 15ml falcon tube at 300g for 5 minutes;

8. Remove the supernatant and resuspend the iPSCs pellet with 10ml fresh IPS-Brew medium (or E8 medium) +2μM of ROCK inhibitor;
9. Replate all iPSCs suspension inside the pre-coated multiwell 10cm petri dish and put the plate into a 37°C, 5%CO_2, 5% CO_2 incubator.
10. Next day, check the cell recovery and remove the ROCK inhibitor by medium changing.

iPSCs freezing:

1. Remove the IPS-Brew medium (or E8 medium) and wash the iPSCs colonies with PBS, twice;
2. Remove the PBS solution and add TryPLE solution over the iPSCs colonies surface evenly;
3. Incubate back in the incubator for 3-4 minutes, check under the microscope to see if all colonies start to be detached;
4. Stop the TryPLE reaction with DMEMF12+20%KSR medium, collect all solution in a 15ml falcon tube;
5. Wash the left cells inside the dish with 3ml PBS and collect into the tube used in the previous step;
6. Centrifugate the 15ml falcon tube at 300g for 5 minutes;
7. Remove the supernatant and resuspend the iPSCs pellet with 1ml fresh IPS-Brew(or E8 medium);
8. Prepare 2 cryovials, add 400μl of KSR and 100μl of DMSO, add 1μl of ROCK inhibitor, mix thoroughly and wait for vials to cool down (DMSO release heat);
9. Add 500μl of iPSCs suspension in each cryovial and mix 1 time; tightly close the lid and put in a cryobox;
10. The cryobox has filled up with isopropanol to slow down the freezing procedure; The cryobox firstly has to be put in -80°C fridge for at least 24 hours, then the cells cryovials have to be moved into liquid nitrogen for long term and high-quality storage.

3.3.9 iPSCs 2D differentiation preparation

When the newly generated iPSCs are extracted from the microfluidics, they are called primed iPSCs and cultured in 2D monolayer format in multiwell plate. In order to test the pluripotency and the differentiation potential, 2D germ layer differentiation are performed. We seed iPSCs and guide the differentiation direction with basal medium, growth factor supplement and signal pathway inhibitors combination.

Endoderm differentiaiton:

1. Dissociate iPSC with TrypLE solution into single cell. Place a 12mm cover slip glass inside a 24-well plate, coat the cover slip with 1% MRF. Seed the iPSCs at 50000cell/24well in order to reach 30% confluency the next day;
2. Prepare the endoderm medium as following:

Table3.2 Endoderm differentiation medium preparation

Medium A			
Components	volume	Stock concentration	Final concentration
RPMI1640 medium	9.568ml		
B-27 supplement minus insulin (50X)	200 µl		
Non-essential Amino Acids (100X)	100 µl		
Pen/Strep (100X)	100µl		
Activin A	2µl	0.5mg/ml	100ng/ml
BMP-4	10µl	10µ/ml	10ng/ml
FGF2	20µl	10µ/ml	20ng/ml
Chrion	3µl	10mM	2µM
Total volume	**10ml**		
Medium B			
RPMI1640 medium	9.568ml		
B-27 supplement minus insulin (50X)	200µl		

Non-essential Amino Acids (100X)	100µl		
Pen/Strep (100X)	100µl		
Activin A	2µl	0.5mg/ml	100ng/ml
Total volume	**10ml**		

3. The next day, change medium with medium A;
4. Change with medium B for two days;
5. Fix the cover slip glass with 4%PFA, and perform the 2D immunofluorescence staining to check if there is early endoderm markers expression. The 2D immunofluorescence staining protocol is listed as below.

   Mesoderm differentiaiton:

1. Dissociate iPSC with TrypLE solution into single cell. Place a 12mm cover slip glass inside a 24-well plate, coat the cover slip with 1% MRF. Seed the iPSCs at 30000cell/24well in order to reach 15%-20% confluency the next day;
2. The mesoderm medium recipe is as following:

Table3.3 Mesoderm differentiation medium preparation

Mesoderm medium			
Components	volume	Stock concentration	Final concentration
DMEM/F12	9.675ml		
Non-essential Amino Acids (100X)	100 µl		
Pen/Strep (100X)	100µl		
Insulin-transferrin-selenium(ITS) 100X	100µl		
Chrion	10µl	10mM	10µM
LDN	15µl	1mM	1.5µM
Total volume	**10ml**		

3. Change with mesoderm medium for three days;
4. Fix the cover slip glass with 4%PFA and perform the 2D immunofluorescence staining to check if there is early mesoderm markers expression. The 2D immunofluorescence staining protocol is listed as below.

   Ectoderm differentiaiton:

1. Dissociate iPSC with TrypLE solution into single cell. Place a 12mm cover slip glass inside a 24-well plate, coat the cover slip with 1% MRF. Seed the iPSCs at 120000-150000cell/24well in order to reach 100% confluency the next day;
2. The ectoderm differerntiation medium is called niN2B27 medium, and the recipe is as following:

Table3.4 Neuroectoderm differentiation medium preparation

niN2B27 medium			
Components	volume	Stock concentration	Final concentration
Advanced DMEM	23.8ml		
Neurobasal	23.8ml		
N2 complete	500µl		
B27 complete	250µl		
L-glutamine	500µl		
β-mercaptoethanol	50µl		
Non-essential amino acid (100X)	500µl		
Pen/Strep (100X)	500µl		
SB	50µl	10mM	10µM
LDN	500µl	1mM	10µM
Total volume	**50ml**		

3. Two inhibitors SB and LDN are added everyday freshly to the base medium in step 2, keep niN2B27 medium change for 5 days;
4. Fix the cover slip glass with 4%PFA and perform the 2D immunofluorescence staining to check if there is early ectoderm markers expression. The 2D immunofluorescence staining protocol is listed as below.

3.3.10 2D Immunostaining

When we perform the 2D immunostaing, iPSCs are usually seed on a cover slip due to the feasibility of the image aquisition under the microscope.

1. PBS washes to the well with the cover slip inside, twice;
2. Add 4%PFA to the well, 10 minutes;

3. PBS washes to remove the PFA and, three time, 5 min interval;
4. Add 500µl 0.1%PBST to the well and keep at room temperature for 10 minutes;
5. Wash one time with 5% (or 10%) horse serum in 0.1%PBST;
6. The blocking: add 1ml of 5% (or 10%) horse serum in 0.1% PBST to the well, keep at room temperature for 45 minutes;
7. In the meantime, prepare an aluminum foil wrapped dark box, place a wet tissue and piece of parafilm on the wet tissue, keep these two layers flat;
8. Two washes with 0.1% PBST 0,1%;
9. Place a lid from the 1.5ml microcentrifuge tubes over the parafilm layer;
10. Use the needle and tweezer to take the cover slip from the well and place it on the lid;
11. Prepare the primary antibody mix, usually diluted in 5% (or 10%) horse serum in 0.1%PBST, the volume is 30 µl/glass; gently add the primary antibody mix drop by drop to the glass, remember the distribute the drops evenly, he side with cells have to face up, contacting the primary antibody;
12. Store the dark box at +4°C, overnight;
13. Put back the glass to the well and three washes with 0.1%PBST, 30 minutes interval;
14. Prepare the secondary antibody mix, usually diluted in 5% (or 10%) horse serum in 0.1%PBST, the volume is 30 µl/glass;
15. Use the needle and tweezer to take the cover slip from the well and place it on the lid again;
16. Gently add the secondary antibody mix drop by drop to the glass, remember the distribute the drops evenly, the glass side with cells have to face up, contacting the secondary antibody;
17. Keep the dark box at room temperature for 1-3 hours;
18. Put back the glass to the well and three washes with 0.1%PBST, 30 minutes interval, remember to protect from the light during the washes;
19. Add PBS+1% Pen/Strep to the well and keep the glass at +4°C for storage;

20. Image acquisition: place a drop (usually 8-15µl) of mounting reagent on a thick glass slide, use the needle and tweezer to take the cover slip from the well ,dip on a piece of paper to remove the drifting PBS and then place upside down, the cell surface has to contact the mounting reagent drop; leave the glass slide to dry at room temperature for 15 minute, protect from the light;
21. Close the cover slip edge with nail polish and let it dry until the glass cannot move anymore. Then the slide is ready for immunofluorescence image acquisition.

3.3.11 iPSCs 3D epiblast formation

1. Place a 12-mm cover slip glass inside a 24-well plate, warm the plate inside the incubator;
2. thaw the 100% matrigel (M01,M02 or M07) on ice. Matrigel has to be placed on ice all the time; take out 20µl of matrigel and draw a small bed on the cover slip glass in step; the bed has to take up most of the cover slip surface.after drawing the bed, slowly move the whole plate back to the incubator and wait for 20 minutues to let the matrigel gellify. When the matrigel bed gellified, the shape is like a half moon; Add DMEM knockout medium around the matrigel beds to prevent drying out;
3. Detached primed iPSCs (Passage 0), which we call nascent iPSCs, with TrypLE solution into single cells, following the dissociation step mentioed above. Count the cell number and adjust the cell density to 10000cell/ml. Add 500µl of the iPSCs suspension plus 1µM ROCK inhibitor, which equals to 25cell/mm^2 to each bed, move it back and forth in a T path, the distribution of iPSCs has to be homogenous on the matrigel bed, in order to form homogenous an epiblast cyst later;
4. The next day, change medium with IPS-Brew with 2% of the same matrigel used for making the matrige beds the day before; The matrigel supplys the

extracellular matrix to environment, which helps the iPSCs to self-assemble into a 3D structure;

5. From day2, the epiblast cyst is formed from the iPSCs with a central lumen inside. IPS-Brew medium plus 2% matrigel is freshly prepared and changed everyday to maintain the 3D format;

3.3.12 3D epiblast cysts germ layer differentiation

The self-assembly 3D epiblast cysts are cultured on beds until day3. From one hand, the neuroectoderm differentiation could start when epiblast cysts are still on bed. On the other hand, we start the endoderm and mesoderm differentiation from the epiblast drops. So on the day3 after the epiblast cyst formed, the beds are detached, epiblast cysts are released from the matrigel beds, they are reembeded in 100%MRF drops. The detalied steps of making epiblast cysts drops are as following:

1. Place 12-mm cover slip glass inside a 24-well plate, warm the plate inside the incubator;
2. Thaw the 100%MRF on ice, the MRF has to be on ice all the time; Take 500µl of cold DMEM knockout medium, push hard on the epiblast cysts bed to destroy the whole bed and release the epiblst cysts; pour three beds, in total 1500µl together in a 1.5ml eppendorf tube and centrifuge at 1000g for 5 minutes, remove the supernatant as much as possible and resuspend the epiblast cysts in 600ul 100%MRF. The resuspend volume of MRF is dependenting on the beds number, usually 200µl MRF is used for resuspend epiblast cysts from 1 bed;
3. After the suspension, take out 20µl from the suspension MRF and leave a drop at the center of the warm cover slip glass mentioned in step 1. The drop has to stay in a dome shape and not spread on the glass. In general, 200µl of matrigel suspension could make 10 drops, but due to the pipetting loss, 7-8 drops could be made out of 200µl matrigel suspension.

   The short-term 3D epiblast cysts endoderm differentiation:

The 3D epiblast cysts endoderm differentiation shares the same medium as we already descriped in 2D endoderm differentiation protocol; Medium A is kept for 1 day, then medium B is kept for 2 days. Compare to the 2D differentiation, we extend the endoderm differentiation with more days in medium C and medium D, also later switch to hepatocytes culture medium for specific endoderm organoids;

The 3D epiblast cysts mesoderm differentiation:

According to the differentiation process, it is mainly divided into two phases, easly stage and late stage, and various factors are required dependenting on the process. The base medium details are listed as below:

Table3.5 3D Mesoderm differentiation medium preparation

Early mesoderm base medium			
Components	volume	Stock concentration	Final concentration
DMEM/F12	46ml		
5%Knockout serum	2.5ml		
Insulin-transferrin-selenium(ITS) 100X	500µl		
Non-essential amino acid (100X)	500µl		
Pen/Strep (100X)	500µl		
Total volume	**50ml**		
Late mesoderm medium base			
DMEM/F12	41.5ml		
15%Knockout serum	7.5ml		
Non-essential amino acid (100X)	500µl		
β-mercaptoethanol	50µl		
Pen/Strep (100X)	500µl		
Total volume	**50ml**		

After the mesoderm drops formed, from day0 to day4, the base medium is early mesoderm base medium, the later days are all late mesoderm base medium. But each day, the combinations of cellular factors and inhibitors are different.

Table3.6 3D mesoderm differentiation factors combination

Day0-day2	
Components	Final concentration
Chiron	10μM
LDN	0.5μM
Day2-day3	
Chiron	10μM
LDN	0.5μM
FGF2	20μg/ml
DMEM/F12	
Day3-day4	
Only early base medium	
Day4-day6	
LDN	0.5μM
FGF2	20μg/ml
HGF	10ng/ml
IGF	2ng/ml
Day6-day11	
IGF	2ng/ml
Day11 on	
HGF	10ng/ml
IGF	2ng/ml

The time for keeping mesoderm in culture is relied on the quality of differentiation. For example, when we perform the first attempt of mesoderm differentiation, after around one month, we found the mesoderm drops started to bacome flat and the 3D structure was decreasing thus we detached them and put them in suspension culture. They were fixed at around day 60.

Timeline of 3D epiblast cysts neuroectoderm differentiation is reported below.

Figure3.4 The schematic of media for neuroectoderm differentiation

1. After the seeding of iPSCs on bed, at day0, keep three days medium change with IPS-Brew plus 2% matrigel to form the 3D epiblast cyst;
2. From day3, induce the neural fate with the niN2B27 medium descriped before, add always 2%matrigel inside;

3. Keep epiblast cyst in niN2B27 medium plus 2%matrigel for 10 days, and then detached the beds with cold medium to release the neural epiblast cysts from the beds and culture in suspension in a low-adhension petri dish, the medium then is switched to niN2B27 plus BDNF and NT3, the two neurotrophic factors to help the maturation of neural organoids;

3.3.14 3D Immunostaining-organoids on bed

1. Remove the medium from the well, no PBS washes;
2. Add 1ml 2% PFA to the organoid on bed, fix under the chemical hood for at least 45 minutes, room temperature;
3. Three washes with PBS, 30 minutes interval, leave the drop inside the washing PBS for as much time as possible before the staining step;
4. Organoid permeabilization and blocking: remove the PBS from the well and add 1ml of 1%BSA in 0.5%PBST solution, leave at room temperature for 1 hour;
5. In the meantime, prepare an aluminum foil wrapped dark box, place a wet tissue and piece of parafilm on the wet tissue, keep these two layers tightly touched and make sure they are flat;
6. Prepare the primary antibody mix, usually diluted in 1%BSA in 0.5%PBST, the volume is 50 µl/bed;
7. Place a lid from the 1.5ml microcentrifuge tubes over the parafilm layer;
8. Use the needle and tweezer to take the cover slip (where the organoid is) from the well and place it on the lid;
9. Gently add the primary antibody mix drop by drop to the organoid, remember the distribute the drops evenly, the side with organoid has to face up, contacting the primary antibody;
10. Store the dark box at +4°C for 24 hours;
11. Put back the organoid to the well and three washes with 0.5%PBST, 30 minutes interval;

12. Prepare the secondary antibody mix, usually diluted in 1%BSA in 0.5%PBST, the volume is 50 µl/bed;
13. Use the needle and tweezer to take the cover slip from the well and place it on the lid again;
14. Gently add the secondary antibody mix drop by drop to the glass, remember the distribute the drops evenly, the glass side with the organoid has to face up, contacting the secondary antibody;
15. Keep the dark box at +4°C for 24 hours;
16. Put back the glass to the well and three washes with 0.5%PBST, 30 minutes interval, remember to protect from the light during the washes;
17. Leave the washing solution as much as possible before the mounting and image acquisition;
18. Add PBS+1% Pen/Strep to the well and keep the organoids at +4°C for storage;

3.3.15 Sample preparation for LC-MS/MS

During reprogramming, at every medium change or reprogramming transfection, medium was collected in three replicates, pooling together the conditioned medium from the same 40 channels for each replicate. The media were stored at -80°C until prepared for proteomic analysis. After thawing, media from four collections (two consecutive days) were pooled together. For example, sample D1-D2 was conditioned by the cells within the microfluidic chamber from day 1 to day 3 mornings. 3kDa cut-off centrifugation membranes (Amicon Ultra 0.5mL, Ultracel 3K, Merck) were used for filter-aided sample preparation (FASP). Proteins were concentrated by centrifugation for 20 minutes at 4°C and 14,000 g, then washed twice with a 50 mM triethylammonium bicarbonate (TEAB) buffer containing 8M urea. Protein content was quantified by Pierce BCA Protein Assay Kit. Each sample proteins were reduced for 60minutes at 56ºC with 100 mM DTT, and alkylated for 30minutes at room temperature in the dark with 55mM iodoacetamide. Samples were washed with 50mM TEAB for three times. An equal amount of proteins for each sample was digested by

trypsin at 37ºC for 16hours. Digested peptides were desalted by C-18 spin column and vacuum dried. Then, labeling by 6-plex Tandem Mass Tag (TMT6) was performed according to manufacturer's instructions using 50μg of peptides from each sample. The six-time point samples of each of the three replicates were pooled, then desalted and vacuum dried.

3.3.16 Mass spectrometry analysis

25 pre-fractions were collected on UPLC (Agilent 1290) with high pH C18 column (2.1mm x 30mm). Before MS analysis, peptides were resuspended in 10μL of 0.1% formic acid. Thermo Fusion Mass Spectrometer coupled with Thermo EasynLC1000 Liquid Chromatography was used to get peptides profiles. 90minutes of LC-MS gradients were generated by mixing buffer A (0.1% formic acid in water) with buffer B (0.1% formic acid in 80% ACN in water) by different proportions. Using NSI as the ion source and Orbitrap as the detector, the mass scan Range was at 300-1800 m/z, and the resolution was set to 120K. The MS/MS was isolated by Quadrupole and detected by Ion trap, whose resolution was set to 60K.

3.3.15 Proteomic bioinformatic analysis

Peak list files were searched against UniProt human reference proteome (UP000005640) by MaxQuant (v.1.6.3.4)[112].TMT6 modification and carbamidomethyl on cysteine were set as fixed modifications. The oxidation of methionine, acetylation of protein N-terminus, and phosphorylation (STY) were set as variable modifications. Peptide-spectrum matches (PSMs) were adjusted to 1% and then assembled further to a final protein-level false discovery rate (FDR) of 1%. Proteins not identified in at least 2 replicates in at least one time point were excluded from further analysis. Common contaminants (keratins and Bos taurus proteins) were also filtered out, for a final number of 4542 proteins identified. Missing values were imputed by the mean value of the other two replicates. TMT intensities were normalized according to BCA

quantification to obtain a relative quantification proportional to protein concentration in culture. The distributions of the three replicates of TMT intensities were scaled by their respective medians. A principal component analysis (PCA) was performed in MATLAB using mean-centered TMT intensities. Differentially secreted proteins between time pairs were assessed with student t-test, using a threshold of 5%. A list of secreted proteins was manually annotated by integrating the following resources: secreted proteins predicted by MDSEC as reported in Protein Atlas database secreted proteins in Gonzalez [113]; a list of ligands from Gene Ontology-Molecular Function categories "cytokine activity", "growth factor activity", and "hormone activity", and senescence-associated secreted proteins (SASP) annotated from literature[114,115,116,117]. Of the proteins identified in this study, only those secreted according to the criteria above were further studied, in order to avoid the proteins possibly derived from cell death. Proteins whose concentration was maximal only at the first time point (D1-D2 sample) were excluded from further analysis, as potential residual proteins from FBS used during fibroblast expansion. Functional enrichment analysis of Reactome pathways was performed using ReactomePA Bioconductor package. Reactome hierarchy was visualized using ClueGO[118]within Cytoscape[119]. Genes specific of different human embryonic stages were derived from a published single-cell RNA-seq study, of these core ECM genes were selected based on the annotations in Naba's group[120]. Proteins playing a role as ligands were taken from Ramilowski's group[121]. Hierarchical clustering with heat map data visualization was performed in MATLAB 2017a, using Euclidean distance and complete linkage.

3.3.17 Sample preparation for single cell sequencing

For each time-point, cells were detached using TrypLE-express. Harvested cells were then centrifuged at 300g and resuspended at the final cell density of 100cells/ml using a solution containing 40% KnockOut Serum Replacement in DMEM. For each timepoint, two replicates were produced, each containing cells from 4 independent chips that were pooled together then divided in aliquots containing 5000-80000 cells.

Samples were cryopreserved in DMEM supplemented with 40% KSR and 15% DMSO and stored in liquid nitrogen. scRNA-seq libraries were generated using one or two samples for each replicate. Each cryopreserved aliquot was thawed at 37 °C until a tiny ice crystal remained in solution. Then each sample was diluted under gentle shaking by dropwise adding 10 volumes of DMEM supplemented with 40% KSR. Cells were washed twice using a washing buffer containing 8% MACS Running Buffer in PBS. Cells were then resuspended in the washing buffer and filtered through a 40µm strainer. Cell viability and concentration were checked by visual inspection using Trypan Blue.

3.3.18 Sample preparation for single-cell ATAC-sequencing

scRNA-seq data pre-processing was mainly performed using the cellranger software (v 2.2). Fastq files were generated using the Cellranger pipeline mkfastq 10X standard Chromium barcode sequences. Alignment, filtering, barcode and UMI counting were performed using the Cellranger count pipeline. Human pre-built genome index has been applied (hg38 genome reference and GRCh38 annotation, including protein coding, and antisense RNAs). Each feature-barcode matrix from each independent sample was merged to build up the final dataset, consisting of 33694 genes and 44197 cells, then subjected to cells and genes filtering.

Cells having less than 1000 detected genes and with the mitochondrial associated reads percentage greater than 10% were filtered out. Furthermore, in order to have a homogenous sampling for each reprogramming day, the cell dataset was randomly subsampled to 2500 cells per time point. The final dataset retained only those genes expressed in at least 5% of all the cells, leading to 12932 total genes. Gene expression values were normalized to CPM (counts per million) and transformed to the log2 scale using a pseudocount. Finally, cell-cycle scores and, consequently, phases were assigned to each cell by Seurat's (v3.1.5)[122] CellCycleScoring function.

3.3.19 3D Immunostaining-Organoids in suspension and embedded

Remember to coat the plasticware used during all steps with 1%BSA solution to prevent the suspension organoids sticking the wall.

1. Coat the 1.5ml tube and the pipette tip with 1%BSA solution and transfer the organoids with the medium to it, keep the organoids environment moisturized;
2. Organoids fixation: remove the medium and add 1ml PFA 4%, leave it overnight;
3. Remove the PFA and wash with PBS at least three time over the day;
4. Cryoprotection: remove PBS and add 1ml 30% Sucrose, leave it overnight at room temperature;
5. Prepare a labelled 1.5ml Eppendorf tubes with a plastic foil (double layer) on the cap; in the meantime, prepare a dry ice box and liquid nitrogen;
6. Embedding and freezing: aspirate most of the sucrose from step 4;
7. Transfer the organoids (usually 3-5 organoids) in sucrose onto the cap that prepared in step 5;
8. Remove the residual sucrose, add OCT solution to embed all organoids;
9. Use a tweezer to pinch the neck of the eppendorf tube, go inside the liquid nitrogen tank, freeze slowly in the nitrogen vapor;
10. Close the eppendorf tube very tightly and transfer to dry ice immediately;
11. The frozen organoid samples should be stored at -80℃.

3.3.20 Blood outgrowth endothelial cells (BOECs) medium preparation

The basal medium package used to isolate and culture blood outgrowth endothelial cells (BOECs) from the peripheral blood mononuclear cells (PBMNCs) is the EBM™-2 Basal Medium and EGM™-2 SingleQuots™ Supplements.

The EGM™-2 SingleQuots™ Supplements contain as following, 1 bottle of FBS, 10.00 ml,1 vial of Hydrocortisone, 0.20 ml, 1 vial of hFGF-B, 2.00 ml, 1 vial of VEGF, 0.50 ml,1vial of R3-IGF-1, 0.50 ml, 1vial of Ascorbic Acid, 0.50 ml, 1 vial of hEGF,

0.50 ml, 1vial of GA-1000, 0.50 ml and 1vial of Heparin, 0.50 ml. Add all supplements(apart from the FBS and Heparin) to the basal medium. Instead of using the normal FBS, we use the defined FBS, which is a stem-cell grade FBS, helpful for the endothelial cells growth.

1.The BOECs generation medium:

40ml of the basal medium;

10ml of defined FBS;

50μl of heparin;

500μl of Pen/Strep;

2. The BOECs reprogramming medium:

50ml of the basal medium;

500μl of Pen/Strep;

The FBS and heparin will affect the transfection efficiency because heparin is a highly charged protein that will interfere with the transfection reagent.

3.3.21 Endothelial cells isolation from peripheral blood

Equilibrium Ficoll-paque solution and BOECs generation at room temperature.
Step 1: Blood Collection and Density Gradient Centrifugation

1. For each donor, collect 50ml of blood by venipuncture from the local hospital. Dilute the blood with 50ml of sterile PBS. It is essential that blood samples are processed within 2 hours of collection. Delayed processing of blood results in a marked reduction in outgrowth colony yield;
2. Prepare new falcon tube containing 20ml of the density gradient centrifugation (Ficoll-paque) solution at the bottom, gently add 20 ml of the diluted blood on the top of Ficoll-paque solution, do not mix these two layers;
3. Centrifuge samples at 400g for 45 minutes at room temperature with the accelerator and the brake off;
4. During this centrifugation period, begin the collagen coating process;

Step 2: Collagen Coating of T-75 Flask and Preparation of Culture Medium

1. Prepare a 50μg/ml collagen solution by diluting stock type I collagen in 10 ml of 0.02M acetic acid;
2. Add 7.5ml of the collagen solution to a T-75 cell culture flask. This volume gives 5μg collagen/cm^2 (or 375μg/flask). Coat flask for 1 hour at room temperature;
3. After the 1-hour coating, aspirate the collagen solution and wash away residual acetic acid by pipetting in 10 ml distilled water, repeat washing for three times. Aspirate off the distilled water and change with 5ml of BOEC generation medium to keep the collagen coating from drying-out;

Step 3: Collection and Plating of PBMNCs

1. Following the density gradient centrifugation outlined in step 1.3, carefully collect the buffy coat layer using a sterile plastic transfer pipette. Collection of the buffy coat should yield approximately 20 ml of cell suspension and plasma from each tube. Avoid transferring the Ficoll-paque solution;
2. Dilute the PBMCs with 1:1 PBS, vortex to dilute thoroughly. Centrifuge at 300g for 35 minutes at room temperate;
3. Following centrifugation, aspirate the supernatant and resuspend cells by adding 1 ml of BOEC generation medium to each pellet and pipetting up and down repeatedly. Pool cell suspensions and top up total volume to 10 ml with the remaining medium;
4. Plate entire cell suspension into a single, collagen-coated T-75 flask, top-up medium volume to 15ml/flask and culture at 37 °C, 5% CO_2 incubator. Cells plated at this time represent passage 0.

3.3.22 Long-term BOECs culture

1. Change medium three times per week, usually on Monday, Wednesday and Friday; Replace 15ml of fresh BOEC generation medium every time;

2. Monitor the BOEC culture flask on days 20-28 for the appearance of outgrowth colonies. Identify colonies as circular groups of cells exhibiting a classic endothelial cobblestone morphology;
3. Once a colony or multiple colonies are identified in the flask, continue with medium changes and allow colonies to grow to approximately 1000 to 2000 cells per colony before passaging. Determine the cell number per colony through a rough visual estimation;
4. Passage cells by rinsing flasks twice with 10 ml of DPBS. Add 5 ml of 0.25% trypsin-EDTA and incubate in a 37°C incubator for 5 minutes. After 5 minutes, neutralize trypsin with 10 ml of medium (containing FBS) and bring cells into suspension with repeated pipetting; Centrifuge suspension at 300g for 5 min, resuspend in 15 ml of fresh BOEC generation medium and plate entire cell suspension into a new T-75 flask (representing passage 1, P1). From P1, collagen coating is optional, but collagen type I coating is highly recommended due to our experience;
5. Continue medium changes as described above until cells are confluent (roughly 3-5 x 10^6 cells per flask). Once confluent, repeat the passage cells as described above;
6. For continued passaging, plate no fewer than 750,000 cells per T-75 flask as low cell densities can cause the BOECs to stop proliferating;
7. Trypsinize cells and centrifuge at 300g for 5 minutes. Aspirate the supernatant and resuspend in 1ml of BOEC generation medium(i.e. we freeze the entire flask in 2 vials). Add 400µl of FBS and 100µl of DMSO to each vial, add 500µl of cell suspension in each vial and transfer to -80°C freezer by the cryobox.
8. For long-term storage, move the vials to liquid nitrogen.

3.3.23 BOECs reprogramming based on the microfluidics

1. Coat the micro-channel with 200µg/ml collagen type I solution in a 37 °C incubator for 2 hours;

2. After the coating, wash the channels with distilled water for 3 times and replace with BOECs generation medium;
3. Rinsing the flask twice with 10 ml of DPBS. Add 5 ml of 0.25% trypsin-EDTA and incubate in a 37 °C incubator for 5 min, stop the trypsin reaction with BOECs generation medium (defined FBS inside). Collect everything and centrifuge at 300g for 5 minutes, remove the supernatant and resuspend the cell pellet in an appropriate amount of BOECs generation medium and count the cell number;
4. Seed 200cells/mm^2 to the microchannel at day0 and place the whole chip inside a 10-cm dish with PBS around, do not let the PBS go inside the chip;
5. From day1, check the confluency of BOECs inside the channel. If the occupancy is less than 50%, wait for 2-3 days for cells to grow. When the cell occupancy reach 80%, the daily mRNA transfection starts;
6. Since BOECs is more dedicate to the microenvironment, we set a gradual reprogramming adaptation steps at night. From day1-day3, the reprogramming medium is 100% BOECs reprogramming medium, from day4-day7, the reprogramming medium is 75% BOECs reprogramming medium plus 25% Nutristem medium, from day8-day10, the reprogramming medium is 50% BOECs reprogramming medium plus 50% Nutristem medium; During the adaptation process, be cautions to check the cell viability all the time. When the BOECs mortality increases too much due to the mRNA transfection, increase the percentage of BOECs generation medium to help them recover. In the morning, the BOECs generation medium is always used;
7. From day11-day13, when the BOECs-iPSCs start to emerge, switch the reprogramming medium to 100% Nutristem medium, there is no more BOECs reprogramming medium for the transfection process. From day15, since big iPSCs colonies begin to form, stop the transfection step and switch the medium to IPS-Brew medium to maintain the newly formed BOECs-iPSCs;
8. Extract the BOECs-iPSCs from the chips, following the instructions in 3.3.7.

Chapter 4 Experiment results

4.1 Explore the reprogramming process under microfluidics

4.1.1 Daily morphology change during the reprogramming steps in microfluidics

After one hour of vitronectin coating at room temperature, fibroblasts (BJ lines are mostly used) are seeded at day0 at the density of 60cells/mm^2, which equals to 1620cells/channel. Because the glass surface sensitivity, in order to maintain the basic starting cell numbers, we seed the double of the cells required due the loss of attachment and death, so actually 3240cells/channel was seeded. From day1, daily mRNA transfection was required, accompanying with the reprogramming medium (Nutristem+20ng/ml FGF2). According to fibroblast proliferation and transition speed, low/medium/high dose are adapted as we mentioned before. After 8days of mRNA transfection, from day9, medium is switched to IPS-brew until the iPSCs extracted on day14.

As we could see from Figure 4.1, after seeding, at day1, the fibroblasts are long, and spread evenly, occupying most of the surface.

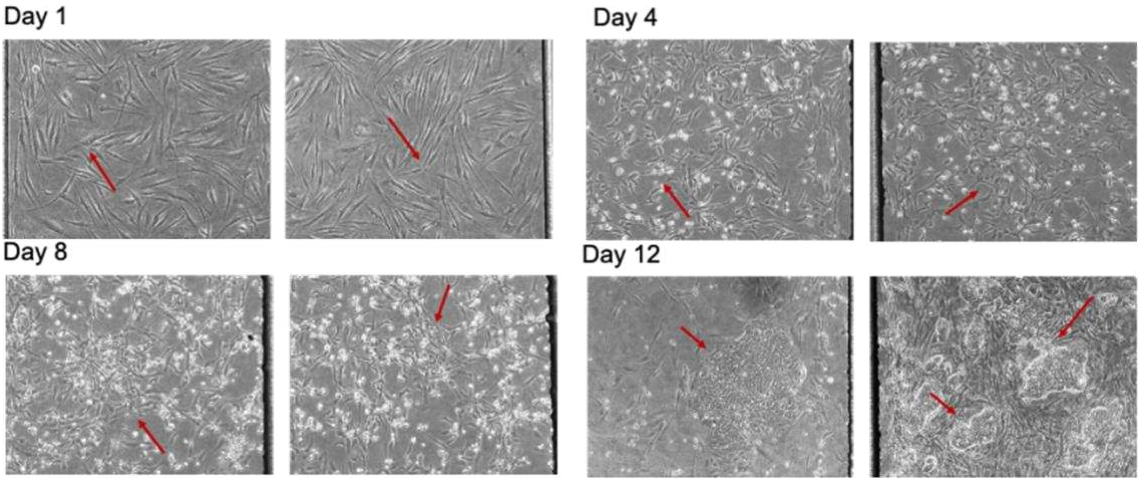

Figure 4.1 the representative morphology changes during the reprogramming process

From day4, their morphology starts to change. The bright spots mean cells go on apoptosis because the mRNA transfection is toxic, but survived fibroblasts keep transition meanwhile proliferating; At day8, the morphology change is more evident. From day 9, medium is switched to IPS-Brew, that is a widely used stem cell maintenance medium, the newly formed iPSCs colonies are maintained and keep growing in dimension. From the picture of day12, we could see the iPSCs colonies are super compact, the single cell inside the colony could not be distinguished from each other.

4.1.2 iPSCs colonies extraction from the micro-channels

At day14, iPSCs colonies are mature and need to be extracted from the micro-channel because the microfluidics are too limited microenvironment for compact colonies to grow, otherwise these iPSCs colonies will start to detach from the bottom glass, also because after two weeks, coating is thoroughly consumed (Figure 4.2).

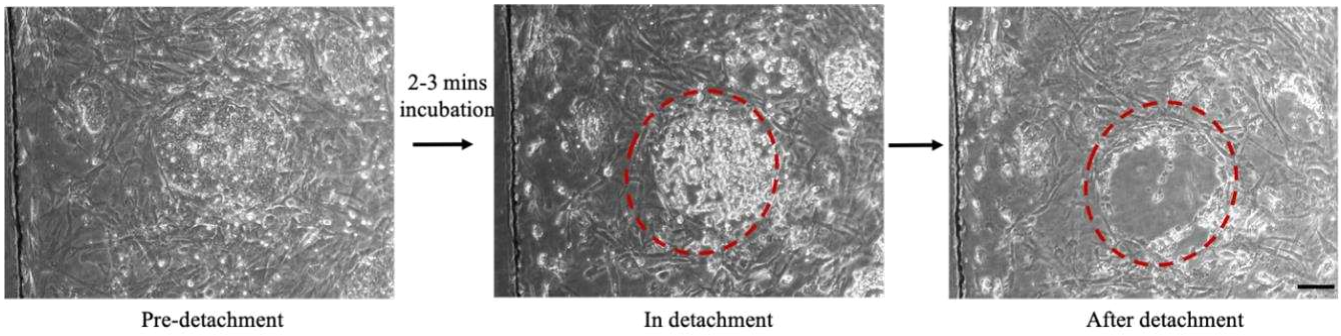

Figure 4.2 the iPSCs colonies detaching from the microfluidic chips

After two washes with PBS inside the micro-channel, 15µl of EZ-LiFT Stem Cell Passaging Reagent is added per channel. EZ-LiFT s a proprietary enzyme-free and chemically defined stem cell dissociation reagent that selectively passages only undifferentiated pluripotent stem cells. The reagent eliminates the need for manual removal of differentiated cells and produces high cell viability. After iPSCs colonies incubating at 37℃ for 2-3 minutes, they start to become bright from the edge to the center and are detaching, while other surrounding cells are still tightly attached. Mechanically pipetting is needed to detach all iPSCs colonies. Then they are collected and transferred to a multi-well plate. After the detachment, as we could see from the

figure 4.2, only the iPSCs colonies are selectively detached, but all other cells around are still left inside the channel.

4.1.3 immunostaining of pluripotency inside the micro-channel

Apart from extraction from the chips, we also keep some microchannels in culture and perform an immunostaining of pluripotency markers inside the chips, like the most frequently used marker, Tra-1-60 and Nanog. The 2D immunostaining inside the microchannels share the same process, but they have to be carefully handled in case that the iPSCs colonies may be washed away by the shear stress.

As we see from the Figure 4.3, firstly, the iPSCs colonies are formed everywhere inside the channel, especially more crowed near the outlet reservoir. It may be due to the less flow and evaporation stress of the outlet. iPSCs colonies have both TRA-1-60 and Nanog strongly expressed. TRA-1-60 is a cell membrane protein, which we could see they are on the surface of the colonies, while Nanog is a transcriptional factor, expressing in the nuclei. However, when image acquired directly from the microchips, there will be problems like the light reflection because of the PDMS layer, that is why we see the light dots near the inlet from Figure 4.3.

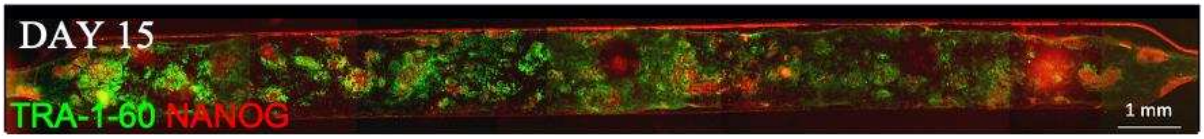

Figure 4.3 2D immunostaining of pluripotency markers, Tra-1-60 and Nanog, inside the microchannel.

4.1.4 Secretome analysis during reprogramming.

Tandem mass spectrometry (LC-MS/MS) was used to examine the dynamic alterations of cell-secreted proteins during the reprogramming of human fibroblasts on conditioned medium collected from microfluidic channels every two days (Fig. 4.4A).

The great effectiveness of microfluidic reprogramming was maintained in a medium that only three types of proteins, the FGF2, INS and transferrin present. We were able to measure each protein relative to the others by protein tagging. We measured 4542 proteins that were found in two (19%) or three replicates (81%) of the

samples. The samples exhibit great reproducibility between replicates and a predictable temporal course, according to a principal component analysis (Fig. 4.4B).

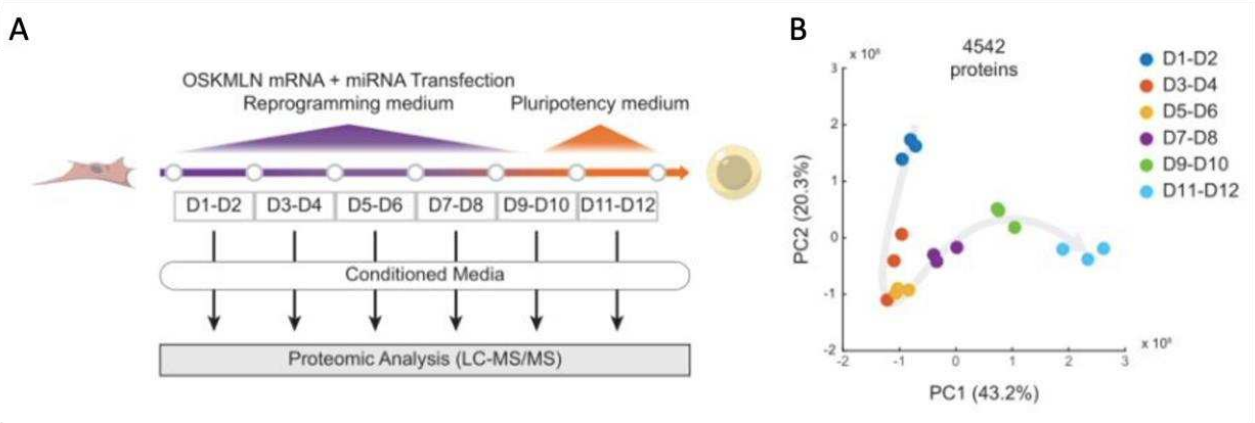

Figure 4.4 Secretome analysis**.** A) Experimental design for proteomic experimental data collection. Proteomic data were obtained by tandem mass spectrometry analysis of conditioned media along the same reprogramming experiments. B) Principal component analysis of the 4542 proteins detected in at least one time point. Each sample of proteomic data refers to medium conditioned over a 48-hour period.

4.1.5 Embryonic ECM accumulates during reprogramming

Many extracellular matrix (ECM) related categories were highly significant, including ECM deposition, degradation and remodeling, and both integrin- and non-integrin-mediated cell-ECM interactions. A previous RNAi screen also identified the critical role of cell adhesion in human reprogramming, highlighting the role of intercellular factors needed for filament assembly, branching, and disassembly[123] .

In our data, we found an overall increasing trend of ECM-related protein accumulation, with different ECM components exhibiting distinct dynamics (Fig. 4.5A). These dynamic changes started already at days 3-4 (SPP1, COL4A1/2, SPARC), in some cases at days 5-6 (LAMC1), or even later (COL18A1). We wondered whether the observed global changes somehow resembled embryo development stages. To address this question, we selected the ECM proteins in our data that were previously reported to be expressed at mRNA level at different stages of human embryo development. The concentration dynamics of these proteins in our system showed the progressive establishment of an ECM that recapitulates the one deposited at the stage

of the late inner cell mass (Fig.4.5A). In conclusion, our data support the idea that during reprogramming, not only fibroblasts are converted to a primed pluripotent phenotype, but also the extracellular context is shaped accordingly.

Looking at the temporal profiles of enriched signaling pathway proteins and ligands (Fig.4.5B), we found a progressive accumulation of proteins that were previously shown to play a role in mouse cell-non-autonomous reprogramming regulation: some senescence-associated secreted proteins (SASP), such as CXCL1 (also known as Gro-α), CXCL8, CCL2, IL6; YAP-target CCN1, also known as CYR61; inflammatory cytokines, such as IL6/11/19, CSF1/2/3, LIF. We found that JAK-STAT pathway, downstream of interleukin signaling, was also significantly differentially expressed at transcriptomic level between freshly-derived microfluidic hiPSC colonies and the same colonies after 3-passage expansion in conventional wells. We conclude that secreted proteins follow precise dynamics during reprogramming and encompass a number of potential regulators of autocrine/paracrine signaling, including those involved in ECM-mediated and soluble communication.

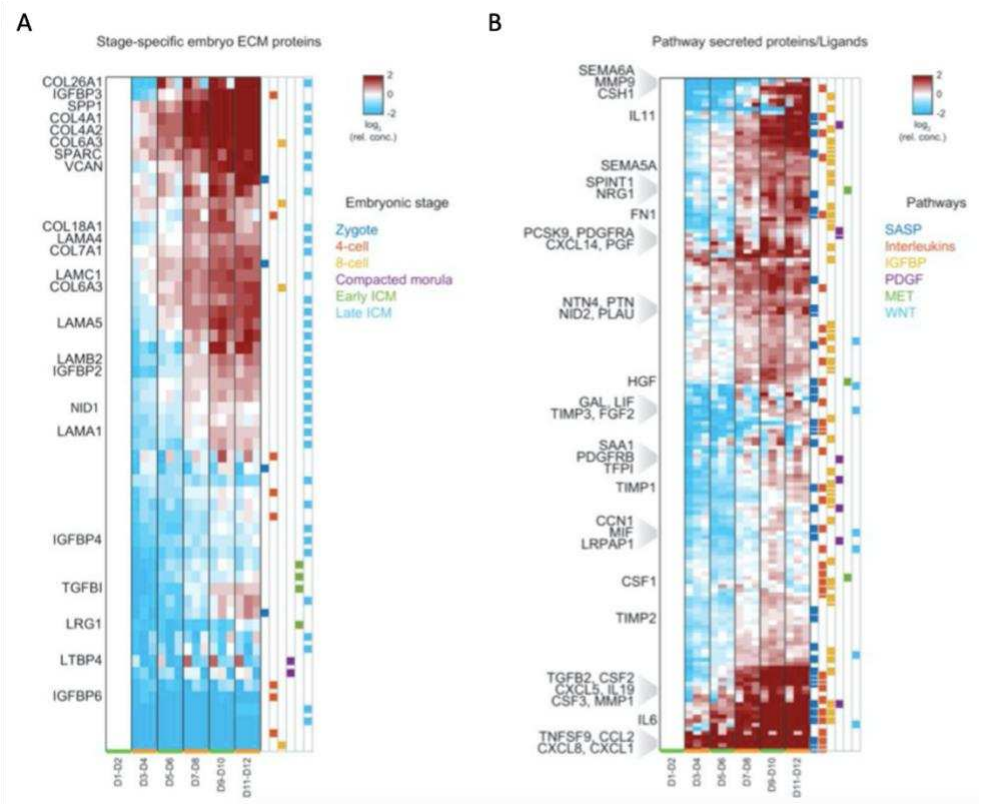

(Figure legends shown in next page)

Figure 4.5 Proteomic analysis of cell-secreted proteins demonstrates a rich extracellular signalling environment along human fibroblast reprogramming. A)Hierarchical clustering of proteins identified in this study and belonging to the core ECM components at specific stages of embryo development. B)Hierarchical clustering of secreted proteins from the following enriched signaling pathways (according to Reactome database)

4.1.6 Single-cell RNA-seq analysis showing cell population heterogeneity during reprogramming

High-throughput single-cell RNA sequencing was used to determine the cellular subpopulations that emerged during human somatic cell reprogramming and their function in the release of signaling molecules (scRNA-seq). Cells were collected before the first transfection (D0), 3 days after transfection (D3) and then every 2 days(D5-D15) during the high-efficiency reprogramming of human fibroblasts in microfluidics. We generated scRNA-seq libraries from independent captures for at least two replicates per time-point, collecting altogether more than 40000 single-cell transcriptomes. Dataset quality control,filtering and down-sampling to 2500 cells per time point produced 20000 high-quality single-cell transcriptome profiles, with a median of 5464 genes detected in each single cell for a total of 12932 total detected genes. Data dimensionality was reduced using the Force-Directed Layout Embedding (FLE) algorithm. The resulting FLE diagram (Fig. 4.6B) illustrates the expression profile of each cell as a point in a Euclidean space where cells are grouped based on their transcriptional similarity.

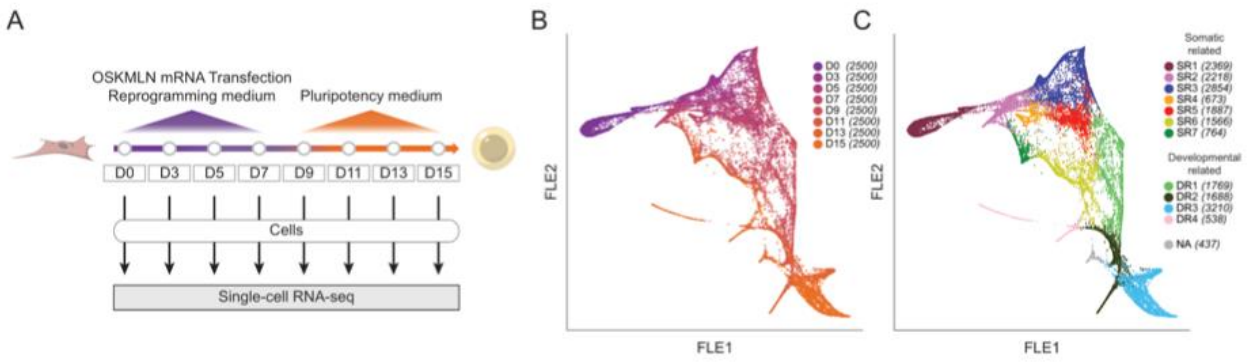

(Figure legends shown in next page)

Figure 4.6 Single-cell RNA-seq analysis of human reprogramming cells. A) the experimental design for single-cell RNA-seq data collection. Human BJ fibroblasts were grown in Pluriton medium and daily transfected with OSKML mRNA. Starting from day 9, cells were grown in IPS Brew Medium till day 15. Samples were collected by stopping parallel experiments at day 0, 3 and every 48 hours. B) Force-Directed Layout Embedding (FLE) map showing the distribution of cells across time-points and C) identified clusters. SR: somatic-related, DR: development-related

We observed high homogeneity of the fibroblasts population at day0 (D0) and higher heterogeneity thereafter. To characterize this heterogeneity, we clustered cells using an 29 unsupervised community detection algorithm , that resulted in 12 clusters (Fig. 4.6C). SR means somatic-related clusters, whereas 4 clusters were highly enriched by the developmenta signature DR stands for developmental-related clusters.

Fibroblasts (SR1) and cells captured at earlier days (SR2-5), while DR clusters were enriched by cells collected at later time points (from D9 to D15) and highly cycling (Fig.4.7A). However, more than 97% of SR6 and SR7 cells were sampled from day11(Fig.4.7A) and were characterized by low but detectable expression of embryonic genes (e.g. POU5F1, LEFTY2) and were negative for NANOG, indicating reshaping of fibroblast identity but at the same time inefficient acquisition of pluripotency. Furthermore, these cells are in the G0/G1 phase of the cell cycle, thus confirming their somatic nature and suggesting peculiar identity in the reprogramming timeline (Fig.4.7A). Despite their developmental features, DR4 cells also did not express NANOG, while showing high and very specific transcriptional levels of mesoderm genes (i.e.CER1, EOMES), suggesting a possible similarity with a differentiating stage. Whilst DR clusters appear to contain the productively reprogramming cells, the role of the SR clusters is less clear (Fig. 4.7B). To address the role of SR clusters we perform Gene Set Enrichment Analysis (GSEA) using the secreted proteins previously identified and some gene signatures that were found enriched in the proteomic analysis (Fig. 4.7B). Surprisingly, the secreted proteins detected by mass spectrometry appear to be transcribed by the cells in the SR clusters, except for SR3 that might not be involved in the secretory phenotype. These results highlight the presence of an unproductive somatic fate, whose role is to express and secrete those factors that we found to be shaping the extracellular environment during

reprogramming and that have been found to characterize later stages of embryonic development.

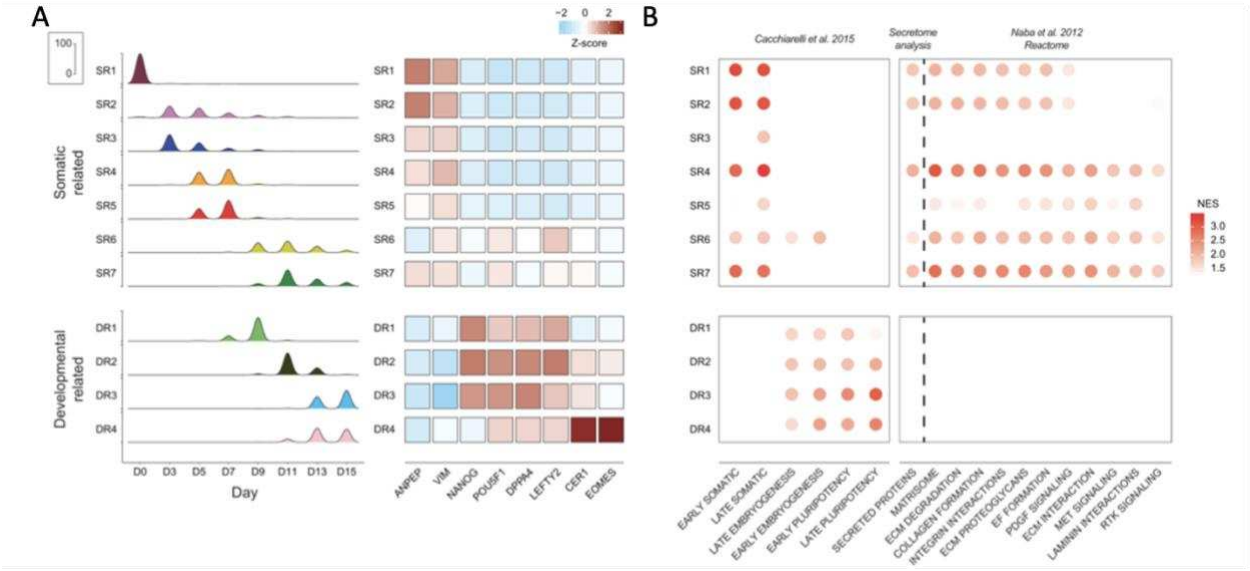

Figure 4.7 Single-cell RNA-seq analysis of human reprogramming cells. D) Time-points enrichment for each cluster (left) and heatmap of Z-scored normalized counts, averaged by clusters, for key reprogramming related genes (right). NA cluster not shown. E) GSEA results for each cluster. Only significant results are shown. NES, Normalized enrichment score.

4.1.7 Signaling contributions from different cellular subpopulations

Among all the gene sets analyzed, matrisome and Late pluripotency associated genes were found to best describe the phenotype of D13-15 endpoints (Fig. 4.8A). Therefore, we decided to computationally investigate the routes linking such states to the somatic start-point by applying Waddington Optimal Transport (WOT). Results showed a common path until day 5 (D5), after which cells started to exhibit different trajectories (Fig. 4.8B).

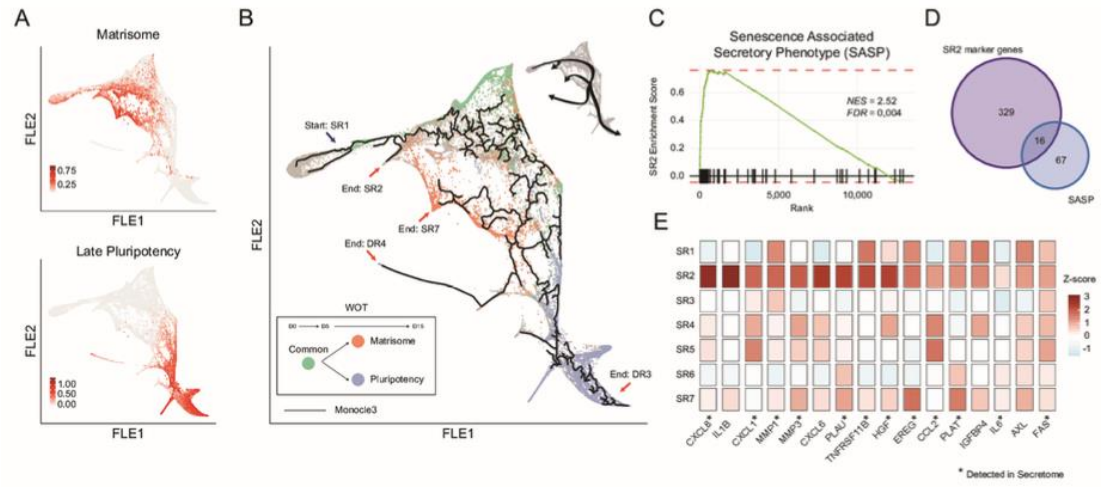

Figure4.8. Trajectory inference reveals different fates during reprogramming. Gene expression-based interaction analysis suggests an existing crosstalk between somatic and reprogramming cells through known and novel ligand-receptor couples. A) Matrisome and Late pluripotency enrichment scores shown along the FLE map. B) Monocle3 (black line) and WOT (colored dots) trajectory inferences are displayed on the FLE graph. Arrows point to the starting point (blue) and 4 end points (red) of the inferred trajectories. A representative scheme of the trajectories is shown on the top-right. C) Enrichment Score graph relative to the GSEA of SR2 cluster for senescence-associated secreted proteins geneset (SASP)50–53. Black lines on the x axis represent a match between the ranked list and the geneset analyzed. NES, Normalized enrichment score. FDR, False Discovery Rate. D) Venn diagram representing the intersection between SASP geneset and SR2 cluster marker genes and their relative gene expression, shown in a E) heatmap of Z-scored normalized counts, averaged by clusters. Genes with * have been detected in secretome analysis

Therefore, we decided to computationally investigate the routes linking such states to the somatic start-point by applying Waddington Optimal Transport (WOT). Results showed a common path until day5 (D5), after which cells started to exhibit different trajectories (Fig.4.8B). We validated these findings through an unsupervised pseudotime-based approach using Monocle, which not only confirmed the bifurcation at day7 (D7) leading to endpoints inside SR7 matrisomal and DR3 pluripotent clusters, also introduced two additional outcomes inside DR4 and SR2, respectively (Fig. 4.8B). While the mesodermal nature of DR4 was previously assessed, we focused on the characterization of SR2. GSEA using common pathways revealed the enrichment for terms related to signaling molecules, therefore, we hypothesized that this cluster might be implicated in the secretion of the ligands detected in the medium. Most of them were significantly enriched, with SASP having the highest enrichment score (Fig. 4.8C). We found SASP genes are highly expressed and specific of this cluster, such as cytokines (CXCL1, IL1B, CXCL8), metalloproteases (MMP1, MMP3), HGF and its activators, PLAU and PLAUR (Fig. 4.8D-E).

In conclusion, we were able to define human somatic reprogramming as a process consisting of two major outcomes, matrisomal and pluripotent, deriving from the same starting cells which bifurcate around day7(D7). Moreover, among matrisomal somatic cells, we identified and characterized an early subpopulation of cells which contributes to the expression and secretion of SASP-related signaling molecules.

4.2 Explore the microfluidics-based nascent iPSCs for modeling human development *in vitro*

4.2.1 Highly efficient generation of nascent iPSCs from microfluidics

The newly generated iPSCs are called nascent iPSCs throughout the whole experiments. Nascent iPSCs were extracted at day14 and transferred to multi-well for expansion. After the centrifugation step, we resuspend the cell pellets to single cell and count the total number we got from each channel from one chip.

As we see from the Figure 4.9, we counted the generation of iPSC from 5 channels of one chip, the average number for one channel is around 3400 cells, while we seed around 3700 fibroblasts at day0. However, there is also great variability among channels, like we could read from the top dot, which means from this channel, 8000 iPSC were generated while at the bottom, we could only generate less then 500 iPSC from another channel. These channels belong to the same chips, but still we see difference between. Also we see the first and the fifth channel, which are at the edges of the chip, usually have low yield of iPSCs and higher mortality. This may due to the PBS or water inside the petri dish are more easily to go in, also sometimes due to the attachment of PLASMA treatment in the micro-chip fabrication process.

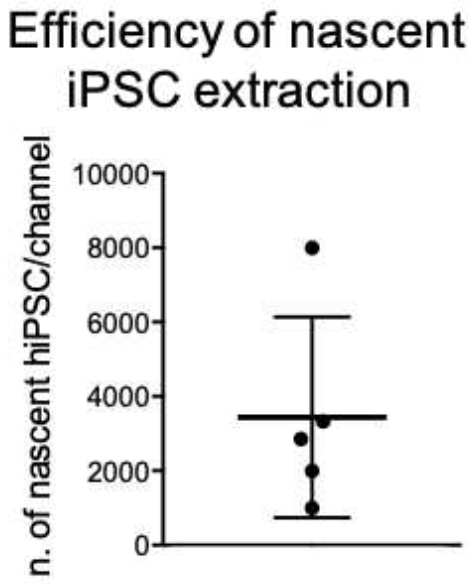

Figure4.9 Nascent iPSCs production efficiency.one dot present one channel.

4.2.2 Nascent iPSCs are less methylated than high passage established iPSCs lines

DNA methylation is an important part of epigenetics. Methyl groups add to the promotors and repress gene transcription. We know from the literature that methylation state increases while the iPSCs passage increasing, which could significantly affect the iPSCs capability of differentiation. 5-Methylcytosine is a methylated form of the DNA base cytosine (5mC) that regulates stable and long-term gene transcription. On the other hand, histone H3 lysine 9 methylation (H3K9me) is marker of heterochromatin methylation that mediates the gene silencing.

Immunofluorescence staining was performed against the 5mC and H3K9me to test the methylation state between the nascent iPSCs (P1) and high passage iPSCs (P18), as shown in Figure 4.10.

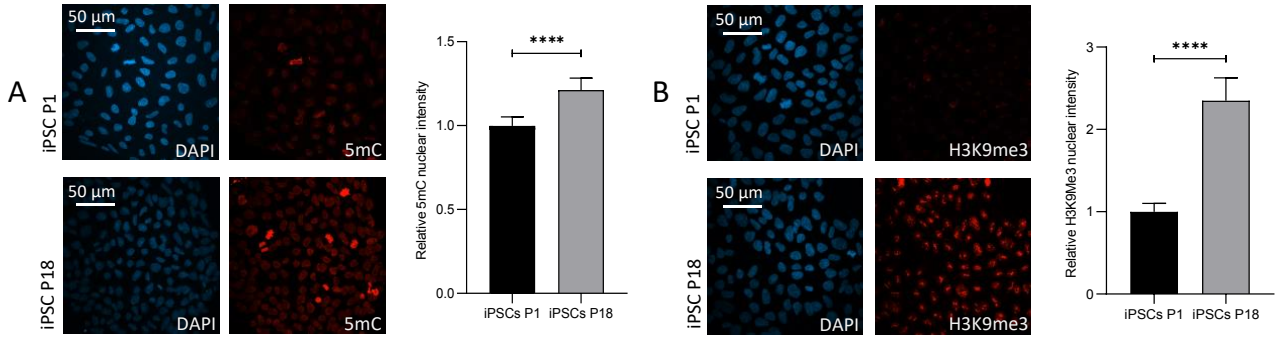

Figure 4.10 Methylation comparison between nascent iPSC(P1) and high passage iPSCs(P18).A) the 5mC staining and quantification; B) the staining of H3K9me3 and quantification.

Both 5mC and H3K9me3 expression are low in nascent iPSCs, especially the H3K9me3, from the staining, there were no signal. But the 5mC and H3K9me3 are both higher in P18 iPSCs line, the H3K9me3 is expressed in all cells. The quantification of 5mC and H3K9me3 are significantly different, which means the nascent iPSCs have low methylation state, owing higher potential and advantages in terms of differentiation capability.

4.2.3 Homogeneity of nascent iPSCs

Nascent iPSCs were extracted from the microchips and cultured in multi-well format for 2 days for cleaning and expansion before seeding into 3D epiblast cysts. In order to test the homogeneity and quality of nascent iPSCs generated from the microfluidics, 2D immunofluorescence staining was firstly performed.

Immunofluorescence staining of pluripotency markers and cell intermediate filament (i.e. OCT4 and phalloidin) showed the homogeneity and robustness of microfluidics-based nascent iPSCs (Figure 4.11). We were able to generate and select high quality of iPSCs and remove all the non-reprogrammed cell population.

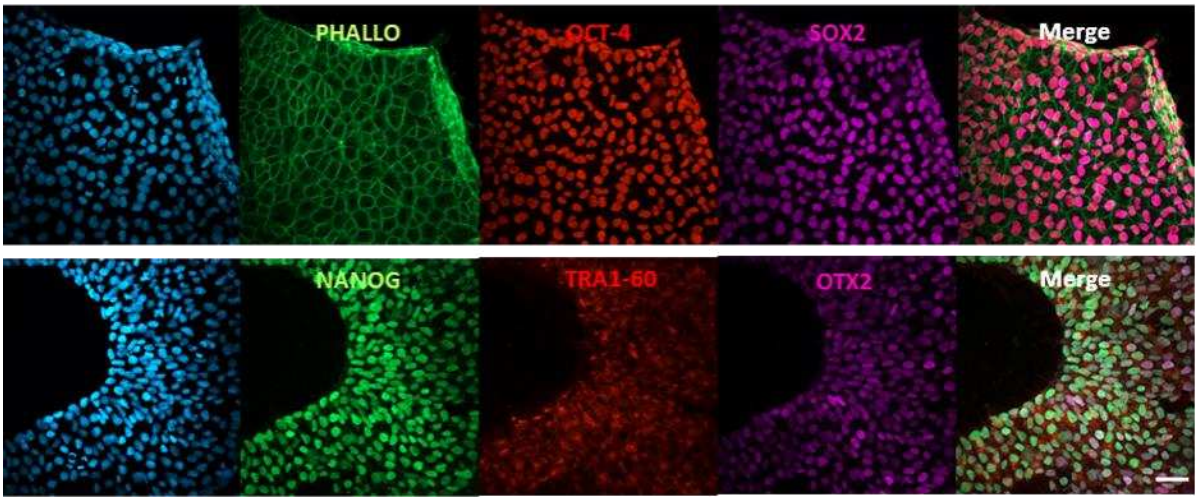

Figure 4.11 Homogeneity of nascent iPSCs.OCT-4, TRA-1-60, SOX2, NANOG and OTX2 are pluripotency markers, phalloidin stands for intermediate filaments. Scale bar: 50μm.

4.2.4 2D differentiation of nascent iPSCs

After the extraction of iPSCs, they are seeded also on monolayer to test their differentiation potential. Following the combination of factors and inhibitors mentioned in Section 3.3.9 and base medium guidance, three germ layer differentiations are directed. Early germ layer markers are tested.

According to 2D differentiation protocols, iPSCs were fixed and checked for the germ layer markers. Ectoderm started from 100% iPSC confluency and checked after 5 days. Pax6 and Sox1 were positive for early neuroectoderm differentiation. Sox17 and FOXA2 showed iPSCs obtained the ability for endoderm differentiation. The non-

expression of OCT4 and NANOG, but the expression of Brachyury showed they could be changed into mesoderm cells. They all exist from pluripotent stage.

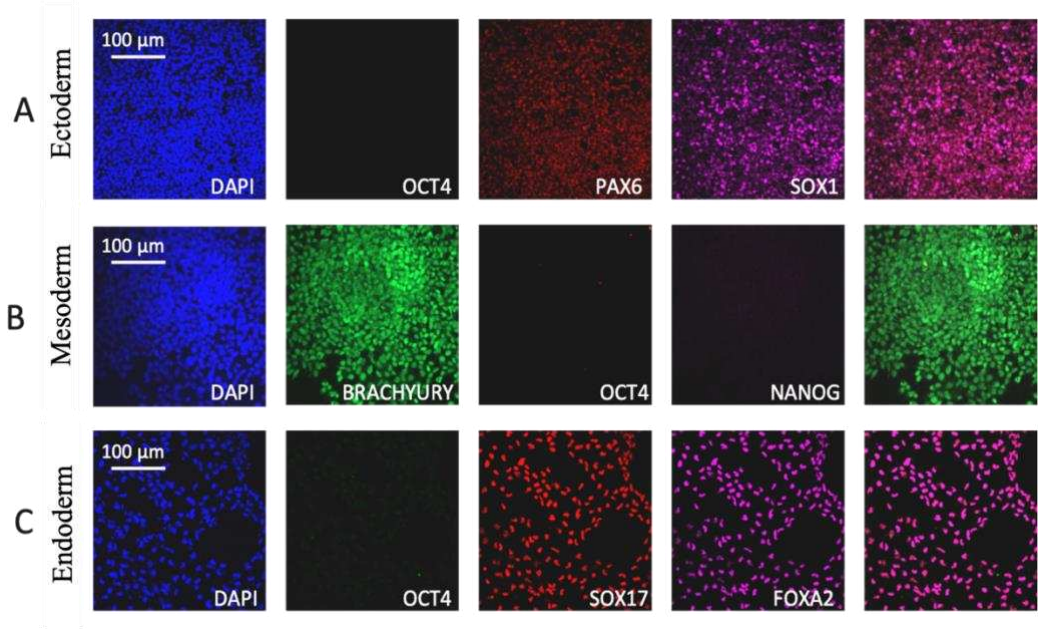

Figure 4.12 2D differentiation of nascent iPSCs into three germ layers. Oct4 and Nanog are pluripotent marker. A)Early ectoderm markers, PAX6 and Sox1;B)Early mesoderm marker, Brachyury; C)Early endoderm marker,Sox17 and FOXA2.

4.2.5 Robust 3D generation of epiblast cysts on bed from nascent iPSCs

Nascent iPSCs are cultured for two days before seeding on matrigel bed. At day 0, nascent iPSCs are detached into single cells. Thanks to the high proliferate rate and plasticity of nascent iPSCs, the seeding density could be cell adjusted to as few as 5000cell/bed. ROCK inhibitor is required only at the seeding day. After 24 hours, medium is changed with 2% matrigel inside. Matrigel adds matrix to the medium, which form a sandwich structure to help the iPSCs assembly and form an epiblast cyst shape from day1. Epiblast cysts are tracked both by numbers and dimension, to check the ability of forming 3D structure for later differentiation. The schematic drawing of seeding nascent iPSCs (P0), without any passaging after extraction, is shown in Figure 4.13.

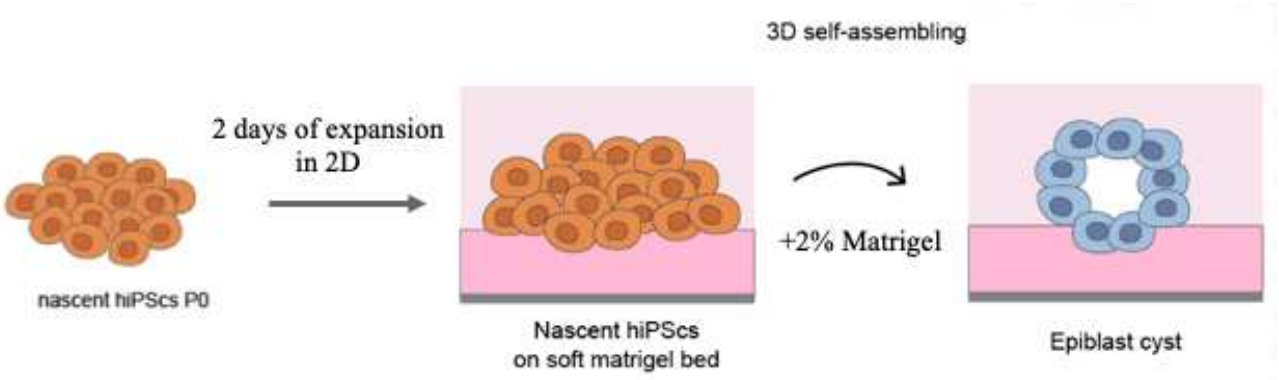

Figure 4.13 Schematic of seeding nascent iPSCs(P0) on matrigel bed.

After 24hours, ROCK inhibitor is removed by medium changing. IPS-Brew medium plus 2% matrigel needs freshly prepared and changed every day to form the 3D epiblast cysts structure (Figure 4.14). Epiblast cysts are kept in culture up to 7days while germ layer differentiation starts from day3.

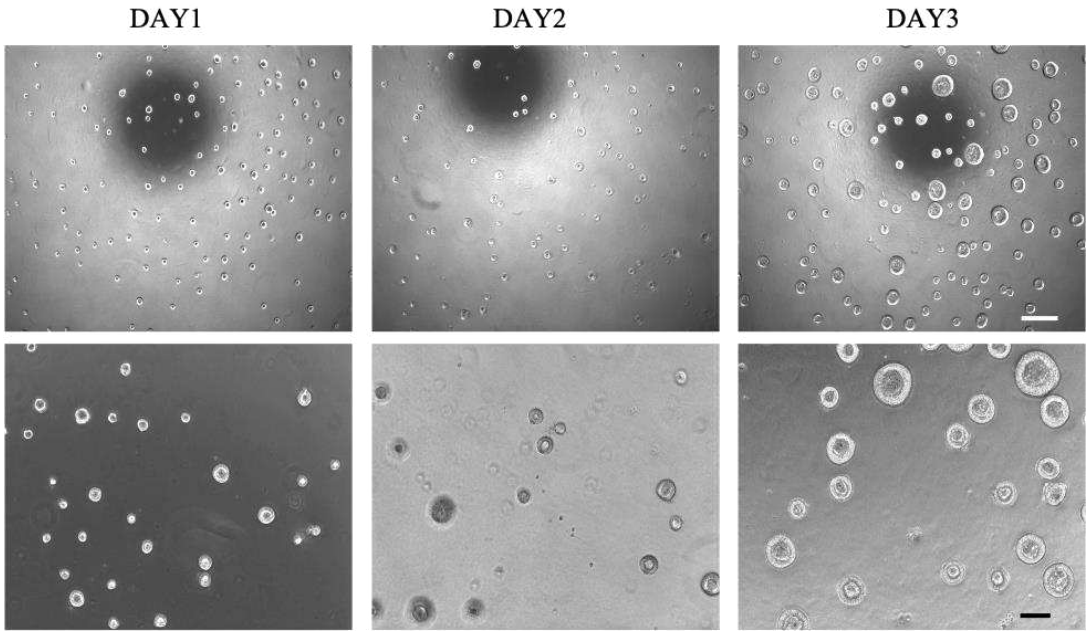

Figure 4.14 Bright field of epiblast cysts from day1-day3. Scale bar:100μm

Epiblast cysts formed from day1 after matrigel was added in the medium at 2%. Here we showed the first 3 days of epiblast cysts cultured on matrigel beds, their size increased during the culture. Also we saw a clear lumen formed inside the epiblast cysts from day1. We tracked the growth rate by measuring the diameter of each epiblast cyst from day 1 to day 7.

The dimension of nascent iPSCs epiblast cysts increased at a steady pace, the diameter of the first day was bigger than 50μm, and when it reached day3, the diameter increased to 130μm. When the epiblast cysts reached day7, cysts were big enough, and since the bed size was around 113mm^2, cysts were close to each other, they started to merge together and formed a cyst cluster, which hindered the measurement of epiblast cysts (Figure 4.15).

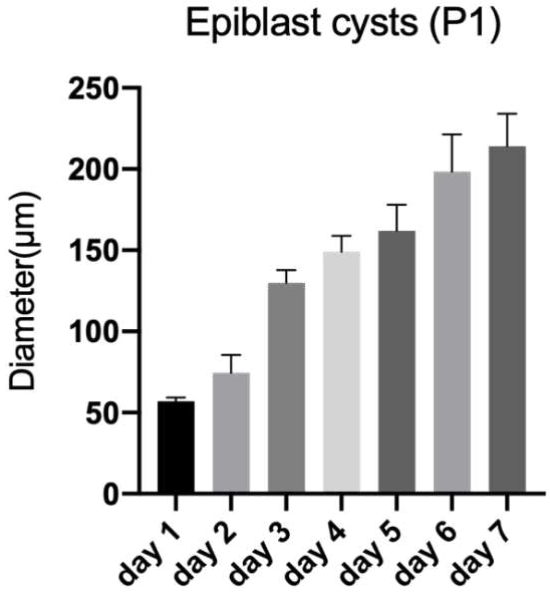

Figure 4.15 Average diameter of epiblast cysts from P1 iPSCs between day1 to day7.

Apart from measuring the diameter of the epiblast cyst (Figure 4.16), we also counted the total cysts number formed from each bed, to check if the starting 5000cells were spreading homogenously and their ability to assembly the epiblast cysts.

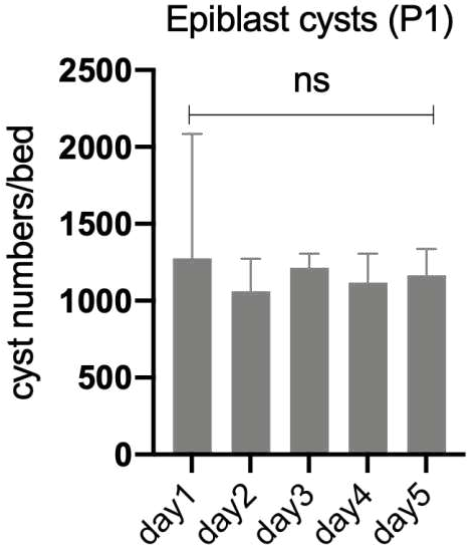

Figure 4.16 Cysts number from nascent iPSCs(P1) between day1 and day5

The self-assembly epiblast cysts from nascent iPSCs (P1) were around 1300 cysts from 5000cells. The great error of day1 was due to the small dimension as we mentioned before, the diameter of the day 1 was only around 50μm, which aroused imprecision when the Image J software performed the automatic counting. But from day 2 to day 5, the epiblast cysts number kept at the same number, about 1300-1400 cysts, the difference between days was not significant, which meant they epiblast cysts numbers was determined at day 1, depending on the seeding cell number. From day 2 to day 5, the epiblast cysts number did not increase many, but the dimension of each cyst grew to more than double size.

4.2.6 Comparison between nascent iPSCs and high passage iPSCs lines

We compared the diameter between nascent iPSCs (P1) and high passage iPSCs, we choose the established iPSCs line, P5, P10 and P15 to check the ability of forming 3D epiblasts, as shown in Figure 4.17. They were seeded at the same cell number, 5000 cell/bed.

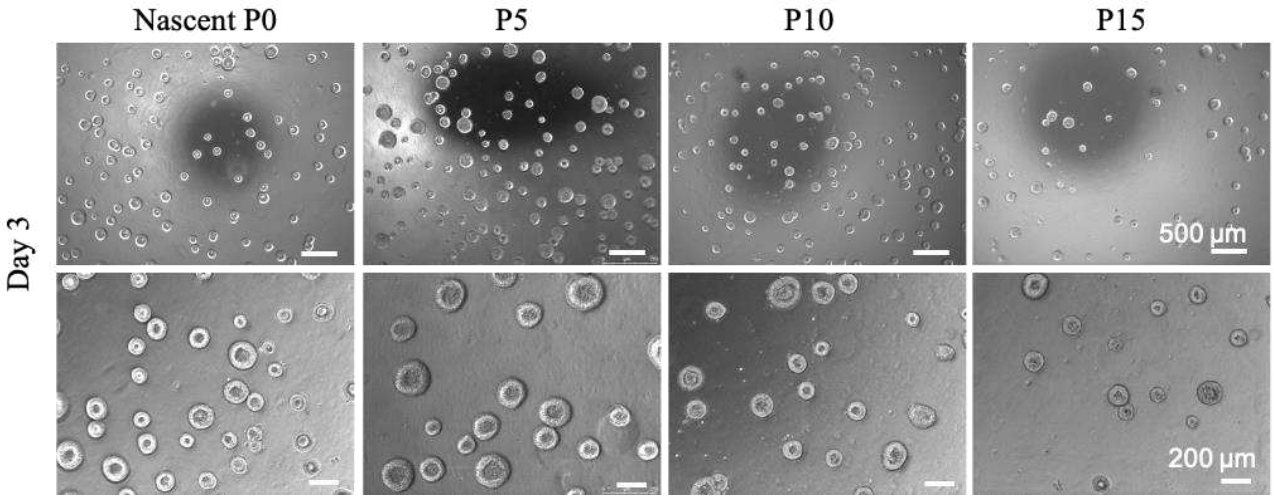

Figure 4.17 Bright field of epiblast cysts from nascent iPSCs, P5, P10 and P15 iPSCs lines.

The dimension difference between high passages and nascent iPSCs were not significantly distinguished from the bright field, but we could clearly see from the picture of P15 that the cyst number was greatly decreased at day 3. So, we measured both the cyst number and cyst dimension from all passage iPSCs lines and figured out the correlation between numbers and dimension at day 3. The result was shown in Figure 4.18.

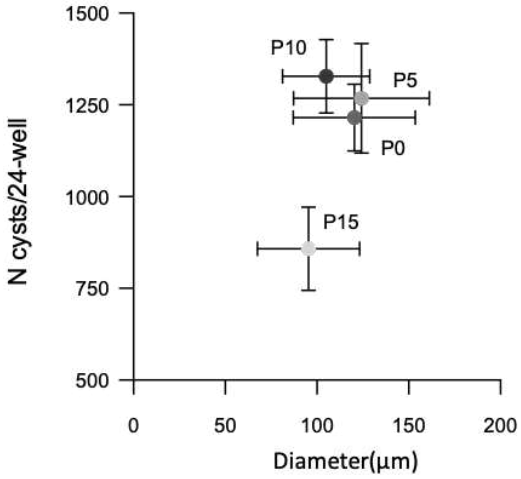

Figure 4.18 Correlation between cyst numbers and dimension of various passages at day 3

The epiblast cysts beds are kept in 24-well plate, thus one 24-well equals to one epiblast cyst bed. Figure4.18 shows that from P0 to P10, the difference in terms of cyst numbers and dimension, was not significant, P0 and P5 obtained the same diameter while P10 cells had the greatest number of cysts. But there was a drop of P15 both from the cyst diameter and the cyst numbersP0, P5, P10 and P15 were mainly divided into 2 clusters. After P10, there was a great difference both from the cyst numbers and diameters. Cell viability and movement could decrease while the passage increasing, which affected the epiblast cyst self-assembly.

Then we seeded higher passage iPSCs, P37, at the same seeding density, 5000cells/bed, the detailed result was shown in Figure 4.19.

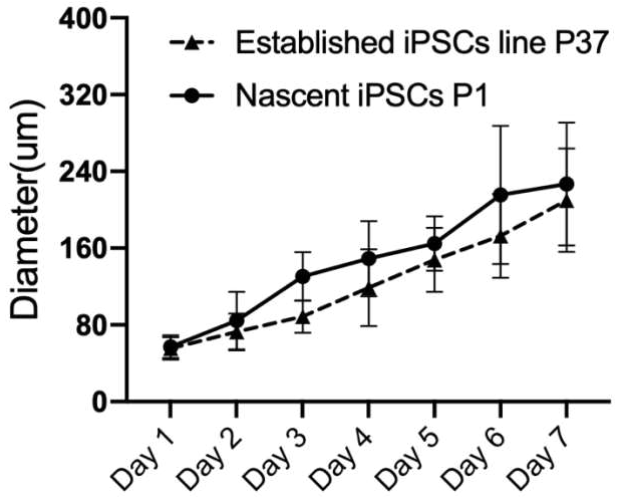

Figure 4.19 Cyst dimension comparison between nascent iPSCs and high passage P37 iPSCs

The cyst diameter of the first day was around 50μm, both from the nascent iPSCs and P37. While from day 2, as the round dots showed, the nascent epiblast cysts started to grow faster, the dimension was bigger than the P37 epiblast cysts. The average diameter was about 120μm for the nascent epiblast cysts at day3, but the high passage epiblast cysts was only 80μm.Also, the growth slope of nascent iPSCs were higher than the high passage epiblast cysts.

In conclusion, we investigated the robustness of generating epiblast cysts on matrigel beds from the nascent iPSCs (P0 or P1), found out that the seeding density is as low as 5000cells/bed, which is able to assemble 1200-1300 epiblast cysts. Meanwhile we also test high passages iPSCs line, to compare the advantages of using nascent iPSCs for generating epiblast cysts and later organoids. Part of results is summarized in Figure 4.20.

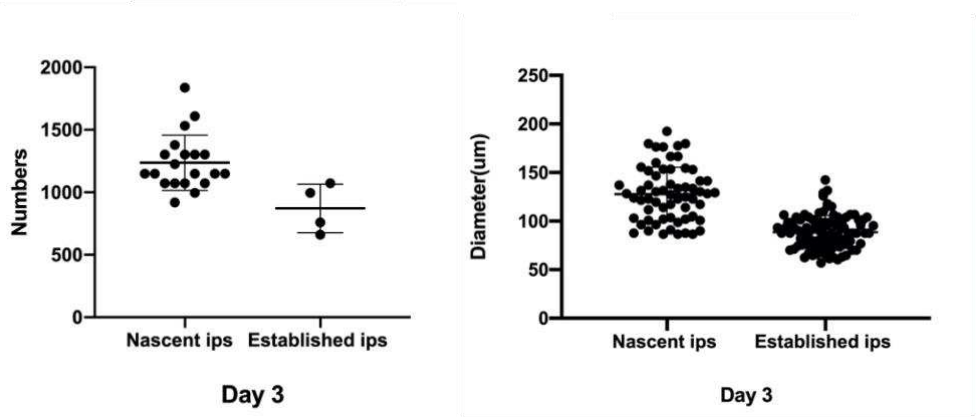

Figure 4.20 Comparison of epiblast cysts numbers and dimension between nascent iPSCs and established iPSCs at day 3. One dot means one matrigel bed.

We took the results of day 3 as an example. The epiblast numbers from nascent iPSCs ranged from 1200 to 1300, while established iPSCs could only generate around 800 epiblast cysts. Also, the diameter of nascent epiblast cysts at day 3 was between 120-130μm, while the high passage epiblast cysts diameter only reached 80μm.

We confirmed the homogeneity and robustness of nascent iPSCs self-assembly epiblast cysts as an ideal starting point for later 3D germ layer differentiation. Also, the high quality and efficient reprogramming from microfluidics facilitate the human development *in vitro*, because the epiblast cysts step requires low amount of cell from the beginning, as few as 5000cells per bed, allowing high throughput assays conducting at the same time. After we established the process of generating epiblast cysts from nascent iPSCs, we start the 3D differentiation procedure, to investigate their capability of differentiating cells into three germ layers and modelling human embryonic development *in vitro.*

4.2.7 3D epiblast cysts from nascent iPSCs are pluripotent

First of all, we asked if the pluripotency is still maintained by the 3D epiblast cysts. As we could tell from the Figure 4.21.

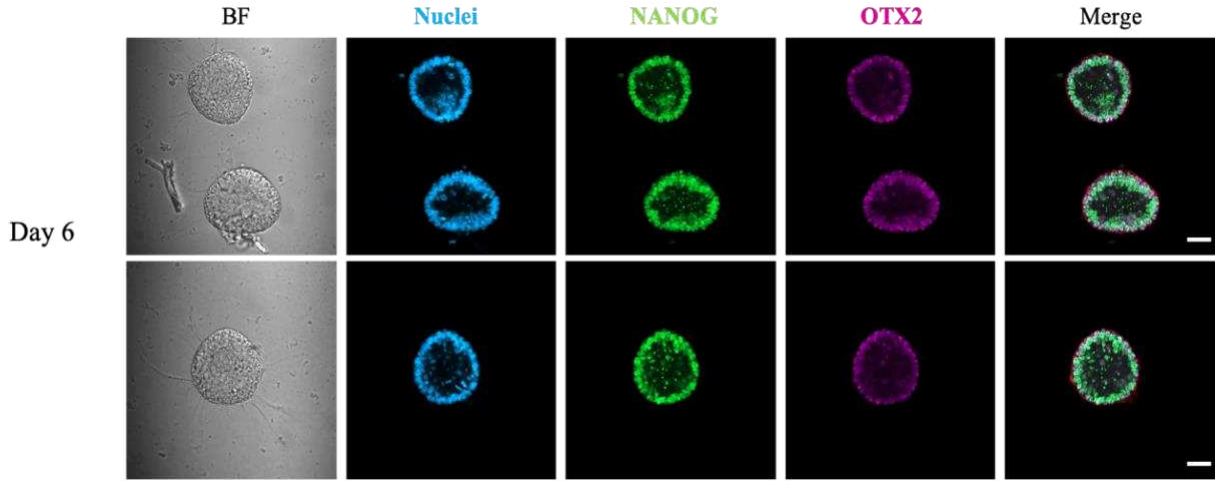

Figure 4.21 Pluripotency immunofluorescence staining of nascent 3D epiblast cysts at day6.scale bar:100μm

The important pluripotency markers, the Nanog, OTX2 express in the nascent 3D epiblasts cysts, Otx2 is a key regulator of the earliest stages of embryonic stem cell differentiation, which shows they are still pluripotent and have the potential to be differentiated into three germ layers.

4.2.8 Endoderm differentiation of epiblast cysts in matrigel drop

After keeping the epiblast cysts in culture for 3 days, we started the three germ layers differentiation. Figure 4.22 showed the early stage of endoderm differentiation at day7, after 4 days of differentiation.

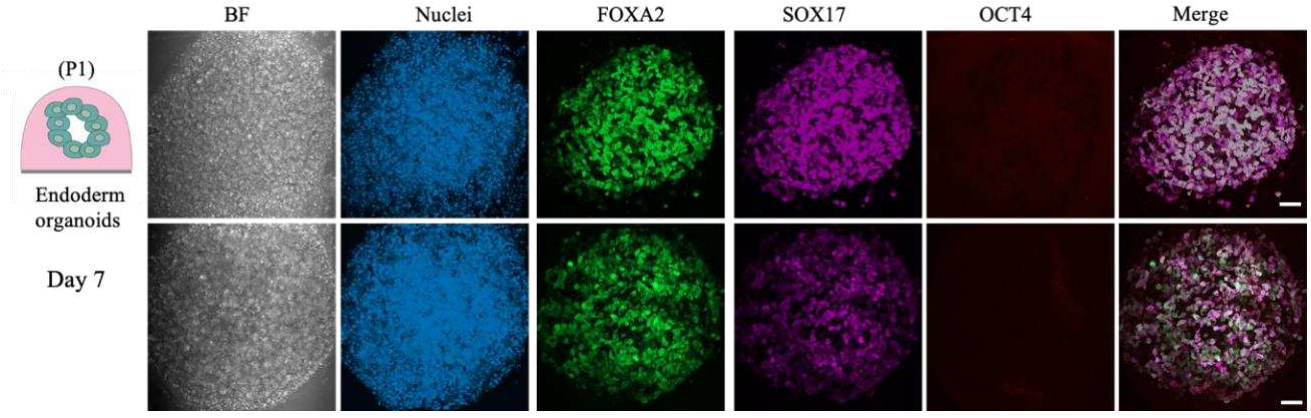

Figure 4.22 Endoderm differentiation IF staining at day7. Scale bar:100 μm.

FOXA2 and SOX17 are two key endoderm development markers to show that we are going in the correct direction for endoderm differentiation. SOX17 is involved in the regulation of vertebrate embryonic development and in the determination of the endodermal cell fate. We could say that the percentage of cells committing endoderm fate was 100%. The encoded protein acts downstream of TGFβsignaling (Activin)and canonical WNT signaling. Especially, the correct phosphorylation of SMAD2/3 within the respective cell cycle is crucial for the activation of cardinal endodermal genes to further enter the definitive endodermal lineage. FOXA2 together with HNF4A could drive differentiation to hepatocyte-like cells. This is also confirmed by the non-expression of OCT4, showing the endoderm epiblast cysts exited the pluripotent state.

4.2.9 Mesoderm differentiation of epiblast cysts in matrigel drop

Mesoderm differentiation started at the same time as for the endoderm differentiation. Also, immunostaining was performed at the early stage for guiding the mesoderm differentiation. IF result is shown in Figure 4.23.

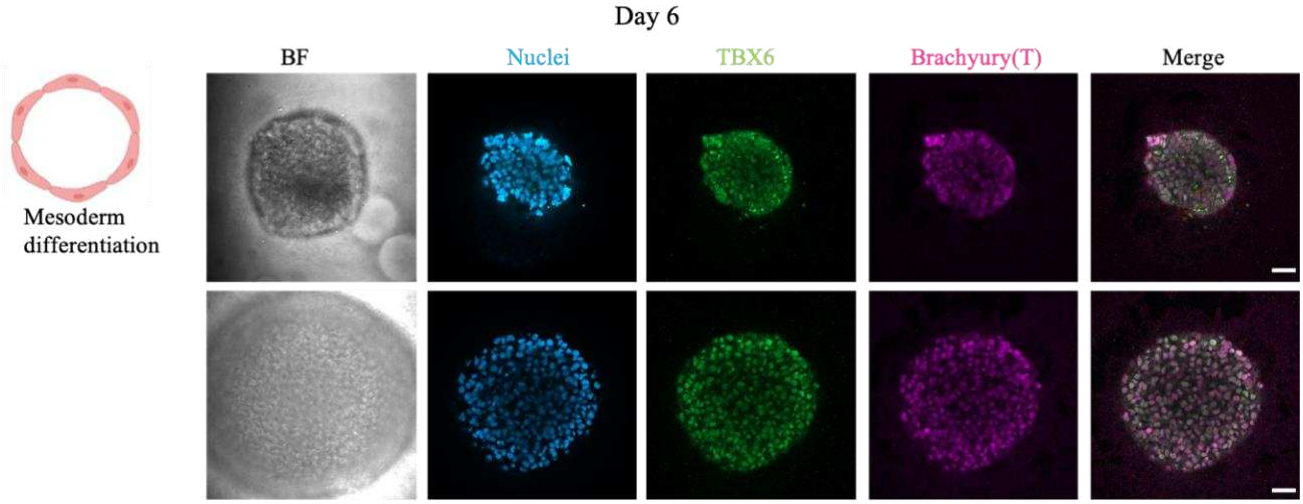

Figure 4.23 Mesoderm differentiation immunostaining at day 6.

TBX6 is also required for the segmentation of the paraxial mesoderm into somites, which could appear as early as one week after the gastrulation in human embryos. Brachyury protein, also known as transcription factor T, has also been shown to help establish the cervical vertebral blueprint during fetal development. They define

the mesoderm during gastrulation. TBX6 and Brachyury both expressed in our mesoderm differentiation from epiblast cysts at early day6.

4.2.10 Neuroectoderm differentiation of epiblast cysts on bed

At the same time, the neuroectoderm started by adding N2 and B27 neurotrophic factors in the neurobasal medium. Neuroectoderm organoids are cultured firstly in matrigel beds, after 7days, they are detached and then re-embedded in matrigel drops. After one month of culture, they are released from the drops, but still embedded by the matrigel and moved to suspension culture as the Figure 4.24 shows.

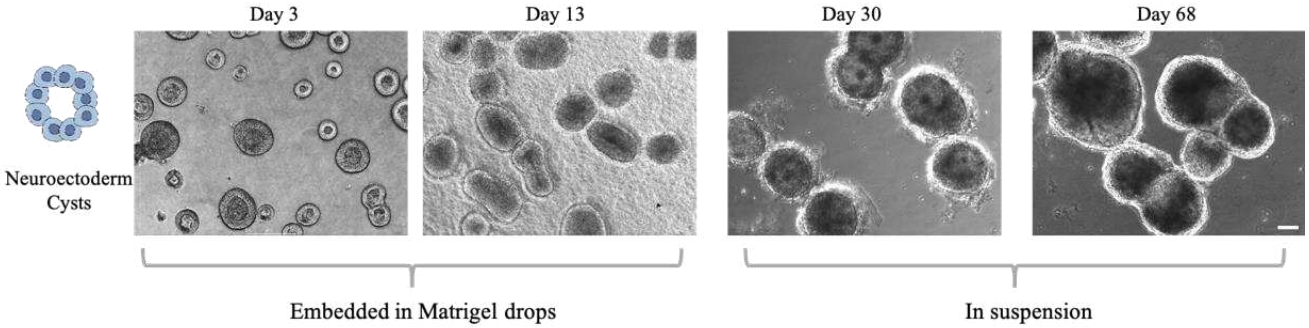

Figure 4.24 Bright field of neuroectoderm organoids are firstly kept in matrigel drops and then moved in suspension culture.

We invest more efforts in 3D neuroectoderm differentiation. Once they are moved into suspension culture, we freeze 3-5 organoids every month to track the development and the maturation process for the brain organoids. Now they have been in culture for more than 360 days.

4.2.11 Neuroectoderm differentiation induction time optimization

When we checked the data of epiblast cysts, we were thinking if the dimension of the epiblast cysts would affect the neuroectoderm differentiation (Figure 4.25).

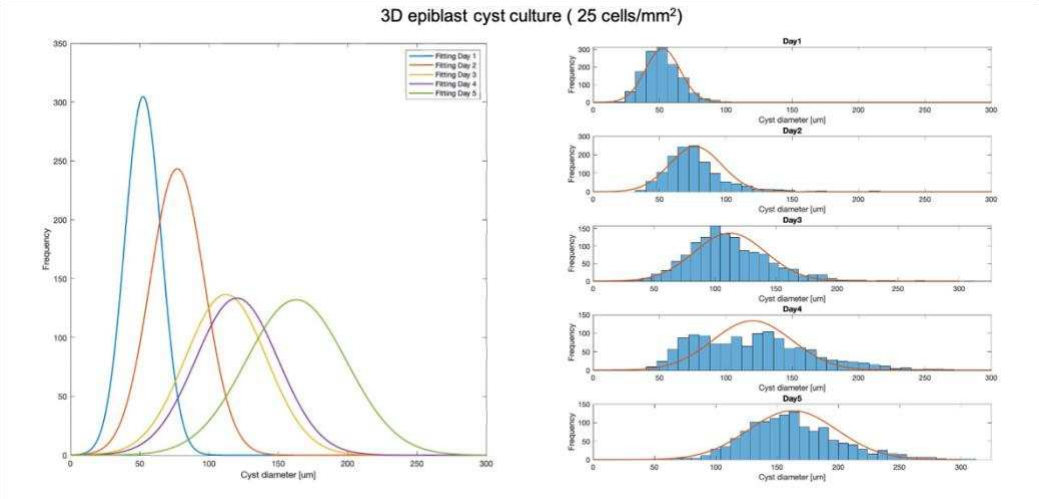

Figure 4.25 Distribution of cyst diameter between day1 and day5

The distribution of the cyst diameter somehow followed a Gaussian curve as figure 4.26 showed, the frequency of median cyst diameter between day2 and day3 was greater than other days. So, we started a time-lapse neuroectoderm differentiation separately from day1, day2 and day 3.

At day 1 of NE differentiation there was almost no Pax6 expression, which was found in proliferative zones of neural progenitors (Figure 4.26A). However, Sox1 started to appear from day 1. SOX1 encourages the development of neural stem cells and the interconnection of neurons. When the NE differentiation started either from day2 or day 3, both Pax6 and Sox2 fully expressed, this was confirmed by the quantification in Figure 4.26B. We saw heterogeneity in day1 NE epiblast cyst, but day2 NE cysts and day3 NE cysts had Pax6 and Sox1 co-expressed. NE differentiation may require a specific dimension of epiblast cysts to be triggered, but still, we do not

know the exact way that how the epiblast dimension affect the NE differentiation efficiency.

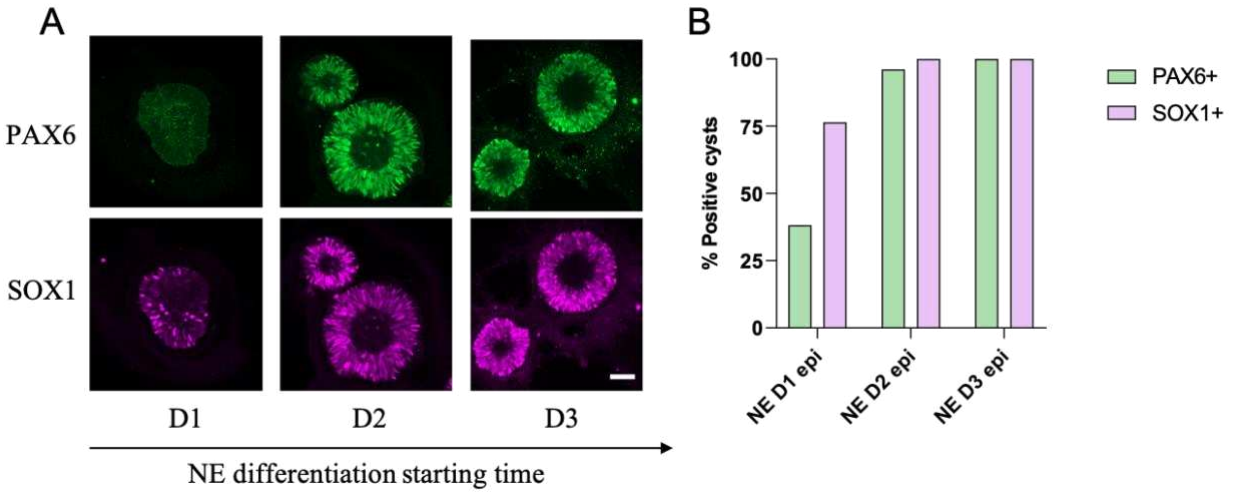

Figure 4.26 Neuroectoderm (NE) differentiation from different days of epiblast cyst. A) IF of NE marker Pax6 and Sox1; B) The quantification of Pax6 and Sox1 expression. Scale bar:50μm.

As we illustrated at the beginning, after 2 days of expansion in multi-well, nascent iPSCs were detached into single cell and seeded in 3D epiblast cysts format in order to proceed the germ layer differentiation part. Even though three germ layer differentiation started at the same time, but we were more focused on neuroectoderm organoid direction, that is why we made more effort to optimize the induction time or the starting epiblast cysts size. But still, the endoderm and mesoderm differentiation protocol optimization are also important for fully characterizing the development potential of microfluidics-based nascent iPSCs.

4.2.12 Long-term maturation of brain organoids from nascent iPSCs

From the preliminary data and the literature, we chose epiblast cysts at day3 as the starting point to trigger the NE differentiation. 10 days of niN2B27 basal medium with two inhibitors SB and LDN adding in the base medium, they were kept on the matrigel bed. These epiblast cysts on matrigel beds were fixed after 10days.

Neuroectoderm markers are stained during the 10 days neuron fate induction process. Figure 4.27 showed that after 10days of NE induction, we saw the presence of PAX6 and SOX1 in all cysts.

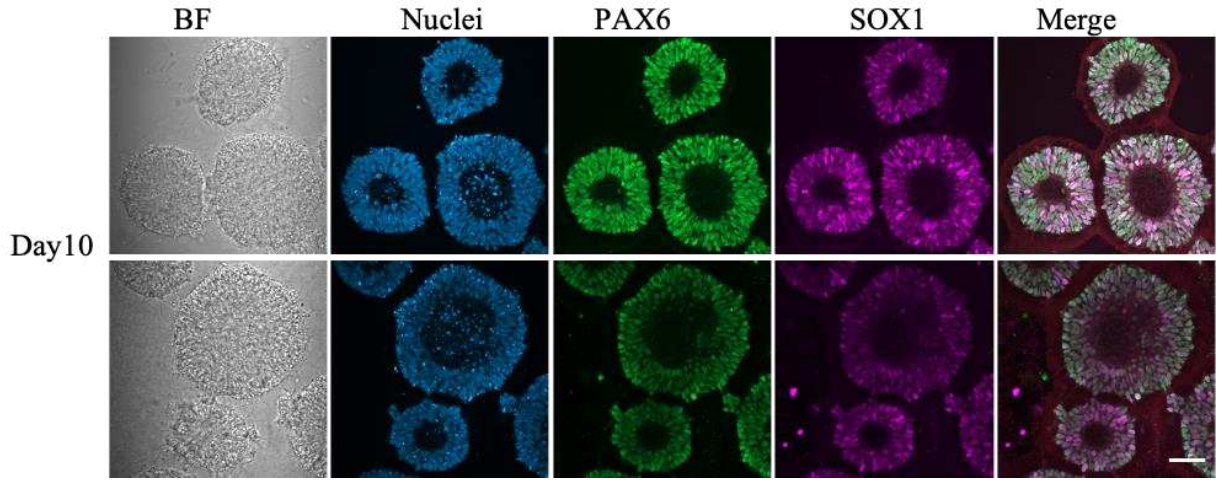

Figure4.27 Neuroectoderm cysts characterization after 10days of differentiation. Scale bar:50μm.

We saw both the presence of PAX6 and SOX1, even PAX6 expression was more even and homogenous while SOX1 showed a salt and pepper patten. When we looked at the merge picture, the co-location of PAX6 and SOX1 was not 100%, which meant that 10days in basal neuroectoderm medium was not sufficient to fully convert the epiblasts cysts.

After 10days of neural fate induction of epiblast cysts on matrigel beds, they are released from the beds and moved in suspension culture. They are maintained in neural maturation medium, with BDNF and NT3, two neurotrophic factors, which promote the nerve and glia cells to grow. Also, after they are moved into suspension, there is also 1% matrigel in presence for continuously supplying matrix to preserve the 3D spherical structure.

When Brain organoids are cultured in suspension, they require a low-adhesion petri dish because once the Matrigel inside attach to the dish bottom, the brain organoids would anchor to the matrix and become flat. Besides, we perform twice per day of the brain organoids pipetting to prevent the merge of close brain organoids. Pipetting also helps to break the adhesion of organoids to the dish bottom.

The suspension brain organoids were fixed at specific time points, like day20, day30, day60, later they were fixed every month, to track the maturation process. Neuroectoderm markers at different stages are checked at each time point.

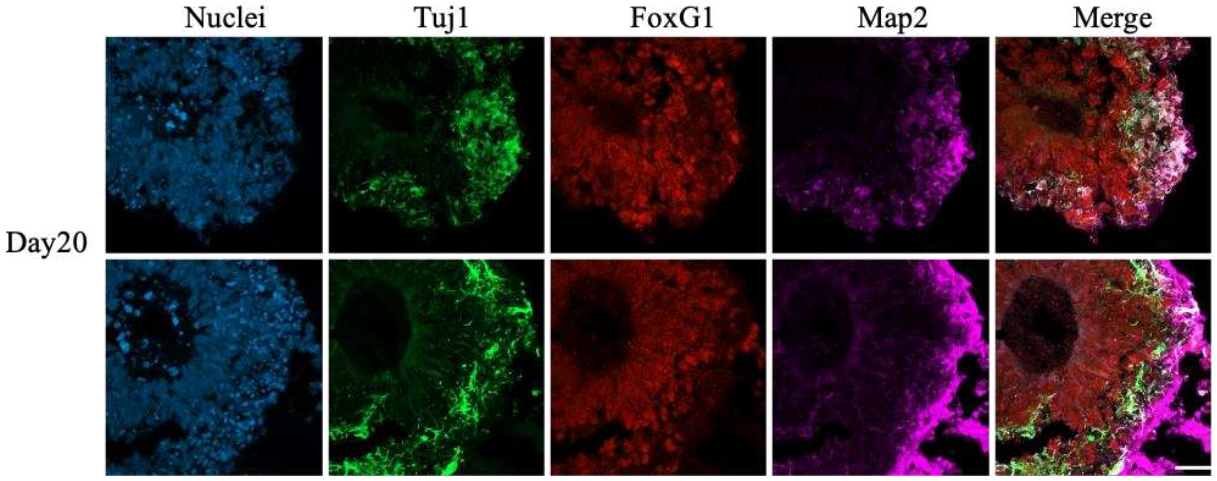

Figure 4.28 Forebrain organoids immunofluorescence characterization at day 20. Scale bar:50μm.

When the brain organoids slices were checked at day 20, β III Tubulin (Tuj1), which was an important role in immature neurons and axon guidance, was found present. FoxG1 refers to brain regionalization, starting to emerge at day 20. Microtubule-associated protein 2 (Map2) was a marker of mature neurons, was not clearly evident inside the brain organoids slice at day 20. Then we continued to characterize the maturity of long-term brain organoids cryosections.

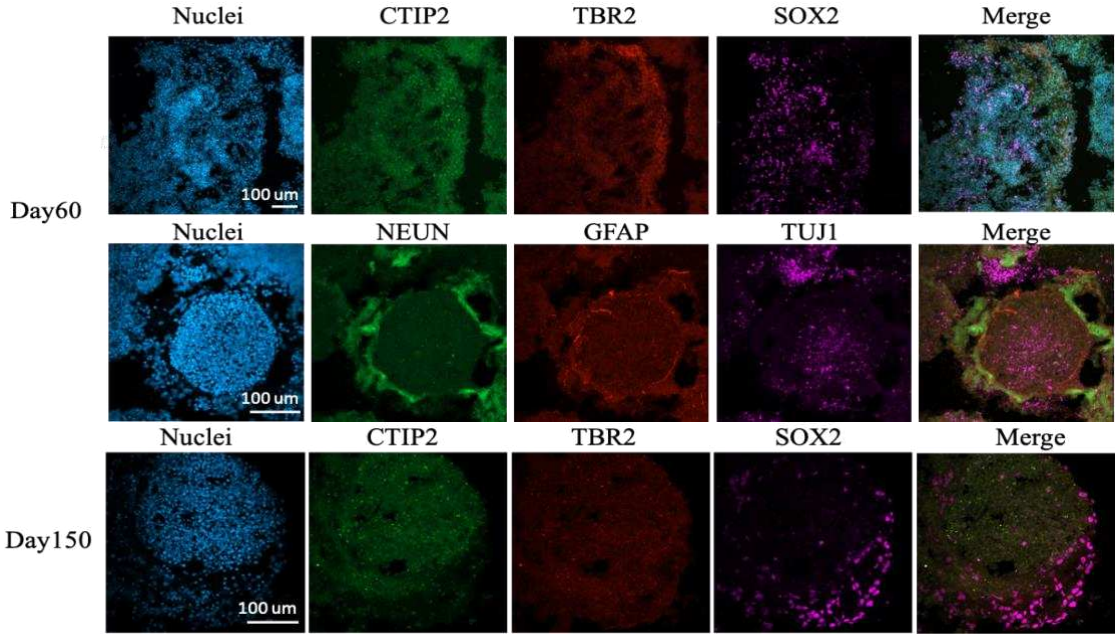

Figure 4.29 Long-term forebrain organoids staining characterization at day 60 and day150.

In Figure 4.29, the presence of SOX2 showed the neural stem cell niche still existed. Neural stem cells designated the region where stem cells were kept after embryonic development in order to produce new nervous system cells. While CTIP2 and TBR2 were the neocortex regulators, but they were not present both at day 60 and day 150. However, at day60, we saw some spots with GFAP positive, GFAP was the Glial fibrillary acidic protein (GFAP), that was an intermediate filament-III protein uniquely found in astrocytes in the central neural system, non-myelinating Schwann cells. NEUN was an important marker localized in nuclei and perinuclear cytoplasm of most of the mature neurons, also started to emerge from some side parts. The positive spots of NEUN and GFAP at day60 showed the heterogenous cell population, which was an advantage of 3D organoids differentiation.

Up to now, we are still working on optimizing the nascent 3D epiblast cysts differentiated into three germ layer organoids. For example, for the endoderm, we are towards the mature hepatocyte differentiation, for the mesoderm differentiation, we started a cardiac muscle differentiation and we found they stared to beat at day17. Long-term culture of mature brain organoids is also ongoing. For example, we are testing if by changing the pipetting orientation, the brain organoids could reach maturity in a shorter time. What is more, we want to test other methods of cutting the frozen organoids slices to improve their quality. For instance, we tried to decrease the PFA concentration in order to minimize the damage of outer layer matrix structure while still maintaining their 3D structure. Because after long time of storage at -80°C, once they are cut, the slices are fragile and can be ruined by the long staining process, which later may affect the detect of mature marker expression in brain organoids.

4.3 Peripheral blood supplies cell sources for reprogramming

Fibroblasts from the skin are most widely used cell source for cellular reprogramming research. We think about looking for other cell sources to avoid the invasive isolation of fibroblasts from the biopsies, especially to prevent the damage to kid patients.

Peripheral blood is more accessible than biopsies by intravenous blood collection. Also, cells circulating inside the peripheral blood are protected from the sunlight rays, which usually bring mutation to genes. We want to test if we could firstly isolate cells from the blood, which are adherent to the glass bottom of the microfluidic chips. we also make attempts to compare if the mRNA transfection is more efficient than other ways of transfection, like the Sendai virus or episomal plasmids. What is more, we test the pluripotency of blood derived iPSCs, also the 2D germ layer differentiation to characterize their development potency.

4.3.1 Peripheral blood mononuclear cells (PBMCs) are isolated from peripheral blood

40ml of peripheral blood (Figure 4.30) was kindly donated from an anonymous patient in the local hospital and had been processed as soon as possible (within 2 hours).

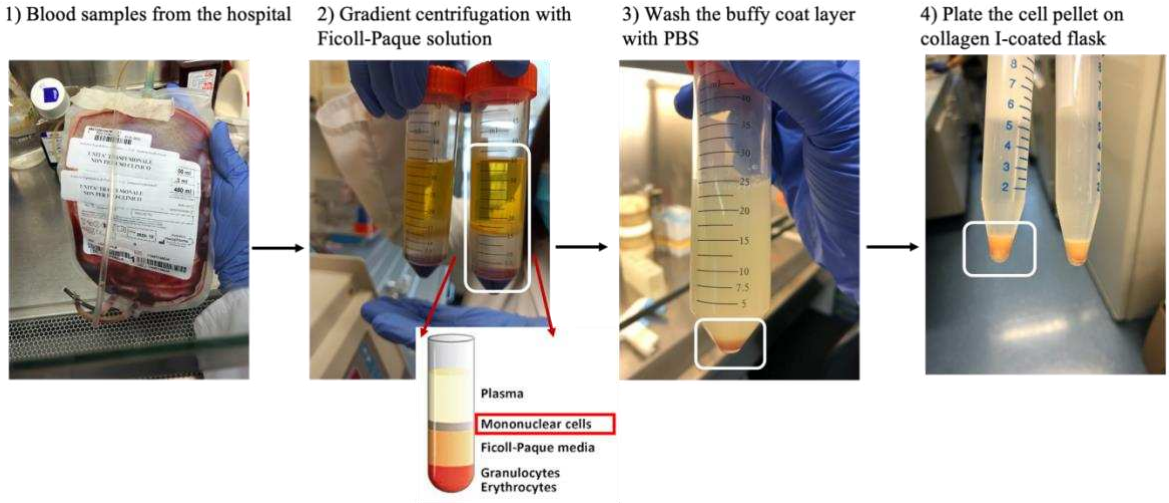

Figure 4.30 Isolation process of mononuclear cells from the peripheral blood.

Dilute 40ml blood with 1:1 PBS solution, 15ml of Ficoll-paque (commercial gradient centrifugation solution) was added at the bottom of a 50ml falcon tube, 20ml of diluted blood was later placed on the top of the Ficoll-paque solution. The most important detail is to set the centrifuge brake off Figure 4.30(2) because after the centrifugation, the sudden stop would force all layers mixed again. Gently absorb the mononuclear cells (PBMCs) layer was gently absorbed with a plastic paster and

washed with PBS twice, at this washing step, the centrifuge brake had to be set at maximum to tighten the PBMCs pellet in Figure 4.30 (3). After all the washing steps, we saw a very big cell pellet, they were around 200.8 million cells in total, and we seeded them all in a collagen type-1 coated flask. We kept them in BOECs generation medium as mentioned before. The medium changing frequency was three times per week.

4.3.2 Blood outgrowth endothelial cells (BOECs) are isolated from PBMCs

When the whole PBMCs were seeded into the flask, only a small portion of them would attach and grow. Most of them were white blood cells and would be removed later by medium change.

The original cell pellet was mixture cell population, but by applying for BOECs generation medium, endothelial progenitor cells (EPCs) would firstly appear around day15, as Figure 4.31 showed.

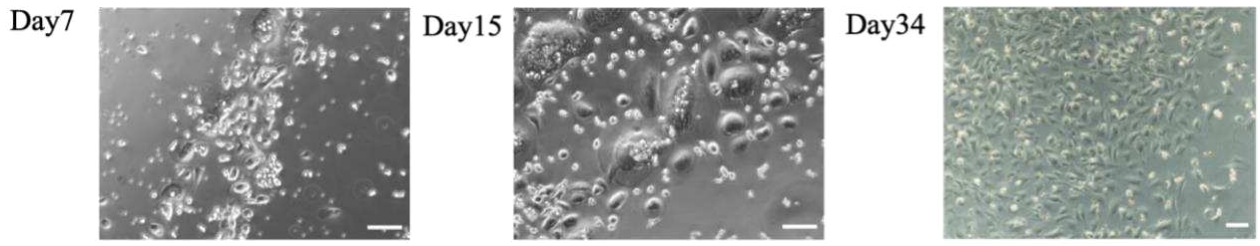

Figure 4.31 Isolation of blood outgrowth endothelial cells (BOECs) from the peripheral mononuclear cells. Scale bar:100μm.

In the meantime, there were also macrophages along EPCs, with a wide and flat morphology comparing to the small and spindle shape of EPCs. At day34, we saw the emergence of cobblestone shape cells, growing a cluster. They were regarded as the blood outgrowth endothelial cells (BOECs). Flow cytometry could also be utilized to characterize these cell identities precisely. They were highly proliferative but also sensitive to the cell density. Once the cluster reaches around 2000 cells by approximate visual estimation, they need to be split.

4.3.3 Attempt of BOECs reprogramming in microfluidics

When the BOECs was stable in culture, we started the mRNA reprogramming in microfluidic chips. Since the dimension of BOECs were much smaller than fibroblasts, by checking the literature and combining with our experience, we set the seeding density of BOECs at 200cells/mm^2. We increased the seeding density to occupy more space of the microchannel, also it helped to modulate the toxicity of mRNA transfection. Beside the seeding density, the coating concentration of collagen type I was elevated from 50μg/ml to 200μg/ml compared to the one used in flask coating because the glass surface was trickier for BOECs to attach and grow.

As we saw the below Figure 4.32, at day1, the BOECs attached and grew well inside the microchannel. From day1, we stared the daily mRNA transfection. What was different between the fibroblasts reprogramming and BOECs reprogramming was that BOECs reprogramming needed a medium adaptation process.

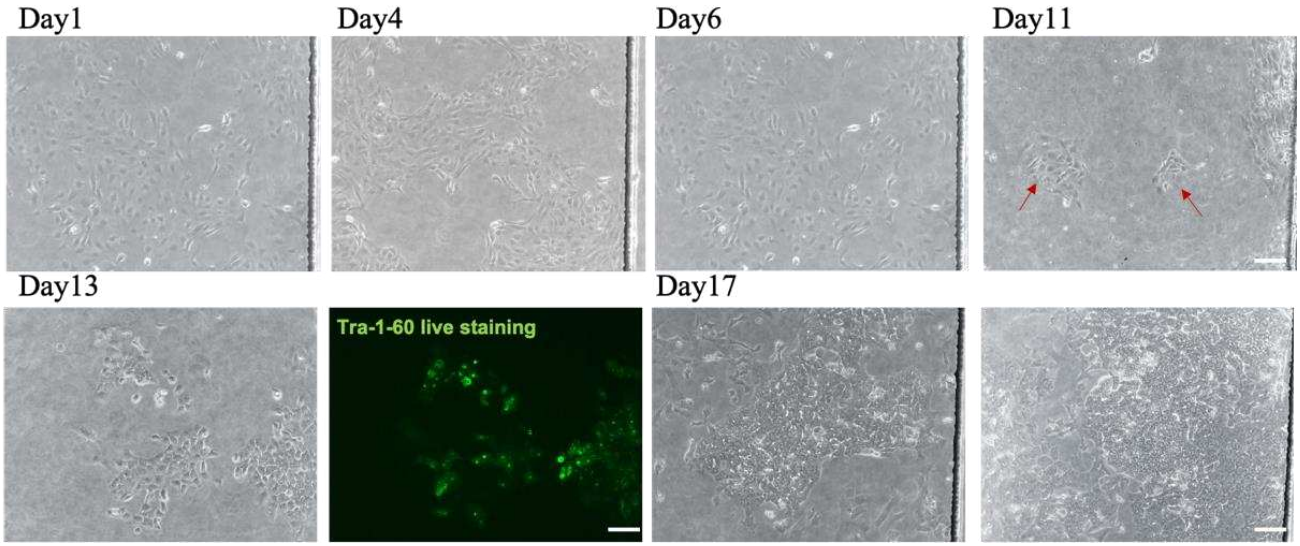

Figure 4.32 Bright field of morphology change of BOECs reprogramming based on the microfluidics. Scale bar:100μm

The default reprogramming medium used in our lab was Nutristem XF plus 20ng/ml FGF2. While since it was the first attempt to perform the BOECs reprogramming, the first day of transfection, we prepared 25% of Nutristem XF plus 20ng/ml FGF2 medium and 75% of the BOECs generation medium (without FBS and

heparin, so they called BOECs reprogramming medium) to maintain first of all the BOECs growth while they were converting towards iPSCs. The medium adaptation process started from 25% Nutristem XF plus 20ng/ml FGF2 composition to 50%, then from day9, they were switched to full Nutristem XF plus 20ng/ml FGF2. As the figure4.27 showed, at day11, we could identify the emergence of new iPSCs colonies, even though after the fully medium switch, most of the not-in-transition or non-reprogrammed cell populations could not resist the toxicity of mRNA transfection and died, that explained why there were empty space surrounding the iPSCs colonies. The iPSCs colonies continued to grow while the transfection going on. At day 13, live staining of Tra-1-60, a cell membrane protein of pluripotency, was conducted to check the quality of these iPSCs. Tra-1-60 was only found positive expression in some spots of the colonies, not 100% iPSCs colonies were positive. Since the iPSCs colonies appeared from day11, we stopped the daily mRNA transfection at day13 and switched the medium to IPS-Brew, the default medium used in our stem cell maintenance. The BOECs derived iPSCs adapted well in the IPS-Brew medium, growing in both in colony numbers and size. At day17, we extracted the BOECs-iPSCs from the microchannels and kept them in culture in multi-well for expansion and later characterization.

4.3.4 2D germ layer differentiation of BOECs-iPSCs

After several passages of stabilization in multi-well plate, BOECs-iPSCs are seeded in monolayer on a cover slip glass at different cell density according to the germ layer differentiation requirement. The results are shown in Figure 4.33.

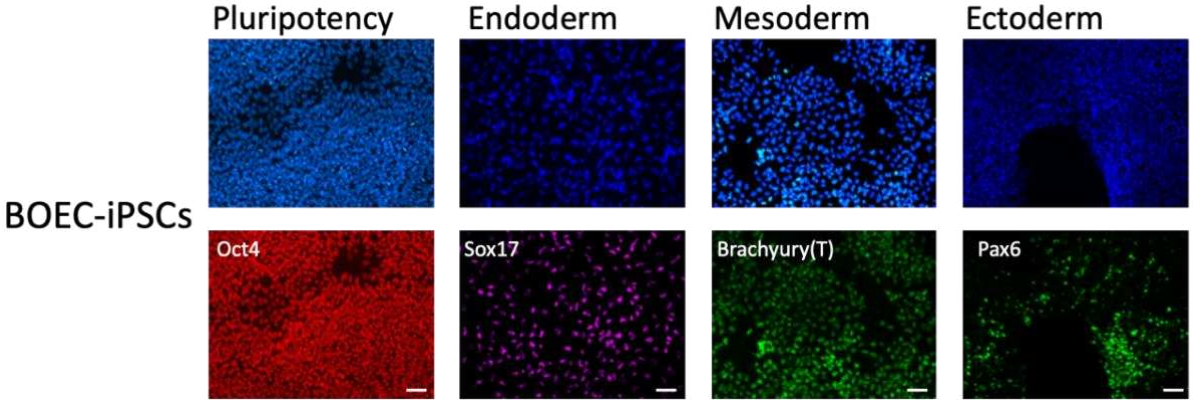

Figure 4.33 2D differentiation of three germ layers from BOEC-iPSCs. Scale bar:100μm.

Even BOECs-iPSCs had been cultured for establishment for around 5 passages before they were seeded on the cover slip glass for differentiation, we still found there was a big problem of attachment and mortality. For example, when firstly seeded at 15% confluency for mesoderm differentiation, the next day we found they did not attach to the glass and all died, we assumed that the problem was due to the low density for single stem cell to grow and the quality of matrigel coating. Then the later attempts, we increased the matrigel coating from 1% to 2%. Besides, the seeding confluency was elevated from 20% to 40% for endoderm differentiation and elevated from 15% to 30% confluency for mesoderm differentiation. Ectoderm differentiation went smoothly thanks to the 100% confluency at the beginning. As we saw from figure 4.32, BOECs-iPSCs had the potential for generating cells from all three germ layers. There were early endoderm key markers, Sox17 expression, the Brachyury presence for mesoderm and abundant Pax6 characterization for ectoderm guidance.

2D monolayer differentiation is a fast and direct assay to test the development potential of BOECs-iPSCs. We intend to also perform 3D organoids differentiation experiments to better characterize their potency.

To summarize, exploring alternative cell sources for reprogramming is of great benefit to personized medicine research. Great efforts have made on skin fibroblasts, fibroblasts isolated from urine, dental pulp or other tissues, to facilitate the cellular reprogramming process. We are working the blood cells reprogramming because they are at the least damage level and is the most feasible material to all laboratories. However, up to now, we just did few attempts to work in a continuous procedure, from the patient peripheral blood to patient specific iPSCs. We have proven that blood cells could be successfully reprogrammed into iPSCs in our microfluidic chips by mRNA transfection, which is more efficient than other systems demand, even though the isolation of blood cells still needs time optimization.

Chapter 5 Conclusion and discussion

Based on the findings of our group that non-modified RNA reprogramming method in microfluidics has greatly improved the efficiency of iPSCs generation, we take advantage of highy efficient reprogramming in microfluidics and temporal multi-omics to identify and resolve distinct subpopulations and their interactions, since secreted signals are accumulated, and distinctive intermediate subpopulations can be effectively captured and characterized in the confined microenvironment of microfluidics. Also, we combine secretome analysis with single-cell transcriptomics to reveal functional extrinsic protein communication channels between reprogramming subpopulations and the reshaping of a favorable extracellular environment. We came to the conclusion that during reprogramming, secreted proteins exhibited precise dynamics and included a variety of possible autocrine/paracrine signaling regulators, including those implicated in soluble and ECM-mediated communication. We were able to characterize human somatic reprogramming as a procedure that yields two main results, matrisomal and pluripotent, from the same beginning cells that split at day7. Additionally, we discovered and characterized an early subpopulation of matrisomal somatic cells that participates in the production and secretion of SASP-related signaling molecules.

Preliminary attemptes of fibroblasts reprogramming to organodis was a success in the microfluidics-based nascent iPSCs. We were able to robustly generate high numbers of homogeneous epiblast cysts from a low starting cell density, to be more sepecific, 1200 organoids generated from 5000 single nascent iPSCs with a uniform eiblast cyst size and morphology. This offered great possibility of large scale and high throughput generation of organoids. Besides, this is beneficial to personized medicine when the patients cell source is limited available. However, there are some aspects that still need optimization. For example, we found variability between nascent iPSCs to produce epiblast cysts. When nascent iPSCs were overmature in microfluidics, they started part of differentiation automatically after the extraction, which affected the quality of pluripotent epiblast cysts formation. Also, for the long-term brain organoids

culture, we still need to figure it out if the matrigel in suspension medium is indispensible and how the organoids orientation modulate the maturity of them. Also, a better immunofluorescence staining technique is in demand to better characterize advanced neuron markers expression. Even though we made more efforts in optimizing the brain organoids maturity, but we were also interested in guiding endoderm and mesoderm orgranoids, to fully describe our concept of from fibroblasts to organoids.

Going back to broaden the cell sources for cellular reprogramming is the third aspect for the whole project, after we established the highly efficient fibroblasts reprogramming process in microfluidic chips, and also figured out practical applications of nascent iPSCs.Blood cells reprogramming by mRNA adapted well in microfluidic system even through it took 13days of transfection instead of 8 days for the standardized fibroblasts reprogramming process, due to the fact that they were more sensitive to the microenvironment and required a gradual medium and transfection adaptation. Also, peripheral blood volume needs to decrease from the current 40ml to less than 10ml, which would be feasible to get more patients blood, especially when we ask for blood from small kids. On the other hand, we need to work on the optimization of isolation period of BOECs. When the BOECs could appear from the blood cell population culture in two weeks, plus the reprogramming procedure, from the patient blood to patient specific iPSCs could be completed within only one month.

Bibliography

1. Driesch, H. The potency of the first two cleavage cells in echinoderm development. Experimental production of partial and double formations. *Found. Exp. Embryol. Hafner, New …* 38–50 (1892).
2. Robinton, D. A. & Daley, G. Q. The promise of induced pluripotent stem cells in research and therapy. *Nature* **481**, 295–305 (2012).
3. Thomson, J. A. Embryonic stem cell lines derived from human blastocysts. *Science (80-.).* **282**, 1145–1147 (1998).
4. Nichols, J. & Smith, A. Pluripotency in the embryo and in culture. *Cold Spring Harb. Perspect. Biol.* **4**, 1–14 (2012).
5. Weinberger, L., Ayyash, M., Novershtern, N. & Hanna, J. H. Dynamic stem cell states: Naive to primed pluripotency in rodents and humans. *Nat. Rev. Mol. Cell Biol.* **17**, 155–169 (2016).
6. Hogan, B. L. M. Changes in the behaviour of teratocarcinoma cells cultivated in vitro. *Nature* **263**, 136–137 (1976).
7. Evans M J & Kaufman M H. Establishment in culture of pluripotential cells from mouse embryos. *Nature* **292**, 154–156 (1981).
8. Rossant, J. & Tam, P. P. L. New Insights into Early Human Development: Lessons for Stem Cell Derivation and Differentiation. *Cell Stem Cell* (2017) doi:10.1016/j.stem.2016.12.004.
9. Watanabe, K. *et al.* A ROCK inhibitor permits survival of dissociated human embryonic stem cells. *Nat. Biotechnol.* **25**, 681–686 (2007).
10. Lawson, K. A., Meneses, J. J. & Pedersen, R. A. Clonal analysis of epiblast fate during germ layer formation in the mouse embryo. *Development* **113**, 891–911 (1991).
11. Stevens, L. C. & Little, C. C. Spontaneous Testicular Teratomas in an Inbred Strain of Mice. *Proc. Natl. Acad. Sci.* **40**, 1080–1087 (1954).
12. Xu, C. *et al.* Feeder-free growth of undifferentiated human embryonic stem cells. *Nat. Biotechnol.* **19**, 971–974 (2001).
13. Silva, J. & Smith, A. Capturing Pluripotency. *Cell* **132**, 532–536 (2008).
14. Desai, N., Rambhia, P. & Gishto, A. Human embryonic stem cell cultivation: Historical perspective and evolution of xeno-free culture systems. *Reprod. Biol. Endocrinol.* **13**, 1–15 (2015).
15. Shi, G. & Jin, Y. Role of Oct4 in maintaining and regaining stem cell pluripotency. *Stem Cell Res. Ther.* **1**, 1–9 (2010).
16. Wang, L. *et al.* NANOG and LIN28 dramatically improve human cell reprogramming by modulating LIN41 and canonical WNT activities. *Biol. Open* **8**, 1–12 (2019).

17. Schaefer, T. & Lengerke, C. SOX2 protein biochemistry in stemness, reprogramming, and cancer: the PI3K/AKT/SOX2 axis and beyond. *Oncogene* **39**, 278–292 (2020).
18. Schopperle, W. M. & DeWolf, W. C. The TRA-1-60 and TRA-1-81 Human Pluripotent Stem Cell Markers Are Expressed on Podocalyxin in Embryonal Carcinoma. *Stem Cells* **25**, 723–730 (2007).
19. Jin Xu, Heather Hardin, Ranran Zhang, Kaitlin Sundling, Darya Buehler, and R. V. L. STAGE SPECIFIC EMBRYONIC ANTIGEN-1 (SSEA-1) EXPRESSION IN THYROID TISSUES. *Physiol. Behav.* **176**, 139–148 (2017).
20. Sivasubramaniyan, K. *et al.* Expression of stage-specific embryonic antigen-4 (SSEA-4) defines spontaneous loss of epithelial phenotype in human solid tumor cells. *Glycobiology* **25**, 902–917 (2015).
21. Ström, S. *et al.* Mechanical isolation of the inner cell mass is effective in derivation of new human embryonic stem cell lines. *Hum. Reprod.* **22**, 3051–3058 (2007).
22. Cowan, C. A. *et al.* Derivation of Embryonic Stem-Cell Lines from Human Blastocysts. *N. Engl. J. Med.* **350**, 1353–1356 (2004).
23. Turetsky, T. *et al.* Laser-assisted derivation of human embryonic stem cell lines from IVF embryos after preimplantation genetic diagnosis. *Hum. Reprod.* **23**, 46–53 (2008).
24. Takahashi, K. & Yamanaka, S. Induction of Pluripotent Stem Cells from Mouse Embryonic and Adult Fibroblast Cultures by Defined Factors. *Cell* **126**, 663–676 (2006).
25. Takahashi, K. *et al.* Induction of Pluripotent Stem Cells from Adult Human Fibroblasts by Defined Factors. *Cell* **131**, 861–872 (2007).
26. Yu, J. *et al.* Induced pluripotent stem cell lines derived from human somatic cells: Commentary. *Science (80-.).* **318**, 1917–1920 (2007).
27. Campbell, K. H. S., McWhir, J., Ritchie, W. A. & Wilmut, I. Sheep cloned by nuclear transfer from a cultured cell line. *Nature* **380**, 64–66 (1996).
28. Tada, M., Takahama, Y., Abe, K., Nakatsuji, N. & Tada, T. Nuclear reprogramming of somatic cells by in vitro hybridization with ES cells. *Curr. Biol.* **11**, 1553–1558 (2001).
29. Zheng, Y. L. Some Ethical Concerns About Human Induced Pluripotent Stem Cells. *Sci. Eng. Ethics* **22**, 1277–1284 (2016).
30. Hawley, R. G. Does retroviral insertional mutagenesis play a role in the generation of induced pluripotent stem cells? *Mol. Ther.* **16**, 1354–1355 (2008).
31. Yu, J. *et al.* Human Induced Pluripotent Stem Cells Free of Vector and Transgene Sequences. **324**, 797–801 (2009).
32. Chang, C. W. *et al.* Polycistronic lentiviral vector for 'hit and run' reprogramming of adult skin fibroblasts to induced pluripotent stem cells. *Stem Cells* **27**, 1042–1049 (2009).
33. Haridhasapavalan, K. K. *et al.* An insight into non-integrative gene delivery approaches to generate transgene-free induced pluripotent stem cells. *Gene* **686**, 146–159 (2019).

34. Fusaki, N., Ban, H., Nishiyama, A., Saeki, K. & Hasegawa, M. Efficient induction of transgene-free human pluripotent stem cells using a vector based on Sendai virus, an RNA virus that does not integrate into the host genome. *Proc. Japan Acad. Ser. B Phys. Biol. Sci.* **85**, 348–362 (2009).
35. Woltjen, K. *et al.* PiggyBac transposition reprograms fibroblasts to induced pluripotent stem cells. *Nature* **458**, 766–770 (2009).
36. Kim, D. *et al.* Generation of Human Induced Pluripotent Stem Cells by Direct Delivery of Reprogramming Proteins. *Cell Stem Cell* **4**, 472–476 (2009).
37. Lee, K. I., Kim, H. T. & Hwang, D. Y. Footprint- and xeno-free human iPSCs derived from urine cells using extracellular matrix-based culture conditions. *Biomaterials* **35**, 8330–8338 (2014).
38. Poleganov, M. A. *et al.* Efficient Reprogramming of Human Fibroblasts and Blood-Derived Endothelial Progenitor Cells Using Nonmodified RNA for Reprogramming and Immune Evasion. *Hum. Gene Ther.* **26**, 751–766 (2015).
39. Li, Z., Dang, J., Chang, K. Y. & Rana, T. M. MicroRNA-mediated regulation of extracellular matrix formation modulates Somatic cell reprogramming. *Rna* **20**, 1900–1915 (2014).
40. Zhang, Z., Xiang, D. & Wu, W. S. Sodium butyrate facilitates reprogramming by derepressing OCT4 transactivity at the promoter of embryonic stem cell-specific miR-302/367 cluster. *Cell. Reprogram.* **16**, 130–139 (2014).
41. Chen, G., Guo, Y., Li, C., Li, S. & Wan, X. Small Molecules that Promote Self-Renewal of Stem Cells and Somatic Cell Reprogramming. *Stem Cell Rev. Reports* **16**, 511–523 (2020).
42. Esteban, M. A. *et al.* Vitamin C Enhances the Generation of Mouse and Human Induced Pluripotent Stem Cells. *Cell Stem Cell* **6**, 71–79 (2010).
43. Zhou, H. *et al.* Generation of Induced Pluripotent Stem Cells Using Recombinant Proteins. *Cell Stem Cell* **4**, 381–384 (2009).
44. Yang, W. iPSC reprogramming from human peripheral blood using Sendai Virus mediated gene transfer. *StemBook* 1–6 (2014) doi:10.3824/stembook.1.73.1.
45. Okita, K. *et al.* A more efficient method to generate integration-free human iPS cells. *Nat. Methods* **8**, 409–412 (2011).
46. Warren, L. *et al.* Highly efficient reprogramming to pluripotency and directed differentiation of human cells with synthetic modified mRNA. *Cell Stem Cell* **7**, 618–630 (2010).
47. Schlaeger, T. M. *et al.* A comparison of non-integrating reprogramming methods. *Nat. Biotechnol.* **33**, 58–63 (2015).
48. Plews, J. R. *et al.* Activation of pluripotency genes in human fibroblast cells by a novel mRNA based approach. *PLoS One* **5**, (2010).
49. Steinle, H. *et al.* Generation of iPSCs by nonintegrative RNA-based reprogramming techniques: Benefits of Self-Replicating RNA versus Synthetic mRNA. *Stem Cells Int.* **2019**,

(2019).
50. Weibel, D. B., DiLuzio, W. R. & Whitesides, G. M. Microfabrication meets microbiology. *Nat. Rev. Microbiol.* **5**, 209–218 (2007).
51. Xia, Y. & Whitesides, G. M. Soft lithography. *Annu. Rev. Mater. Sci.* **28**, 153–184 (1998).
52. Whitesides, G. M., Ostuni, E., Jiang, X. & Ingber, D. E. Soft lithography in biology and biochemistry. *Annu. Rev. Biomed. Eng.* **3**, 335–73 (2001).
53. Bax, D. V. *et al.* Plasma processing of PDMS based spinal implants for covalent protein immobilization, cell attachment and spreading. *J. Mater. Sci. Mater. Med.* **29**, (2018).
54. Bae, S.-I., Kim, K., Yang, S., Jang, K. & Jeong, K.-H. Multifocal microlens arrays using multilayer photolithography. *Opt. Express* **28**, 9082 (2020).
55. Scott, S. M. & Ali, Z. Fabrication methods for microfluidic devices: An overview. *Micromachines* **12**, (2021).
56. Kim, E., Xia, Y. & Whitesides, G. M. Polymer microstructures formed by moulding in capillaries. **376**, 7666–7667 (1995).
57. Khadpekar, A. J., Khan, M., Sose, A. & Majumder, A. Low Cost and Lithography-free Stamp fabrication for Microcontact Printing. *Sci. Rep.* **9**, 1–8 (2019).
58. Chan, E. K. L., Wong, C. K. Y., Lee, M., Yuen, M. M. F. & Lee, Y. K. Using PDMS micro-transfer moulding for polymer flip chip packaging on MEMS. *Proc. - Electron. Components Technol. Conf.* **2**, 1071–1076 (2005).
59. Whitesides, G. M. The origins and the future of microfluidics. *Nature* **442**, 368–373 (2006).
60. Leung, C. M. *et al.* A guide to the organ-on-a-chip. *Nat. Rev. Methods Prim.* **2**, (2022).
61. Zhang, B., Korolj, A., Lai, B. F. L. & Radisic, M. Advances in organ-on-a-chip engineering. *Nat. Rev. Mater.* **3**, 257–278 (2018).
62. Luni, C., Michielin, F., Barzon, L., Calabrò, V. & Elvassore, N. Stochastic model-assisted development of efficient low-dose viral transduction in microfluidics. *Biophys. J.* **104**, 934–942 (2013).
63. Giobbe, G. G. *et al.* Functional differentiation of human pluripotent stem cells on a chip. *Nat. Methods* **12**, 637–640 (2015).
64. Luni, C. *et al.* High-efficiency cellular reprogramming with microfluidics. *Nat. Methods* **13**, 446–452 (2016).
65. Gagliano, O. *et al.* Microfluidic reprogramming to pluripotency of human somatic cells. *Nat. Protoc.* **14**, 722–737 (2019).
66. Shahbazi, M. N. Mechanisms of human embryo development: From cell fate to tissue shape and back. *Dev.* **147**, (2020).
67. Bailey A.T. Weatherbee,Tongtong Cui, M. Z.-G. Modeling Human Embryo Development with Embryonic and Extra-Embryonic Stem Cells. *Sensors Actuators B. Chem.* 130836 (2021).
68. Moris, N. *et al.* An in vitro model of early anteroposterior organization during human

development. *Nature* **582**, 410–415 (2020).
69. Stemple, D. L. Quick guide:The notochord. *Curr. Biol.* 873–874 (2004).
70. Huch, M. & Koo, B. K. Modeling mouse and human development using organoid cultures. *Dev.* **142**, 3113–3125 (2015).
71. FLEMING, A., KEYNES, R. J. & TANNAHILL, D. The role of the notochord in vertebral column formation. *J. Anat.* **199**, 177–180 (2001).
72. Pera, M. F. Human embryo research and the 14-day rule. *Dev.* **144**, 1923–1925 (2017).
73. Peng, Y., Lv, J., Xiao, Z., Ding, L. & Zhou, Q. A framework for the responsible reform of the 14-day rule in human embryo research. *Protein Cell* **13**, 552–558 (2022).
74. Castelyn, G. Embryo experimentation: is there a case for moving beyond the '14-day rule'. *Monash Bioeth. Rev.* **38**, 181–196 (2020).
75. Cohen, D. E. & Melton, D. Turning straw into gold: Directing cell fate for regenerative medicine. *Nat. Rev. Genet.* **12**, 243–252 (2011).
76. Osafune, K. *et al.* Marked differences in differentiation propensity among human embryonic stem cell lines. *Nat. Biotechnol.* **26**, 313–315 (2008).
77. Fang, Y. & Eglen, R. M. Three-Dimensional Cell Cultures in Drug Discovery and Development. *SLAS Discov.* **22**, 456–472 (2017).
78. Little, M. H. Organoids: A special issue. *Development* **144**, 935–937 (2017).
79. Sato, T. *et al.* Single Lgr5 stem cells build crypt-villus structures in vitro without a mesenchymal niche. *Nature* **459**, 262–265 (2009).
80. Kretzschmar, K. & Clevers, H. Organoids: Modeling Development and the Stem Cell Niche in a Dish. *Dev. Cell* **38**, 590–600 (2016).
81. Orkin, R. W. *et al.* A murine tumor producing a matrix of basement membrane. *J. Exp. Med.* **145**, 204–220 (1977).
82. Weiss, P. & Taylor, A. C. Reconstitution of Complete Organs From Single-Cell Suspensions of Chick Embryos in Advanced Stages of Differentiation. *Proc. Natl. Acad. Sci.* **46**, 1177–1185 (1960).
83. Eiraku, M. *et al.* Self-Organized Formation of Polarized Cortical Tissues from ESCs and Its Active Manipulation by Extrinsic Signals. *Cell Stem Cell* **3**, 519–532 (2008).
84. Huch, M., Knoblich, J. A., Lutolf, M. P. & Martinez-Arias, A. The hope and the hype of organoid research. *Development* **144**, 938–941 (2017).
85. Mariani, J. *et al.* FOXG1-Dependent Dysregulation of GABA/Glutamate Neuron Differentiation in Autism Spectrum Disorders. *Cell* **162**, 375–390 (2015).
86. Chlebanowska, P., Tejchman, A., Sułkowski, M., Skrzypek, K. & Majka, M. Use of 3D organoids as a model to study idiopathic form of parkinson's disease. *Int. J. Mol. Sci.* **21**, (2020).
87. Lancaster, M. A. *et al.* Cerebral organoids model human brain development and

microcephaly. *Nature* **501**, 373–379 (2013).

88. Kyle W. McCracken1, Emily M. Catá1, Calyn M. Crawford1, Katie L. Sinagoga1, Michael Schumacher2, Briana E. Rockich3, Yu-Hwai Tsai4, Christopher N. Mayhew1, Jason R. Spence3, 4, Yana Zavros2,*, and James M. Wells1, 5. Modeling human development and disease in pluripotent stem cell-derived gastric organoids. *Physiol. Behav.* **176**, 139–148 (2017).
89. Ryan, S. L. *et al.* Drug Discovery Approaches Utilizing Three-Dimensional Cell Culture. *Assay Drug Dev. Technol.* **14**, 19–28 (2016).
90. Freedman, B. S. *et al.* Modelling kidney disease with CRISPR-mutant kidney organoids derived from human pluripotent epiblast spheroids. *Nat. Commun.* **6**, 1–13 (2015).
91. Rossi, G., Manfrin, A. & Lutolf, M. P. Progress and potential in organoid research. *Nat. Rev. Genet.* **19**, 671–687 (2018).
92. K.T, N., Prasad, K. & Singh, B. M. K. Analysis of red blood cells from peripheral blood smear images for anemia detection: a methodological review. *Med. Biol. Eng. Comput.* **60**, 2445–2462 (2022).
93. Nwogoh, B., Transfusion, B., State, E., Transfusion, B. & State, R. The Peripheral Blood Film. *Peripher. Blood Film* **12**, 71–79 (1974).
94. Aasen, T. *et al.* Efficient and rapid generation of induced pluripotent stem cells from human keratinocytes. *Nat. Biotechnol.* **26**, 1276–1284 (2008).
95. Gaignerie, A. *et al.* Urine-derived cells provide a readily accessible cell type for feeder-free mRNA reprogramming. *Sci. Rep.* **8**, 2–11 (2018).
96. Zhou, T. *et al.* Generation of induced pluripotent stem cells from urine. *J. Am. Soc. Nephrol.* **22**, 1221–1228 (2011).
97. Oda, Y. *et al.* Induction of pluripotent stem cells from human third molar mesenchymal stromal cells. *J. Biol. Chem.* **285**, 29270–29278 (2010).
98. Loh, Y. H. *et al.* Generation of induced pluripotent stem cells from human blood. *Blood* **113**, 5476–5479 (2009).
99. Zhang, X. B. Cellular Reprogramming of Human Peripheral Blood Cells. *Genomics, Proteomics Bioinforma.* **11**, 264–274 (2013).
100. Kim, Y. *et al.* The Generation of Human Induced Pluripotent Stem Cells from Blood Cells: An Efficient Protocol Using Serial Plating of Reprogrammed Cells by Centrifugation. *Stem Cells Int.* **2016**, (2016).
101. Bardelli, D. *et al.* Reprogramming fibroblasts and peripheral blood cells from a C9ORF72 patient: A proof-of-principle study. *J. Cell. Mol. Med.* **24**, 4051–4060 (2020).
102. Seki, T. *et al.* Generation of induced pluripotent stem cells from human terminally differentiated circulating t cells. *Cell Stem Cell* **7**, 11–14 (2010).
103. Nishimura, T. *et al.* Generation of rejuvenated antigen-specific T cells by reprogramming to

pluripotency and redifferentiation. *Cell Stem Cell* **12**, 114–126 (2013).
104. Baghbaderani, B. A. *et al.* CGMP-manufactured human induced pluripotent stem cells are available for pre-clinical and clinical applications. *Stem Cell Reports* **5**, 647–659 (2015).
105. Chou, B. K. *et al.* Efficient human iPS cell derivation by a non-integrating plasmid from blood cells with unique epigenetic and gene expression signatures. *Cell Res.* **21**, 518–529 (2011).
106. Pelosi, E., Castelli, G. & Testa, U. Endothelial progenitors. *Blood Cells, Mol. Dis.* **52**, 186–194 (2014).
107. Ormiston, M. L. *et al.* Generation and culture of blood outgrowth endothelial cells from human peripheral blood. *J. Vis. Exp.* **2015**, 1–7 (2015).
108. Hebbel, R. P. Blood endothelial cells: Utility from ambiguity. *J. Clin. Invest.* **127**, 1613–1615 (2017).
109. Toshner, M. *et al.* Evidence of dysfunction of endothelial progenitors in pulmonary arterial hypertension. *Am. J. Respir. Crit. Care Med.* **180**, 780–787 (2009).
110. Eminli, S. *et al.* Clinically compatible advances in blood-derived endothelial progenitor cell isolation and reprogramming for translational applications. *N. Biotechnol.* **63**, 1–9 (2021).
111. Yoshida, Y., Takahashi, K., Okita, K., Ichisaka, T. & Yamanaka, S. Hypoxia Enhances the Generation of Induced Pluripotent Stem Cells. *Cell Stem Cell* **5**, 237–241 (2009).
112. Tyanova, S., Temu, T. & Cox, J. The MaxQuant computational platform for mass spectrometry-based shotgun proteomics. *Nat. Protoc.* **11**, 2301–2319 (2016).
113. Gonzalez, R. *et al.* The Senescence-Associated Secretory Phenotype: The Dark Side of Tumor Suppression. *Proc. Natl. Acad. Sci. U. S. A.* **107**, 3552–3557 (2010).
114. Coppé, J.-P., Desprez, P.-Y., Krtolica, A. & Campisi, J. The Senescence-Associated Secretory Phenotype: The Dark Side of Tumor Suppression. *Annu Rev Pathol* **8**, 99–118 (2010).
115. Coppé, J. P. *et al.* Senescence-associated secretory phenotypes reveal cell-nonautonomous functions of oncogenic RAS and the p53 tumor suppressor. *PLoS Biol.* **6**, (2008).
116. Acosta, J. C. *et al.* A complex secretory program orchestrated by the inflammasome controls paracrine senescence. **15**, 978–990 (2014).
117. Lopes-Paciencia, S. *et al.* The senescence-associated secretory phenotype and its regulation. *Cytokine* **117**, 15–22 (2019).
118. Bindea, G. *et al.* ClueGO: A Cytoscape plug-in to decipher functionally grouped gene ontology and pathway annotation networks. *Bioinformatics* **25**, 1091–1093 (2009).
119. Paul Shannon, 1 *et al.* Cytoscape: A Software Environment for Integrated Models. *Genome Res.* **13**, 426 (1971).
120. Naba, A. *et al.* The matrisome: In silico definition and in vivo characterization by proteomics of normal and tumor extracellular matrices. *Mol. Cell. Proteomics* **11**, 1–18 (2012).

121. Ramilowski, J. A. *et al.* A draft network of ligand-receptor-mediated multicellular signalling in human. *Nat. Commun.* **6**, 1–11 (2015).
122. Satija, R., Farrell, J. A., Gennert, D., Schier, A. F. & Regev, A. Spatial reconstruction of single-cell gene expression data. *Nat. Biotechnol.* **33**, 495–502 (2015).
123. Jun Qin, A. M. G. Weak protein complexes: challenging to study but essential for life. *Physiol. Behav.* **176**, 139–148 (2017).

Acknowledgements

First of all, I must give my great gratitude to Chinese Scholarship Council, who is super kind to offer me this precious opportunity for going abroad to pursue the doctoral degree. Without the funding support and the help from the Chinese embassy, I would never make it to come here. Besides, during the Covid19 epidemic period, I received many supplies from my motherland-China, with their great love and care, to help me go through it.

Many thanks to my supervisor, professor Nicola Elvassore. Without his help, I would not get this Ph.D. opportunity to enter the department of industrial engineering. Many thanks to professor Onelia Gagliano for giving instructions and guidance to my doctoral project.

Many thanks to Silvia Angiolillo, Luca Brandolino and Elisa Cesare for taking care of me when I just arrived in Italy. At that time, I was scared of the new environment and new people since I knew nobody here, but they are so nice people who always keep me company and take care of me.

Many thanks to Roberta Frison and Pietro Bellet, I do enjoy spending time in making chips with you in DII, that is the most relaxed time during the work.

Many thanks to Martina Dercole, Lisa Agostini, Alessia Gesualdo, Andrea Maset and Carmela Ribecco. Even though we meet each other later, I also appreciate it that we spend the time together. I also enjoyed all activities with you outside of VIMM.

Special thanks to Camilla, Seba and Erika, whom I met in China and also later here in Italy. I always have the greatest fun whenever I stay with them.

Many thanks to those whom I did not mention here. You are always in my mind.

I feel great pain when I say goodbye to all my friends here, but I must move forward. However, saying goodbye is just a pause, not meaning we are saying farewell forever. As long as we want, we will always meet.

致 谢

首先要感谢国家留学基金委给我的提供的奖学金，让我能有这个机会，没有后顾之忧地来到意大利进行学习。与此同时还要感谢中国大使馆和驻意大利领事处各位老师的关心和帮助，除了平日里学业和生活上的帮助之外，尤其感谢在疫情期间所提供的物资资助。

其次要特别感谢我的导师 Nicola Elvassore 教授。十分感谢他为我提供的这个读博的机会，让我能够来到意大利完成自己的学业。

最后要感谢 VIMM 实验室所有的人，尤其是每天和我朝夕相处的学生们，感谢他们帮我融入意大利的学习和生活，感谢他们在我看不懂意大利语的时候给予的各种耐心的帮助。

我三年前来到意大利的时候，没有想过会在三年多的时间里，一次都回不了家。疫情改变了很多事情，当然我没有理由去埋怨，因为相比于那些在 2020 年春天失去了生命的人来说，我现在还能健康自由地生活，我需要感恩。疫情阻断了我很多的计划，有关于学习的，有关于旅行的，也有很多其他自己来自己设想好要去做，但是后来又没有能去做的事情。

在我出国的这三年里， 我的父母和弟弟是最担心我的人，担心我一个人出门，一个人回家，担心我有没有朋友，担心我有没有好好吃饭。我很想念我的弟弟，今年夏天他毕业了，选了一份自己非常满意的工作，现在过得很开心。这让我感到非常地欣慰。我的弟弟是这个世界上最好，最善良的人，不接受反驳。我和我的父母保持着每周固定时间视频的习惯，尽管大多数时候我妈妈都是在跟我说一些家长里短的事情，但是我知道这是她表达思念和爱意的方式，她做饭很好吃。

在这三年里，国内很多的人和事情都发生了改变。我有很多同学毕业了，工作了。也有很多朋友结婚了，甚至生了小孩，我很遗憾错过了很多好朋友的婚礼，也很遗憾没有能分享他们初为人父人母时的喜悦。他们总是会在微信上嘱咐我在国外要好好照顾自己，也总是问起我什么时候能回去。

首先感谢我的意大利室友，虽然我们经常会因为很多事情互相争执，但是我仍然十分感谢我室友在这两年朝夕相处里面对我的包容。

很想念大海。她是我最好的朋友，是那种无时无刻无条件支持我的朋友。在这三年里，她换了新工作，加班很多，有很多辛苦，但是也成长和收获了很多。我要谢谢她对我无时无刻的陪伴。希望我们都能成为理想中的自己，也希望今后能一起创造更多共同的回忆。

要感谢何早柯。他今年终于下定决心去了洛杉矶，我非常为他感到骄傲。希望他在美国一切顺利。

还有很多因为篇幅有限，在这里没能提到但是仍然要感谢的朋友们，感恩你们的关心和支持。

最后要感谢我自己，在过去的三年乃至过去人生中的某些至暗时刻，托住了自己不往下掉。借用龙队最爱的那句话，秦葳，你的美好人生才刚刚开始。

少年哪来多感伤，一心向南墙。从我在 3000 米的高空，往机舱外纵身一跃的那刻起，我所有的恐惧就都留在身后的云中了。

我们后会有期。

2022 年 11 月 30 日